

Magnetic impurities in non-magnetic metals

To cite this article: G Gruner and A Zawadowski 1974 *Rep. Prog. Phys.* **37** 1497

View the [article online](#) for updates and enhancements.

You may also like

- [Impurity transport driven by kinetic ballooning mode in the strong gradient pedestal of tokamak plasmas](#)

Shanni Huang, Weixin Guo and Lu Wang

- [The influence of electrode for electroluminescence devices based on all-inorganic halide perovskite CsPbBr₃](#)

Zhuo-Liang Yu, Yu-Qing Zhao, Peng-Bin He et al.

- [Direct d-d interactions among transition metal impurities in III-V semiconductors](#)

Takeshi Fujita and Hannes Raebiger

www.hidenanalytical.com
info@hiden.co.uk

HIDEN ANALYTICAL

Instruments for Advanced Science

Mass spectrometers for vacuum, gas, plasma and surface science



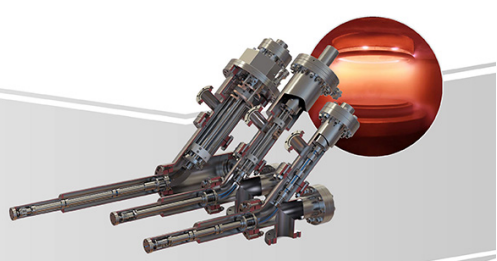
Residual Gas Analysis

Perform RGA at UHV/XHV. Our RGA configurations include systems for UHV science applications including temperature-programmed desorption and electron/photon stimulated desorption.



Thin Film Surface Analysis

Conduct both static and dynamic SIMS analysis with a choice of primary ions for full chemical composition and depth profiling. Our SIMS solutions include complete workstations and bolt-on modules.



Plasma Characterisation

Fully characterise a range of plasmas: RF, DC, ECR and pulsed plasmas, including neutrals and neutral radicals. Extend your analyses to atmospheric pressure processes using the HPR-60, with time-resolved mass/energy analysis.

Magnetic impurities in non-magnetic metals

G GRÜNER

Department of Physics, Imperial College, London and
Central Research Institute for Physics, Budapest, Hungary†

AND

A ZAWADOWSKI

Central Research Institute for Physics, Budapest, Hungary† and
Institute Laue-Langevin, Grenoble, France

Abstract

In this article the properties of 3d transition metal impurities in simple metal hosts are summarized.

The microscopic models of Friedel, Anderson and Wolff are reviewed, and the question of the formation of the magnetic moment on the impurity is briefly discussed. The structure of the Anderson model in the Hartree-Fock approximation and the correlation effects in the weakly magnetic limit when the Coulomb correlation energy U is smaller than the width Δ of the d states are summarized, together with the perturbational treatments of the model in the strongly magnetic limit $U/\Delta \gg 1$.

The s-d exchange model and the Kondo effect (the logarithmic increase of the resistivity with decreasing temperature) are discussed, and the various approximations of this model are compared. The relation between the Anderson model and the s-d exchange model is derived, and the nature of the Schrieffer-Wolff transformation is analysed, in particular the question of the polarization of the s and d states.

The experimental state of affairs is reviewed next, and the experimental data—obtained mainly on alloys of noble metals and aluminium with 3d elements—are collected to answer the questions raised in the previous sections. Experimental evidence on the singlet ground state, on charge neutrality and on the single-particle and many-body resonances is summarized. The question of the validity of the various approximations of the models is answered by comparing the experimentally found behaviours with theoretically derived formulae; this comparison leads to an indication of the basic unresolved questions in this field.

Finally, the latest developments in the theory are reviewed. These developments involve the consideration of the Kondo problem as a typical case of infrared divergencies, and are based on scaling and renormalization group techniques; they may bridge the gap between the earlier theories and the experimental facts.

This review was completed in January 1974.

† Permanent address.

Contents

	Page
1. Introduction	1500
2. Basic models	1502
2.1. Virtual bound state model	1502
2.2. Anderson model	1503
2.3. Wolff model	1505
2.4. Estimates of the basic parameters of the Friedel and Anderson models	1506
3. Basic results in the Anderson model	1507
3.1. General structure of the Anderson model	1508
3.2. Hartree-Fock treatment of the Anderson model	1509
3.3. Correlation effects in the non-magnetic limit	1514
3.4. Correlation effects in the magnetic limit	1519
3.5. General results in the Anderson model at zero temperature	1519
3.6. Hartree-Fock picture versus singlet ground state at $T = 0$	1522
4. Kondo effect and s-d model	1524
4.1. s-d model	1524
4.2. Kondo effect in third order of perturbation theory	1525
4.3. Kondo effect in leading logarithmic orders	1528
4.4. Different methods in the one-particle intermediate state approximation	1532
4.5. Results in the one-particle intermediate state approximation and the unitarity limit	1534
4.6. Kondo effect including potential scattering	1536
4.7. Variational calculations for the ground state	1537
4.8. Derivation of the s-d model from the Anderson model: Schrieffer-Wolff transformation	1540
4.9. Conduction electron density of states and charge oscillation around the impurities	1543
4.10. Spin perturbation in the s-d model and the spin compensation cloud	1545
4.11. General remarks	1548
5. Experiments on dilute alloys	1549
5.1. Introduction	1549
5.2. Basic parameters of the Anderson model; HF analysis	1550
5.3. The magnetic-non-magnetic transition: the Kondo effect	1555
5.4. Physical properties in the Kondo state	1557
5.5. Relation between the single-particle and many-body resonances	1564
6. Recent theoretical developments: infrared divergencies and scaling laws	1565
6.1. Many particles in the intermediate states	1565
6.2. Infrared divergencies	1566
6.3. Thermodynamical scaling	1568

6.4. Diagram techniques and the dynamical renormalization group	1570
6.5. Wilson's theory	1574
6.6. Functional integral method	1576
6.7. Some comparisons and some problems to be solved	1576
7. Conclusions	1577
Acknowledgments	1579
References	1579

1. Introduction

The subject of magnetic impurities in non-magnetic metals involves a rather wide range of alloys: the host can be a simple metal like copper or aluminium or a transition metal like palladium; and impurities with unfilled d or f shells both belong to this category. The great variety of different alloys leads naturally to widely diverging physical phenomena and different models to account for these observations. We do not survey all of them, but merely confine ourselves to simple but rather interesting cases where a strong correlation between theory and experiment is most promising: we discuss the situation where a 3d transition metal impurity is imbedded into a simple (free-electron-like) metal.

The first experiments date back to the early thirties, when a resistance minimum was found in certain pure metals at low temperatures; it became clear only much later that this effect is caused by a small amount of magnetic impurities. The term 'magnetic' here derives from the susceptibility measurements, which show a Curie-Weiss behaviour in these cases. Impurities which have a temperature-independent Pauli susceptibility do not cause such drastic effects in the resistivity. As a rather small amount of impurities can often lead to easily observable anomalies, metallurgical factors play a crucial role.

Nuclear magnetic resonance and electron spin resonance experiments have brought the question of polarization caused by a magnetic field as well as the question of the dynamical properties of the impurities into the limelight. A simple model was constructed to account for the experimental observations; in this so-called s-d model the impurity is represented by a spin operator with momentum $[S(S+1)]^{1/2}$, and this spin interacts with the conduction electrons through an exchange interaction J . This interaction is weak; the dimensionless coupling constant $J\rho_0(E_F)$, where $\rho_0(E_F)$ is the density of the host conduction electron states at the Fermi level, is of the order of 0.1. Due to the weakness of this interaction a perturbation treatment was expected to work and to give reasonable answers to questions concerning the polarization, resistivity, specific heat, etc. The main interest was focused on impurity-impurity interactions, which play an important role even for concentrations as small as 1 at%.

Another line of approach attempted to give an answer to the question of the existence of magnetic moment on the impurity. Friedel first addressed himself to solve this problem using scattering theory; the models of Anderson and Wolff rely heavily on Friedel's arguments. For single impurities the mean field approximation of the models was successful in dividing the impurities into magnetic and non-magnetic according to the ratio of two parameters, the Coulomb correlation energy U and the width Δ of the d states. The models were also thought to be appropriate for discussions of the pure 3d metals, and although this problem is more complicated due to the d-d interactions, for s-d hybridization the models are appropriate starting points in band structure calculations. It also turned out that the s-d model can be derived from the Anderson model when U is much larger than Δ .

A milestone in the development was Kondo's observation that a third-order calculation of the resistivity in the s-d model can account for the resistance minimum.

In this calculation a term $\log(kT/D)$ appears in third order, where D is the free-electron band width; the next correction is of the order of $J\rho_0(E_F)\log(kT/D)$ and it diverges at $T = 0$. This so-called Kondo effect placed this problem at the focus of solid state physics for a few years after 1964. Abrikosov and Suhl have demonstrated that the logarithmic terms are the consequence of a many-body resonance appearing at the Fermi level, and subsequent theoretical papers tried to determine the properties of this resonance; the main goal was to achieve a good quantitative agreement between theory and experiment.

A new line of approach has appeared in this period; this is called the localized spin fluctuation theory. According to this theory the appearance of the magnetic moment is the consequence of fluctuations at the impurity site. This model, which was supposed to work for nearly magnetic impurities, can also lead to anomalous transport, thermal and magnetic properties, and was in good agreement with the experimental observations on certain alloys.

In parallel with the theoretical development, more and more alloys were demonstrated to have anomalous properties; they were interpreted sometimes as Kondo, sometimes as localized spin fluctuation effects. The previous classification of alloy systems which was based on the Hartree-Fock approximation has been extended; the notation of Kondo or LSF alloys derived from this period. The overall confusion was enhanced by the fact that the experimental results were heavily influenced by impurity interactions, and a nearly perfect agreement between theory and experiment was in some cases merely an artefact rather than real progress. The theoretical and experimental states of affairs up to this point were reviewed by Kondo (1969) and Heeger (1969), and later by Fischer (1970, 1971a).

Since 1969 the experimental development has been characterized by very careful macroscopic experiments which have separated the effect of single impurities from spurious anomalies, resulting in a completely different overall picture than that apparent in 1969; this has forced the re-examination of the theory. This renewal of theoretical interest, however, was also initiated by the expectation that a final solution of this particular problem would have a much broader aspect, and might be rather useful in other branches of physics, like catalysis, chemisorption, etc.

It was realized that the main shortcoming of the classical ‘solutions’ lies in the fact that only one electron-hole intermediate state is considered in the approximations; this has required an approach to the problem based on a new physical concept. It was first used in other fields of solid state physics, such as x-ray absorption, where the response of an electron gas to a sudden change in a well-localized potential was investigated. The effect is an example of the so-called infrared divergency; a spin rotation is a typical case of this effect. The approach—in which an infinite number of electron-hole excitations are considered in the intermediate state—leads to scaling laws with the characteristic feature that the high-temperature logarithmic behaviours change to simple power laws at low temperatures. It seems that this approach has cleared up the basic physics behind the s-d model, although it still does not predict definite formulae which can match the experimental findings.

The experimental situation appears to be clear again (the main feature is that no real difference appears between various alloys, and any kind of distinction is artificial) and complete enough to build up a phenomenological picture which absorbs all the main experimental features; a model of this kind serves as the backbone of this review.

Our discussion differs from that expected of a review intended to serve as a guideline to a basic understanding of the dilute alloy problem. This is because we believe that in this particular field of solid state physics theory and experiment are strongly correlated, and extensive mathematical calculations of simple models are still expected to have their echoes in experimentally determined behaviours.

We start with a short discussion of the basic microscopic models and the relation between them. The structure of the Anderson model will be discussed in more detail in § 3, where the Hartree–Fock approximation and correlation effects in different limits will be examined. Section 4 is devoted to the s-d model, and we review the perturbational treatments of the Kondo effect, the one-particle intermediate state approximations and the variational treatments of the singlet ground state. The connection between the Anderson model and the s-d model will also be discussed in this section. We next review the main features of the experiments and contrast the results of various macroscopic and local methods with the theoretical situation; the structure of the discussion closely follows the arrangement of the previous sections. This will bring us to the still unresolved basic questions in the field of dilute alloys, and § 6 is devoted to a discussion of the latest development of the theory which aims to solve these questions in principle without attempting to account for experimental details.

It would be impossible to give a full list of works which have contributed to this field. We have selected those papers which we believe are the most instructive and which contain an extensive list of publications on the particular subject. The reference list relevant to the section on the experimental situation is far from being complete; for the reader who is interested in the details we refer to the review papers of Rizzuto (1974) and Grüner (1974).

2. Basic models

In order to account for physical phenomena caused by a transition metal impurity in a non-magnetic metallic host one should start with the electronic structure of the impurity atom and describe the interaction of this impurity with the host. In other words one should find a basic set of wavefunctions for the collective conduction electron states and for the localized magnetic orbitals, and afterwards describe the interaction between them (this interaction is called the s-d hybridization). This procedure is analogous to the band structure calculations of transition metals, where one starts with d electron and conduction electron wavefunctions. To account for dynamical processes, however, it is not necessary to perform a complete *ab initio* calculation of the electronic structure, but merely to find good and simple models which show realistic dynamical behaviour. In the following we briefly describe the three basic models applied to this problem: (i) Friedel's virtual bound state model (Friedel 1956, 1958); (ii) the Anderson model (Anderson 1961); (iii) the Wolff model (Wolff 1961).

2.1. Virtual bound state model

Friedel (1958) has represented the impurity by a potential. For a given total momentum quantum number l the potential consists of a deep hole at the core of the impurity and a centrifugal potential barrier $l(l+1)/r^2$, where the distance r is measured from the centre of the impurity (see figure 1).

In this potential hole a bound or resonance state can be formed. Here we deal with resonances which are near the Fermi level and are thus only partially occupied by electrons, rather than with deep-lying bound states which are full. If the resonance levels corresponding to the different spin directions are non-degenerate, a magnetic moment is formed at the impurity site. For a transition metal impurity of d or f type the resonance is characterized by the quantum numbers $l = 2$ and $l = 3$ respectively; later, however, we confine ourselves to 3d transition metal impurities. The resonance level has a finite width because the electron may jump from the potential hole to the metallic host by tunnelling through the centrifugal barrier. Since the barrier increases with increasing l , relatively narrow levels are expected for $l > 2$. Friedel has suggested a very elegant description of the resonance

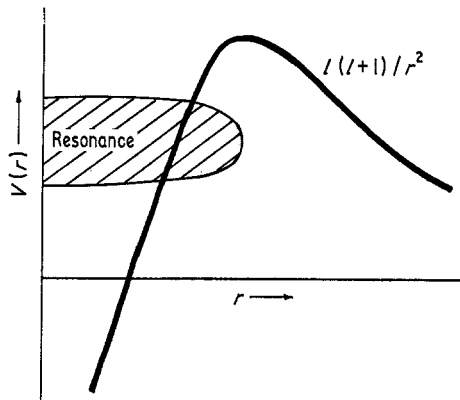


Figure 1. The potential around the impurity with a deep hole in the centre and with a potential barrier $l(l+1)/r^2$. The position of the resonance is also shown.

formation in terms of scattering theory. According to this the conduction electrons undergo a resonance scattering due to the processes in which the intermediate state is the resonance state. This resonance scattering can be characterized by an energy-dependent phase shift $\delta_{l,\sigma}(E)$ and the intermediate state by its density of states $\rho_{l,\sigma}(E)$, where σ denotes the spin index. These quantities are given by formulae well known in scattering theory:

$$\rho_{l,\sigma}(E) = \frac{1}{\pi} \frac{\Delta}{(E - E_{l,\sigma})^2 + \Delta^2} \quad (2.1)$$

and

$$\tan \delta_{l,\sigma}(E) = \frac{\Delta}{E_{l,\sigma} - E} \quad (2.2)$$

where Δ is the width and $E_{l,\sigma}$ the position of the resonance with spin direction σ . Many of the physical quantities can be expressed by the phase shifts, which can be treated phenomenologically; these results will be summarized in §§ 3 and 4.

2.2. Anderson model

Anderson (1961) has suggested a simple model which is based on Friedel's arguments but which allows direct calculations. In this model the metallic host is represented by electron bands with Bloch states (in the following only one band is

retained) with energy ϵ_k for momentum k . The resonant states discussed by Friedel are treated as extra orbitals; in the most simple idealistic case one orbital with two spin directions $\sigma = +, -$ and energy ϵ_d is considered. (The energies ϵ_k and ϵ_d are measured from the Fermi level.) The transition between this orbital and the conduction electron states with momentum k is represented by an extra term in the hamiltonian, where the transition amplitude V_{kd} is introduced phenomenologically. Furthermore, Anderson has introduced an intra-atomic Coulomb repulsion between two electrons at the localized level to reduce the probability of double occupation. This term plays an important role in the formation of a magnetic moment on the localized orbital and thereby in the magnetic properties of the impurity, since in order to be 'magnetic' this orbital must be singly occupied. Collecting all the terms, the Anderson hamiltonian is written in the following form:

$$H = \sum_{k,\sigma} \epsilon_k a_{k\sigma}^+ a_{k\sigma} + \sum_{\sigma} \epsilon_d a_{d\sigma}^+ a_{d\sigma} + \sum_{k,\sigma} (V_{kd} a_{k\sigma}^+ a_{d\sigma} + cc) + U n_{d\sigma} n_{d-\sigma} \quad (2.3)$$

where $a_{k\sigma}^+$ and $a_{d\sigma}^+$ denote the creation operators of the conduction electrons and the localized d electrons respectively with spin σ , $n_{d\sigma} = a_{d\sigma}^+ a_{d\sigma}$ is the occupation number of the localized level, and U is the interatomic Coulomb interaction.

The mixing term has a strong resemblance to that used in band structure calculations where the transition between the d orbitals and the conduction band is treated by introducing the mixing of matrix elements (Heine 1967). In the present case the electron may stay on the localized level for a finite time only, because due to the mixing it will sooner or later go into the conduction band; thus this mixing term determines the width Δ of the resonance via the 'golden rule'

$$\Delta = \pi V^2 \rho_0(\epsilon_d) \quad (2.4)$$

where V^2 denotes an appropriate average of $|V_{kd}|^2$, and $\rho_0(\epsilon_d)$ stands for the density of states of the conduction electrons in the host metal at the energy of the resonance level. Using this width given by equation (2.4) the density of states of the localized level can be obtained from equation (2.1).

The Anderson model in its original form given by equation (2.3) does not take into account the orbital degeneracy of the d level; therefore it has been generalized in several steps. The most general form of the hamiltonian is

$$\begin{aligned} H = & \sum_{k,\sigma} \epsilon_k a_{k\sigma}^+ a_{k\sigma} + \sum_{\sigma,m} \epsilon_d n_{m\sigma} + \sum_{k,m,\sigma} (V_{km} a_{k\sigma}^+ a_{m\sigma} + cc) \\ & + \frac{1}{2} U \sum_{m,m'} n_{m\sigma} n_{m'-\sigma} + \frac{1}{2}(U-J) \sum_{m \neq m', \sigma} n_{m\sigma} n_{m'\sigma} \\ & - \frac{1}{2} J \sum_{m \neq m', \sigma} a_{m\sigma}^+ a_{m-\sigma} a_{m'-\sigma}^+ a_{m'\sigma} + \frac{1}{2} J \sum_{m,\sigma} n_{m\sigma} n_{m-\sigma} + (\text{crystal field}) \end{aligned} \quad (2.5)$$

where the index m labels the different d orbitals, and J is the intra-atomic exchange integral between two different orbitals. The 'crystal field' terms responsible for the crystalline splitting caused by the non-spherical symmetric crystalline surroundings are not given explicitly, because for d electrons they probably can be neglected.[†] In the second and third terms on the right-hand side of equation (2.5) the degeneracy has been taken into account by extending the summation to the different orbitals. The fourth term describes the Coulomb repulsion between two arbitrary electrons with opposite spin. Similarly, the fifth term corresponds to the Coulomb interaction between electrons of parallel spin on different orbitals, and it is completed by

[†] This is not necessarily the case for f electrons, where the crystalline splitting has a larger effect because of the very narrow resonances.

the intra-atomic exchange interaction. The next terms do not occur in the original paper of Anderson (1961). As was recognized later by Caroli *et al* (1969), the first five terms are not invariant under a rotation in spin space, and in order to restore this symmetry they added the sixth term. Finally, in a similar way, Dworin and Narath (1970) noticed that the hamiltonian is still not invariant under a rotation in coordinate space, and they completed it by adding a seventh term.

As will be discussed later, several of the results are modified compared with the non-degenerate model in such a simple way that formally J is replaced by $U+4J$ in the final formulae. The quantity $U+4J$ can be considered as an effective Coulomb integral; and later, where it does not lead to misunderstanding, it will be simply referred to as a Coulomb integral.

The essential feature of the Anderson model is that by introducing extra orbitals one arrives at a dynamical model which fits Friedel's picture perfectly as far as the formation of the virtual bound state is concerned. Conceptually, however, there is a serious difficulty: namely, the translationally invariant conduction electron wavefunctions form a complete set; thus the extra orbitals are not orthogonal to this set. Similar orthogonalization problems appear in the different band structure calculations for normal metals, and more seriously for transition metals (Heine 1967). However, in the present case this non-orthogonality is not expected to influence essentially the dynamical properties, but its effects might rather show up in comparison with *ab initio* calculations. As the Anderson model is usually used to investigate the dynamical behaviour of the impurity, this orthogonality problem is rather academic in that context.

2.3. Wolff model

Another simple model has been constructed by Wolff (1961). The electronic states are restricted to a single band described in terms of Wannier functions localized at atomic sites. The impurity potential is represented by the shift of energy V of the Wannier function centred at the impurity site i . The width of the energy band is determined by the hopping matrix elements T_{ij} between Wannier functions centred at sites i and j . The matrix elements connecting the impurity orbital to the host states are different from the hopping matrix element between the host atoms. Finally, as in the Anderson model, a Coulomb repulsion U is introduced which acts between two electrons with opposite spins at the impurity. The hamiltonian is given as

$$H = \sum_{i \neq j, \sigma} T_{ij} d_{i\sigma}^+ d_{j\sigma} + \frac{1}{2} U \sum_{\sigma} n_{0\sigma} n_{0-\sigma} + V \sum_{\sigma} n_{0\sigma} \quad (2.6)$$

where $d_{i\sigma}^+$ is the creation operator of an electron with spin σ and orbital centred at site i , and $n_{0\sigma} = d_{0\sigma}^+ d_{0\sigma}$ with the impurity site labelled by 0.

This model has strong resemblance to the Anderson model discussed before, which is obvious if in the Anderson model the conduction electron wavefunctions are transformed to a Wannier representation (Rivier and Zitkova 1971) involving all the conduction bands; in the Wolff model, however, only one band is considered.

The most attractive feature of the Wolff model is that no extra orbital has been introduced for the impurity. However, other serious conceptual problems must be raised; for example, the impurity orbital is not well localized since it is represented by a Wannier function, contrary to the Anderson model where the localized orbital is constructed using several bands.

The dynamics in the Wolff model show a behaviour similar to that found for the Anderson model, which will be discussed later in this review (see eg Appelbaum and Penn 1969, 1971); however, there are also essential differences (see eg Fischer 1971b). The differences can be demonstrated by the following example of the electrical resistivity. In the Anderson model, if the transition rate from the conduction band to the impurity level V_{kd} tends to zero, a free-electron band is obtained which is not coupled to the impurity level, and the impurity resistivity vanishes. In the Wolff model, however, taking the hopping matrix elements T_{i0} and T_{0i} which connect the impurity level to the other electrons to be zero, a large impurity resistivity must be expected, because the conduction electrons must avoid the impurity atoms. In this sense, a careful analysis of the applicability of the Wolff model is needed, which may result in a better understanding of the theories obtained in this model (eg Kaiser and Doniach 1970).

2.4. Estimates of the basic parameters of the Friedel and Anderson models

In order to estimate the width Δ , Anderson and McMillan (1967) performed an *ab initio* calculation starting with the ‘muffin-tin’ idea (see eg Ziman 1972) worked out for band structure calculations. In this method atomic wavefunctions are used inside a sphere surrounding the core of the atoms, with free electrons outside the sphere. A special matching condition was elaborated in the augmented plane wave (APW) method. Anderson and McMillan adapted this method to the single-impurity problem, where atomic wavefunctions are used inside the muffin-tin sphere of the impurity and free-electron wavefunctions outside. As in the APW method, one determines the phase shifts of the conduction electrons scattered by the atomic core inside the sphere. Such a calculation fits perfectly Friedel’s description sketched briefly in § 2.2. By making use of the Friedel sum rule to be discussed in § 3.5, Anderson and McMillan have determined the extra density of states localized at the impurity site in terms of the energy derivatives of the phase shifts $\partial\delta_l(E)/\partial E$. By calculating these derivatives the additional density of states $\Delta\rho(E)$ produced by the impurity in the free-electron gas can be obtained from the formula

$$\Delta\rho(E) = \frac{1}{\pi} \sum_l (2l+1) \frac{\partial\delta_l(E)}{\partial E} \quad (2.7)$$

where the summation is over the different angular momenta l and the factor $2l+1$ is due to orbital degeneracy. The actual calculation has been performed for Fe impurity in Cu and yields the density of states given in figure 2, in which a pronounced resonance is formed with a width of 1–2 eV. This value of the width allows us to determine the average value of the mixing amplitude V_{kd} of the Anderson model by equation (2.4). The position of the resonance is about 10 eV measured from the bottom of the conduction band, and therefore the resonance can be found in the neighbourhood of the Fermi level. One cannot calculate the Coulomb integral by considering the atomic orbital in a simple way, because the Coulomb interaction is strongly screened by the conduction electron. This screening may reduce its value essentially to 1–3 eV (see eg Herring 1966), while the integration of atomic wavefunctions yields about 10 eV. Furthermore, using the estimation $J \sim 0.5\text{--}1$ eV we get an effective Coulomb integral $U+4J \sim 5$ eV.

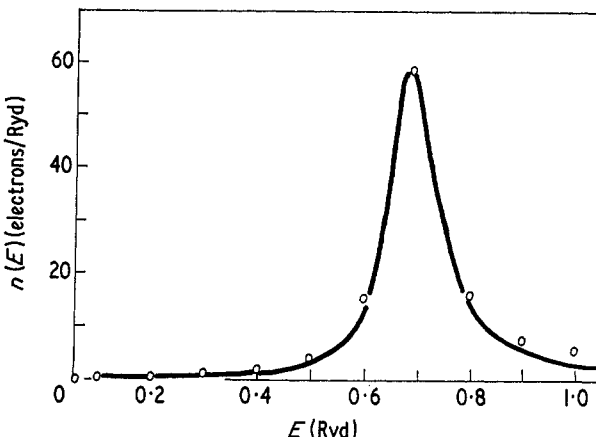


Figure 2. The extra density of states associated with an iron impurity in copper (after Anderson and McMillan 1967).

3. Basic results in the Anderson model

The three models discussed so far are capable of describing the resonance formation due to a transition metal impurity embedded in a metallic host. Since from the physical point of view the Anderson model is nearer than the Wolff model to the situation in which we are interested, and can be treated mathematically more exactly than Friedel's description, in the following we restrict our discussion to the analysis of the Anderson model. It should be pointed out, however, that the dynamical properties of these models are very similar; for example, the localized spin fluctuations (LSF)—which will be discussed later—exhibit similar features in the Anderson and Wolff models (Appelbaum and Penn 1969, 1971).

First let us discuss two limiting cases of the Anderson model. In one limit the broadening of the localized level can be neglected in comparison with the Coulomb interaction, ie $\Delta \ll |\epsilon_d|$ and $\Delta \ll U$. If the impurity level is below the Fermi level ($\epsilon_d < 0$), it is at least singly occupied in thermal equilibrium. Assuming that there are two electrons on the impurity level, the total energy due to the Coulomb repulsion becomes $2\epsilon_d + U$. If $2\epsilon_d + U < 0$, the level is doubly occupied and the magnetic moments of the two electrons localized on the impurity compensate each other; thus the impurity is non-magnetic. If, on the other hand, $2\epsilon_d + U > 0$, the impurity is singly occupied† and a magnetic moment is formed with spin $\pm \frac{1}{2}$. We will be interested mainly in the latter case, where the impurity can be magnetic.

The other limit of considerable interest is the situation when a broad resonance level is formed at the Fermi level and the Coulomb energy is relatively small compared with the width of this level, ie $|\epsilon_d|, U \ll \Delta$. In this case the Coulomb energy U , being small, cannot modify essentially the density of states related to the localized level. Thus the impurity is partially occupied with spin-up and spin-down electrons. This state is obviously non-magnetic; only the fluctuation in the occupation numbers for different spins can result in a magnetic moment formed temporarily for a short time. This phenomenon is known as localized spin fluctuation, LSF.

If we change the relative value of the parameters Δ , U and ϵ_d between these two limiting cases, the magnetic limit goes over continuously to the non-magnetic one.

† We assume implicitly that the Friedel sum rule is maintained by adjustments in phase shifts (say $l = 0$) other than that of the level with which we are concerned.

The Hartree–Fock (HF) approximation (Anderson 1961) leads to a sharp transition between the magnetic and non-magnetic cases, since it corresponds to the approximation of a static mean field theory neglecting fluctuations.

In the following subsections, after referring to some general features of the theory, we shall discuss: (i) the Hartree–Fock approximation; (ii) the localized spin fluctuation including electron–hole and electron–electron correlation; (iii) the perturbational treatment of the Anderson model in the large- U/Δ limit; and finally (iv) we list a series of arguments valid generally in the Anderson model.

3.1. General structure of the Anderson model

The hamiltonian can be given by equation (2.3) in the simplest case with only one localized orbital, where there are two different interaction terms: the s–d mixing characterized by the transition rate V_{kd} , and the intra-atomic Coulomb repulsion U . Since the first of these interactions is quadratic in the operators, if we neglect the Coulomb repulsion U the hamiltonian can be diagonalized exactly. In the case $U = 0$ the conduction electrons can be eliminated by introducing a broadening for the localized level. This broadening can be given by

$$\Delta = \pi \overline{|V_{kd}|^2} \rho_0(E_{d,\sigma}) \quad (3.1)$$

where the bar over $|V_{kd}|^2$ means an average over the directions of k . Thus Δ is proportional to the density of states of the conduction electrons at $E_{d,\sigma}$, which in turn may depend on the spin direction and will be determined later. Usually $\rho_0(E_{d,\sigma})$ is replaced by the density ρ_0 , taken at E_F . In this way the one-particle Green function for the extra orbital can be written at zero temperature as

$$G_{d,\sigma}^{(0)}(\omega + i\epsilon) = \frac{1}{\omega - E_{d,\sigma} + i\Delta}, \quad \epsilon \rightarrow +0 \quad (3.2)$$

where the index (0) indicates that the Coulomb interaction has not been taken into account except for the fact that the position of the resonance $E_{d,\sigma}$ depends on U . The density of states of this single orbital, which can be obtained from the Green function of equation (3.2) as

$$\rho_{d,\sigma}^{(0)}(\omega) = -\frac{1}{\pi} \text{Im } G_{d,\sigma}^{(0)}(\omega + i\epsilon) = \frac{1}{\pi} \frac{\Delta}{(\omega - E_{d,\sigma})^2 + \Delta^2} \quad (3.3)$$

has a simple lorentzian form for $U = 0$. By comparing this formula with equation (2.1), the connection between the Friedel resonance theory and the Anderson model can be demonstrated. It is important to note that this density of states is normalized to unity, and that this normalization is not changed by including the effect of the Coulomb interaction, ie

$$\int \rho_{d,\sigma}^{(0)}(\omega) d\omega = \int \rho_{d,\sigma}(\omega) d\omega = 1. \quad (3.4)$$

The impurity Green function, and in particular its spectral function the density of d states $\rho_{d,\sigma}(\omega)$, is of primary importance, as the various physical parameters are determined by this quantity.

First of all we will consider that part of the one-electron scattering amplitude in which only one electron is in the scattered state and the spin is not changed during the scattering process. Since the conduction electrons are directly involved only

in the mixing interaction, when we consider an arbitrary one-electron scattering process the first interaction is a transition of the conduction electron to the localized level and the last one is the reverse process. All the processes in between can be related to the behaviour of the broadened localized level, which can be described by the localized level Green function $G_{d,\sigma}(\omega)$ renormalized by the Coulomb repulsion.

Thus

$$t_{kk',\sigma}(\omega) = V_{kd} G_{d,\sigma}(\omega) V_{dk'} \quad (3.5)$$

where $t_{kk',\sigma}(\omega)$ is the non-spin-flip scattering amplitude of the conduction electrons with incoming and outgoing momenta k and k' .

Taking the imaginary part of equation (3.5) with variables $k = k'$ and using equation (3.3) one obtains

$$\text{Im } t_{kk,\sigma}(\omega) = \pi |V_{kd}|^2 \rho_{d,\sigma}(\omega) \quad (3.6)$$

ie $\text{Im } t_{kk,\sigma}(\omega)$ is entirely determined by the density of states of the d level.

This equation plays a central role in the dilute alloy problem because according to the ‘optical theorem’ the total scattering cross section is proportional to the imaginary part of the forward scattering amplitude $t_{kk,\sigma}(\omega)$, and therefore it is proportional to $\rho_{d,\sigma}(\omega)$. This connection is the reason for the many theoretical attempts which have been made to calculate the renormalized density of states of one localized level. This renormalization, in spite of the apparent simplicity of the corresponding term $U n_\sigma n_{-\sigma}$ in the model, is still missing for finite Coulomb interaction, and no reasonable approximation is yet known which works for arbitrary Coulomb energies. The approach as outlined above treats first the mixing between the d and conduction electron states, and then includes the effect of the Coulomb interaction; thus clearly this procedure should be more appropriate for small U values.

Finally it should be mentioned that if we were to consider the more realistic case where the d level is five-fold degenerate and the hamiltonian is given by equation (2.3), then we should take into account the symmetry of the d level ($l = 2$). Due to this symmetry the product $V_{kd} V_{dk'}$ occurring in many formulae (see eg equation (3.5)) has an angular dependence

$$V_{kd} V_{dk'} = V^2 P_l(\cos \gamma_{kk'}) = V^2 (2l+1) \sum_{m=-l}^l Y_l^{m*}(k) Y_l^m(k') \quad (3.7)$$

where P_l is the Legendre polynomial, Y^m are the spherical harmonics, $\gamma_{kk'}$ is the angle between momenta k and k' , and V is the transition amplitude. Furthermore, according to equations (3.5) and (3.7) the scattering amplitude can be given in the form

$$t_{kk'}(\omega) = t_{l=2}(\omega) P_{l=2}(\cos \gamma_{kk'}) \quad (3.8)$$

where $t_l(\omega)$ denotes the partial scattering amplitude for angular momentum l .

3.2. Hartree-Fock treatment of the Anderson model

In the Hartree-Fock approximation (Anderson 1961, Blandin 1973) the effect of the Coulomb interaction is taken into account by an ‘effective field’ which results in energy shifts $E_{d,\sigma} - \epsilon_d$ but does not alter the shape (lorentzian for $U = 0$) of the levels. These shifts should be determined in a self-consistent way, allowing for different occupation of the levels.

Let us restrict our treatment to the most simple case given by equation (2.4), with two levels $\sigma = \pm 1$. The occupation numbers are expressed as

$$\langle n_{d\sigma} \rangle = \int_{-\infty}^0 \rho_{d,\sigma}^{(0)}(\omega) d\omega = \frac{1}{\pi} \cot^{-1} \left(\frac{E_{d,\sigma}}{\Delta} \right) \quad (3.9)$$

where the energy ω is measured from the Fermi energy and equation (3.3) has been applied. The averaged Coulomb field acting on the level σ is $U\langle n_{d-\sigma} \rangle$; thus

$$E_{d,\sigma} = \epsilon_d + U\langle n_{d-\sigma} \rangle. \quad (3.10)$$

When we insert these results into equation (3.9) two coupled equations are obtained:

$$\langle n_{d+} \rangle = \frac{1}{\pi} \cot^{-1} \left(\frac{\epsilon_d + U\langle n_{d-} \rangle}{\Delta} \right)$$

and

$$\langle n_{d-} \rangle = \frac{1}{\pi} \cot^{-1} \left(\frac{\epsilon_d + U\langle n_{d+} \rangle}{\Delta} \right). \quad (3.11)$$

Depending on the relative values of the different parameters ϵ_d , U and Δ , this system of equations may have a single solution with $\langle n_{d+} \rangle = \langle n_{d-} \rangle$, in which case the impurity is non-magnetic; or in addition two symmetrical solutions with $\langle n_{d+} \rangle \neq \langle n_{d-} \rangle$, in which case the impurity is magnetic. For $U = 0$ the trivial solution $E_{d,\sigma} = \epsilon_d$ corresponds to a non-magnetic state. On increasing the value of U the impurity remains non-magnetic, until at a critical value of U it becomes magnetic. Equation (3.11) can be solved graphically by plotting $\langle n_{d+} \rangle$ against $\langle n_{d-} \rangle$ using the first equation and vice versa for the second equation; the crossing points of these curves yield the solutions. Two typical diagrams are given in figure 3(a) for parameter values (i) $U/\Delta = 5$, $\epsilon_d = -U/2$ and (ii) $U/\Delta = 1$, $\epsilon_d = -U/2$. The magnetic and non-magnetic regions of the parameters are plotted in figure 3(b).

The boundary line separating the magnetic and non-magnetic regions can be derived in a simple way. Let us suppose that the occupation number at a given point of the boundary is n_c . By increasing U one may get a solution in the form $\langle n_{d+} \rangle = n_c + \delta n$, $\langle n_{d-} \rangle = n_c - \delta n$. This solution must satisfy equation (3.11) at this point with infinitesimally small δn ; thus n_c must be a solution of the derivative of equation (3.7):

$$1 = \frac{U}{\pi\Delta} \frac{1}{1 + [(\epsilon_d + Un_c)/\Delta]^2}. \quad (3.12)$$

This result can be rewritten by using equation (3.3) as

$$U\rho_d^{(0)}(0) = 1 \quad (3.13)$$

and shows that a system is more likely to be magnetic if the density of d states is large at the Fermi level. Thus the most favourable case for formation of a magnetic moment is that where the impurity levels of lorentzian shape are half filled by electrons (eg as we shall see later Mn in Cu). Furthermore, if the impurity levels are nearly empty or almost completely full then the impurity is more likely to be non-magnetic, as $\rho_{d,\sigma}^{(0)}(0)$ is relatively small. This condition can be obtained immediately by considering the balance of the 'kinetic energy' increase and the interaction

energy gain near the boundary. Since due to a polarization $\langle n_{d\pm} \rangle = n_c \pm \delta n$ the kinetic energy increases by $(\rho_d^{(0)}(0))^{-1}(\delta n)^2$, this condition has the form

$$(\rho_d^{(0)}(0))^{-1}(\delta n)^2 + U[(n_c - \delta n)(n_c + \delta n) - n_c^2] = 0$$

which is equivalent to equation (3.13). The relation derived here has the same form as the Stoner condition obtained for the magnetic instability of an electron gas (Stoner 1938, 1939).

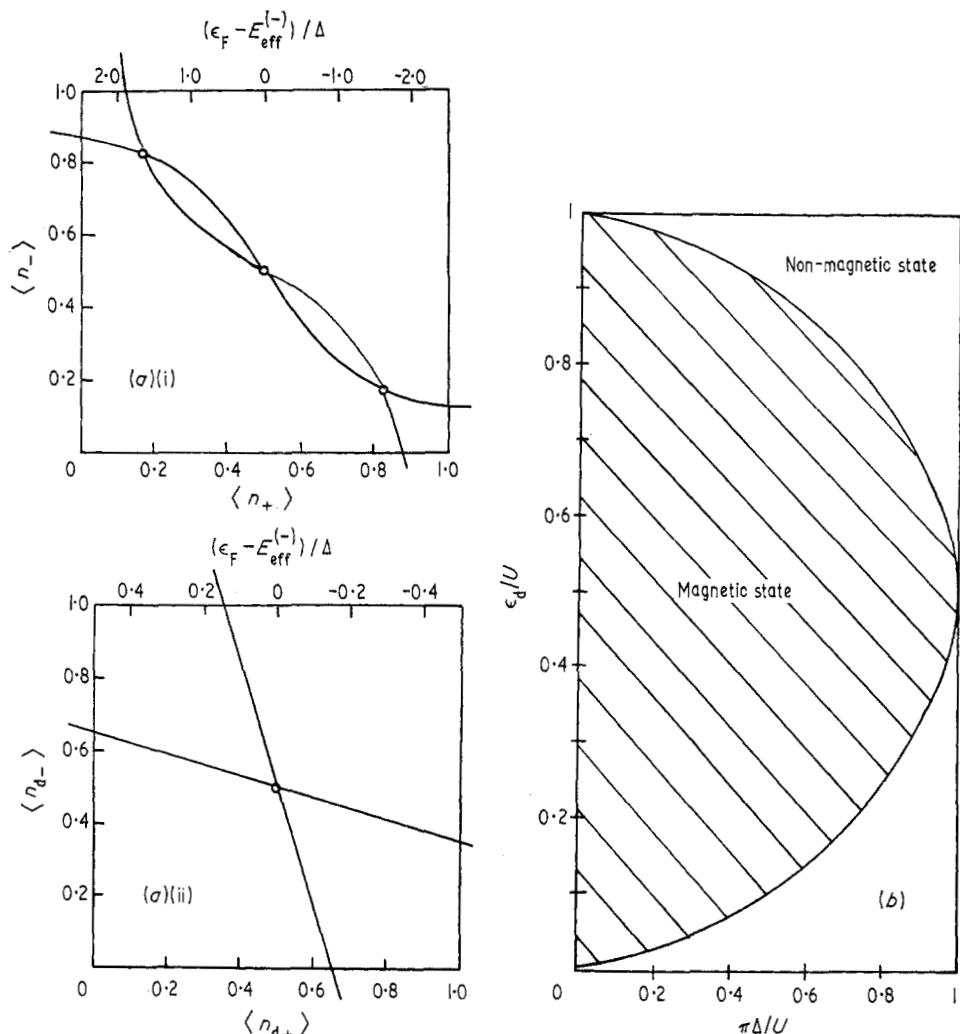


Figure 3. (a) Self-consistency plot of $\langle n_- \rangle$ against $\langle n_+ \rangle$: (i) typical magnetic case with $U/\Delta = 5$, $\epsilon_d/U = -\frac{1}{2}$; (ii) a non-magnetic case with $U/\Delta = 1$, $\epsilon_d/U = -\frac{1}{2}$. (b) Magnetic and non-magnetic regimes as a function of $(U/\pi\Delta)^{-1}$ and $-\epsilon_d/U$.

Similar considerations can also be applied to the five-fold degenerate case $l = 2$, where the levels are labelled by the quantum numbers $m = -2, -1, 0, 1, 2$. In this case, however, there might be two different kinds of magnetism: spin magnetism and orbital magnetism. For spin magnetism the different levels are equally polarized and thus near the boundary $\langle n_{dm\pm} \rangle = n_c \pm \delta n$ for arbitrary m . By repeating our previous reasoning for the hamiltonian given by equation (2.5), we find that the last

two terms of the hamiltonian do not contribute to the HF energy, because they are off-diagonal; thus the condition for spin magnetism is

$$(U + 4J) \rho_d^{(0)}(0) > 1. \quad (3.14)$$

For the investigation of orbital magnetism we take as a simple example an impurity with two-fold orbital degeneracy. Orbital magnetism appears if the populations of the two orbitals are different, but this difference is spin-independent. Denoting the orbitals by 1 and 2, $\delta n_{1\sigma} = -\delta n_{2\sigma}$ for arbitrary σ and σ' . The condition necessary for orbital magnetism can be obtained in a simple way as

$$(U - J) \rho_d^{(0)}(0) > 1. \quad (3.15)$$

As the exchange integral J is positive, we can immediately see by comparing equations (3.14) and (3.15) that the occurrence of spin magnetism is more favoured than the occurrence of orbital magnetism; furthermore, spin magnetism is more likely for a degenerate orbital than for a non-degenerate one.

In the HF approximation several quantities can be expressed in terms of phase shifts which are the key quantities in Friedel's theory. The requirement that the conduction electron scattering amplitude can be expressed by phase shift in an angular momentum channel l is that the scattering be elastic and only the one excitation channel without spin-flip be effective. This is an extremely strong condition; it is, however, satisfied in the HF approximation because the dynamical effects are excluded. The phase shift is related to the scattering amplitude as

$$t_{l,\sigma}(\omega) = (1/\pi\rho_0) \sin \delta_{l,\sigma}(\omega) \exp(i\delta_{l,\sigma}(\omega)) \quad (3.16)$$

where $t_{l,\sigma}(\omega)$ is defined by equation (3.8). The phase shifts $\delta_{l,\sigma}(\omega)$ depend on energy, and in the magnetic case on σ as well. By considering equations (3.16), (3.8), (3.3) and (3.1) the phase shift can be expressed as

$$\delta_\sigma(\omega) = \cot^{-1}\left(\frac{E_{d,\sigma}}{\Delta}\right) = \cot^{-1}\left(\frac{\epsilon_d + U\langle n_{d-\sigma} \rangle}{\Delta}\right) = \pi\langle n_\sigma \rangle \quad (3.17)$$

where the last equality follows from equation (3.9). It is a special case of the Friedel sum rule (see eg Ziman 1972) which relates the phase shifts to the number of electrons screening the excess charge of the impurity. In the present case the Friedel sum rule is satisfied by considering only the electrons on the impurity level.

The ionic charge Z of the impurity ion (measured in electronic units) must be screened by the electrons on the impurity level and by the conduction electrons. However, according to our previous result the conduction electrons do not contribute to the Friedel sum rule; therefore, the screening is entirely due to the electrons on the impurity level. Thus the condition of screening is

$$Z = 5(\langle n_{d\sigma} \rangle + \langle n_{d-\sigma} \rangle) = 5(\delta_\sigma + \delta_{-\sigma})/\pi \quad (3.18)$$

where the orbital degeneracy is responsible for the factor of 5 and equation (3.17) has been applied.

The condition of screening occurs in the mathematical schema in the following way. In the Anderson model the quantities V_{kd} , U and J can be obtained at least in principle by calculating the electronic structure of the impurity, and they are more or less independent of the particular 3d impurity in the same host. On the other hand, the position of the d level ϵ_d depends strongly on the occupation of the d

level, and thus on the charge of the impurity ion. The impurity ion produces a strong Coulomb field which shifts the value of ϵ_d in such a way that the ion is completely screened at the impurity site. This screening can be formulated as a self-consistent condition to determine the position of the d level ϵ_d .

Let us now turn to the discussion of the magnetic polarization of the impurity. The magnetic moment of d electrons can be expressed in a way similar to (3.18) by the occupation number of d electron levels:

$$M = \mu_B \sum_{m=-l}^l (\langle n_{dm+} \rangle - \langle n_{dm-} \rangle) = 5\mu_B(\delta_+ - \delta_-) \quad (3.19)$$

where μ_B is the Bohr magneton. Thus in the HF approximation the magnetic moment localized on the d level is proportional to the difference of the phase shifts. Furthermore, it is important to point out that the conduction electrons are not essentially polarized, as has been shown by Anderson (1961). Thus the s-d mixing term may lead to a polarization of the conduction electrons which is parallel to that of the d electrons, because the polarized d electrons can jump to the conduction band and vice versa; this effect is, however, compensated by the energy shift of the conduction electrons caused by the presence of the resonance (Anderson's 'compensation theorem'). In other words, the conduction electron-impurity scattering does not change the total conduction electron density of states in the region of the Fermi level, provided the scattering is independent of the momenta of the conduction electrons and the band is symmetric to the Fermi level. The fact that these assumptions are fulfilled only approximately does not change the compensation drastically. Thus in the HF approximation the magnetic moment is completely localized on the d level.

The magnetic susceptibility can be calculated by using expression (3.19) and we arrive at a Curie-like temperature dependence μ^2/T . This result may be modified going beyond the HF approximation; however, a clear distinction between the magnetic and non-magnetic limits can be made on the basis of the HF approximation.

The density of states of the d level is entirely different in the non-magnetic and magnetic limits. In the non-magnetic limit a simple lorentzian density of states is obtained which is filled in by electrons to the same energy for both spin directions. In the magnetic limit, however, according to equation (3.10) the positions of the two lorentzian levels are different and

$$E_{d,\sigma} - E_{d,-\sigma} = U(\langle n_{-\sigma} \rangle - \langle n_{\sigma} \rangle). \quad (3.20)$$

The density of states for different spin directions is shown in figure 4, where the occupied regions are shaded in different ways for spin-up and spin-down electrons; the total density of states

$$\rho_{d,tot}(\omega) = \rho_{d,\sigma}(\omega) + \rho_{d,-\sigma}(\omega) \quad (3.21)$$

is represented by the broken curve. The separation between these peaks is proportional to the Coulomb energy and to the magnetization; see equations (3.20) and (3.19).

At zero temperature the impurity resistivity R is proportional to $\rho_{d,tot}(0)$, since the cross section for the conduction electrons is expressed by the forward scattering amplitude (optical theorem), which in turn is given by equation (3.6).

Summing over the spin directions, the electrical resistivity has the form

$$\begin{aligned} R(T=0) &= (1/4\pi k_F e) \operatorname{Im}(t_{kk,\sigma}(\omega=0) + t_{kk,-\sigma}(\omega=0)) \\ &= (1/4\pi k_F e) |V_{kd}|^2 \rho_{d,\text{tot}}(\omega=0) \end{aligned} \quad (3.22)$$

where k_F is the Fermi momentum and e is the electronic charge.

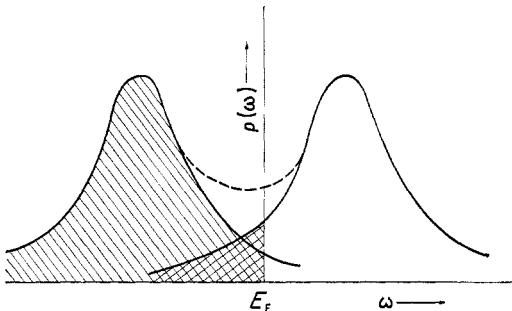


Figure 4. The density of d states for the two spin directions σ and $-\sigma$ in the HF approximation: the total density of states is represented by the broken curve; the occupied regions are shaded in different ways.

Applying this formula to interpret the experiments, the electrical resistivity can be used to obtain information on the structure of the d level. One can distinguish between non-magnetic and magnetic cases by measuring the resistivity as a function of the atomic number of the impurities (Friedel 1958). A similar situation can be expected for the amplitude of the charge polarization around an impurity, and this effect will be discussed in § 5.

It is very important to emphasize that these considerations are valid only in the HF approximation. At low temperature, strong correlations in the neighbourhood of the Fermi energy might give rise to an essential modification of the HF results.

As will be shown later, these correlations might be suppressed by increasing the temperature; thus one may expect that the HF situation is a good approximation at high temperatures where the different quantities depend only slightly on temperature, as kT is always negligible compared with U and Δ . Therefore Friedel's argument on the resistivity holds only in the high-temperature region, and at low temperatures intensive many-body effects can be expected.

In the following we speak about magnetic or non-magnetic impurities depending on whether the total density of states is well-split or non-split; the relation of this behaviour to the magnetic properties has been shown before. The case where there is only a relatively small splitting will be referred to as the intermediate case. The aim of the next section is to study the effect of correlations in the limit where $U \ll \Delta$; the magnetic limit will be the subject of § 3.4.

3.3. Correlation effects in the non-magnetic limit

In the non-magnetic limit the position of the resonances and the occupation numbers are independent of the spin direction σ . The results of the HF approximation are not different from the $U=0$ limit, except that the position of the resonance level is shifted by $U\langle n_\sigma \rangle$. Correlation effects due to the Coulomb repulsion appear only beyond the HF approximation. Two types of correlation may occur

when we consider the localized level: electron-electron with total spin $S = 0$, and electron-hole with spin $S = 1$. In diagrammatic representation these correlations can be characterized in lowest order by the first-order vertex corrections containing two parallel or two antiparallel lines respectively. These diagrams are shown in figure 5, where the full and broken lines represent the electrons and the Coulomb interaction respectively. The strengths of the different correlations depend very much on the density of electrons $n = \langle n_\sigma \rangle$, therefore the discussion is split into two parts: (i) low-density $n \ll 1$ limit (which is equivalent to the high-density limit $n \approx 1$ due to electron-hole symmetry); (ii) symmetrical case when $n = \frac{1}{2}$.

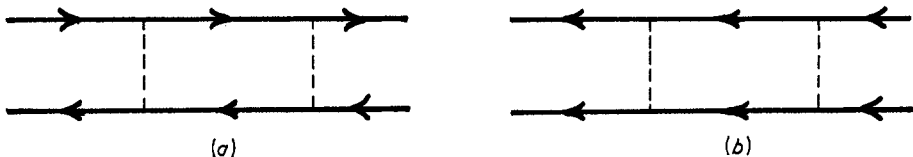


Figure 5. The simplest diagrams which contribute to (a) the electron-electron and (b) the electron-hole correlations. The full lines represent electrons or holes; the Coulomb interaction is represented by broken lines.

(i) *Low-density limit.* As has been pointed out by Schrieffer and Mattis (1965), in the low-density limit the electron-hole correlation can be neglected, because the amplitude of any process in which a hole is involved is proportional to the probability of creation of a hole, and thus to the density of electrons, which is a small quantity $n \ll 1$. Therefore the amplitude of any correlation effect in which electron-hole pairs are involved is negligible compared with processes in which two electrons are interacting. In diagrammatic representation only the electron-electron ladder diagrams shown in figure 5(b) are important. According to Schrieffer and Mattis (1965) these electron-electron correlations can be taken into account by introducing an effective Coulomb interaction $U_{\text{eff}}^{(e-e)}$ which is the sum of a geometric series corresponding to successive electron-electron scatterings. For zero frequency this interaction has the form

$$U_{\text{eff}}^{(e-e)} = \frac{U}{1 + (U/\pi\Delta) \tan^{-1}(\epsilon_d/\Delta)} \quad (3.23)$$

where $\epsilon_d < \Delta$. Furthermore, the condition for the formation of a magnetic moment is

$$U_{\text{eff}}^{(e-e)} \rho_d^{(0)}(0) > 1 \quad (3.24)$$

which is similar to the condition obtained in the HF approximation (see equation (3.13)) except that U is replaced by $U_{\text{eff}}^{(e-e)}$.

Inserting the expression for $\rho_d^{(0)}(0)$ given by equation (3.3), it is easy to see that this condition is never satisfied. Therefore Schrieffer and Mattis concluded that at least in the low-density limit the correlations are of extreme importance, as fluctuations can prevent the system from undergoing a transition to the magnetic limit. For degenerate d levels, however, they have found that although the condition for magnetic transition is weaker than in the HF approximation, the formation of a magnetic moment is still possible, because the exchange interaction tends to align the spins.

(ii) *Symmetrical case.* In this case the position of the localized impurity level is symmetric with respect to the Fermi level, ie $E_{d,\sigma} = \epsilon_d + U/2 = 0$. The problem in

this case is more difficult than in the previous limit, because both channels are of equal importance. In spite of this, a large amount of theoretical work has been based on the supposition that the dominant correlation is the electron-hole one, as the formation of a magnetic moment is the result of this correlation effect. A detailed analysis of these theories is given by Mills *et al* (1973); the present discussion will be restricted solely to the main ideas.

The dominance of the electron-hole correlation was first suggested probably by Suhl (1967), and many details have been worked out by him and his co-workers (Levine and Suhl 1968, More and Suhl 1968, Levine *et al* 1968). Lederer and Mills (1967) presented a similar theory which closely follows their previous work (Mills and Lederer 1966) on nearly magnetic metals, where they describe the dominant electron-hole correlation as a localized paramagnon. Concerning measurable quantities, the most detailed version of this theory, called the localized spin fluctuation (LSF) theory, has been presented by Rivier and Zuckermann (1968) and by Rivier *et al* (1968), and they have even made an attempt to find equivalence between this problem and the Kondo effect.

The mathematical treatment is similar to the theory of Schrieffer and Mattis (1965) discussed previously, but here successive electron-hole scatterings are considered, and thus the electron-hole ladder diagrams are summed up. Here again an effective Coulomb interaction $U_{\text{eff}}^{(\text{e-h})}$ can be introduced as

$$U_{\text{eff}}^{(\text{e-h})} = \frac{U}{1 - U\rho_d^{(0)}(0)}. \quad (3.25)$$

By comparing this formula with equation (3.23) one finds an essential difference, namely in the sign appearing in the denominator. This formula describes an enhancement of the interaction and diverges as the HF instability given by equation (3.13) is approached. A further important consequence of this theory is that at low frequencies ω the dynamical susceptibility of the electrons on the d level $\chi(\omega)$ exhibits a peak which is narrowed due to this enhancement and can be written in the form

$$\chi(\omega) = \frac{1}{\pi} \frac{1}{\omega + i\tau_0^{-1}} \quad (3.26)$$

where τ_0 is the lifetime of the localized spin fluctuations. It contains the enhancement factor $(1 - U\rho_d^{(0)}(0))^{-1}$ as

$$\frac{1}{\tau_0} = \frac{\pi\rho_d^{(0)}(0)}{1 - U\rho_d^{(0)}(0)}. \quad (3.27)$$

The most important consequence of this enhancement is the deformation of the density of states $\rho_d^{(0)}(0)$ in such a way that the second derivative of $\rho_d^{(0)}(0)$ taken at $\omega = 0$ is enhanced by the factor $(1 - U\rho_d^{(0)}(0))^{-1}$; furthermore, the temperature and energy dependence is similar to that of a lorentzian resonance. Using equation (3.6), similar results can also be derived for the imaginary part of the forward scattering amplitude. At low temperature this behaviour leads to an enhanced T^2 temperature dependence, which occurs in several physical quantities. As these predicted temperature dependences and enhancements are in accordance with experiment, the localized spin fluctuation theory is believed by many to be verified experimentally. Although since that time great efforts have been made to clarify whether the electron-hole correlations dominate over the electron-electron correlations,

unfortunately only a few relevant papers have been published. Beal-Monod *et al* (1971) still preferred the paramagnon propagation, but they have concluded that the ladder approximation is not sufficient. Furthermore, Weiner (1971) made an attempt to treat both channels—ie electron-electron and electron-hole correlations—simultaneously without arriving at a definite conclusion.

Realizing the above-mentioned difficulties, Iche and Zawadowski (1972) have recently focused their attention on the symmetry properties of the symmetric Anderson model ($\epsilon_q + U/2 = 0$) instead of performing concrete calculations. In this case the Anderson hamiltonian given by equation (2.3) can be written in the form

$$H = -U/4 + H_U$$

where

$$H_U = \sum_{k,\sigma} \epsilon_k a_{k\sigma}^+ a_{k\sigma} + \sum_{k,\sigma} (V_{kd} a_{k\sigma}^+ a_{d\sigma} + cc) + U(n_{d+} - \frac{1}{2})(n_{d-} - \frac{1}{2}). \quad (3.28)$$

It is easy to show that the hamiltonian H_U exhibits electron-hole symmetry if the conduction electron band is symmetric with respect to the Fermi level. According to Iche and Zawadowski (1972), one can perform an electron-hole transformation for one spin direction without any change in the Hilbert space of the other spin direction, and then the hamiltonian is invariant under this transformation if one changes simultaneously the sign of the Coulomb interaction as well. This means that if repulsion acts between two electrons then the electron-hole interaction is similar but attractive. This symmetry provides us with several identities (eg $\langle H_U \rangle = \langle H_{-U} \rangle$); thus disregarding the term $-U/4$ the ground state energy is an even function of U , as has been previously shown by Yosida and Yamada (1971) using time-dependent Green functions. A similar result follows for the self-energy. Generally, one can connect the electron-electron and electron-hole correlation functions by the exact identity

$$\langle a_{d\sigma}(t) a_{d-\sigma}(t) a_{d-\sigma}^+(t') a_{d\sigma}^+(t') \rangle_U = \langle a_{d\sigma}^+(t) a_{d-\sigma}(t) a_{d-\sigma}^+(t') a_{d\sigma}(t') \rangle_{-U} \quad (3.29)$$

where the subscripts U and $-U$ refer to the sign of U in the hamiltonian occurring in the thermodynamical average. This identity obviously shows that the two different correlations have the same amplitude in any order of perturbation theory; there is only a difference in sign in odd orders. As a special case this shows that the two unrenormalized (with respect to U) correlation functions have the same analytical form. In this way it has been generally proved that a correct theoretical answer can be expected on the basis of such theory only where the electron-electron and electron-hole correlations are treated on an equal footing. The diagrams where the two channels are mixed together are the so-called ‘parquet diagrams’, whose calculation seems to be a very difficult task. Finally, it must be mentioned that the symmetry consideration discussed above cannot be generalized to the case of orbital degeneracy with exchange interaction.

Recently the symmetrical Anderson model has been the subject of investigations using the scaling idea in two different ways. Hertz (1971) has worked with the functional integral method applied to the Anderson model by Wang *et al* (1969), and Iche (1973) has turned to the renormalization group technique. These methods will be discussed in § 6; here we refer only to some important results. In the first method the fluctuations of high frequencies, and in the second method the scattering processes with higher energies have been eliminated by introducing a new, effective coupling constant U_{eff} . Using the renormalization group technique in the

first approximation—which is equivalent to considering the ‘parquet diagrams’ only—it has been found that $U_{\text{eff}} = U$, while in the second approximation—going just beyond the ‘parquet diagrams’— $U_{\text{eff}} \leq U$ has been obtained, in agreement with the functional integral method. It is worth mentioning that considering the localized paramagnons only, by neglecting the electron–electron correlations, the renormalization group method reproduces the expression for U_{eff} given by equation (3.25), with the enhancement factor $(1 - U\rho_d^{(0)}(0))^{-1}$. In this way it is shown that the more accurate theories do not yield an enhancement of this type; thus the localized paramagnon picture with such an enhancement is not realistic at all.

Finally we mention the recent works by Menyhárd (1972, 1973), who has made an attempt to re-investigate the question of dominant diagrams. She has calculated the ground state energy and the static susceptibility up to fourth and third orders respectively, using a time-ordered diagram technique developed by Yosida and Yamada (1971). The conclusion was that in a given order in U the contribution of all the diagrams is of the same order of magnitude. Furthermore, the ground state energy E_g and the static susceptibility χ were compared with the expressions obtained considering electron–hole correlations only. The results

$$E_g = -\frac{U}{4} + \left[-0.11\left(\frac{U}{\pi\Delta}\right)^2 + 0.006\left(\frac{U}{\pi\Delta}\right)^4 + \dots \right]\Delta \quad (3.30)$$

and

$$\chi = \frac{\mu_B^2}{2\pi\Delta} \left[1 + \frac{U}{\pi\Delta} + 0.54\left(\frac{U}{\pi\Delta}\right)^2 + 0.21\left(\frac{U}{\pi\Delta}\right)^3 + \dots \right] \quad (3.31)$$

are in strong disagreement with those obtained by considering the electron–hole correlations only:

$$E_g^{\text{LSF}} = -\frac{U}{4} + \left[-0.11\left(\frac{U}{\pi\Delta}\right)^2 - 0.048\left(\frac{U}{\pi\Delta}\right)^4 + \dots \right]\Delta \quad (3.32)$$

and

$$\chi^{\text{LSF}} = \frac{\mu_B^2}{2\pi\Delta} \frac{1}{1 - U/\pi\Delta} = \frac{\mu_B^2}{2\pi\Delta} \left[1 + \frac{U}{\pi\Delta} + \left(\frac{U}{\pi\Delta}\right)^2 + \left(\frac{U}{\pi\Delta}\right)^3 + \dots \right]. \quad (3.33)$$

It is evident that the LSF theory overestimates the amplitudes of the third- and fourth-order terms by factors of about 5 and 6 respectively. It is interesting to note that the obtained static susceptibility is in fairly good agreement with the exponential form†

$$\chi \sim \frac{1}{\pi\Delta} \exp\left(\frac{U}{\pi\Delta}\right)$$

surprisingly derived by Iche (1973) in his first parquet approximation. The reason for this surprisingly good agreement should be the subject of further investigations.

A comparison of the results given by equations (3.30)–(3.33) confirms our previous conclusions that the enhancement factor appearing in expression (3.25) for the effective Coulomb interaction is not relevant in the behaviour of measurable quantities, and that the concept of localized spin fluctuation is not well established.

† This expression reminds one of the form of the inverse Kondo temperature derived in the opposite limit, $U/\pi\Delta \gg 1$, by using the Schrieffer–Wolff transformation (see § 4.8), but Iche’s expression is inversely proportional to Δ instead of the conduction electron band width. The similar analytical form supports the idea which will be discussed in the following section that the physical quantities should be expressed by formulae analytical in the coupling U .

3.4. Correlation effects in the magnetic limit

The starting point of the previous treatment was to consider first the s-d mixing and then to apply perturbation theory for the intra-atomic Coulomb repulsion U assuming that $U \ll \Delta$. This approach is not appropriate if the impurity has a well-established magnetic moment. In the case of a magnetic impurity, the Coulomb term U should first be considered in order to produce the splitting of the impurity levels, and afterwards the effect of the mixing term can be treated as perturbation. This schema works if $U/\pi\Delta \gg 1$; thus the overlap of the split impurity level is very small. This problem has been worked out in great detail, and the results obtained are related to those provided by the s-d model; therefore here we refer to §4 which deals with this problem. The connection between the results of this perturbation procedure and of the s-d model is established by the Schrieffer-Wolff transformation (Schrieffer and Wolff 1966, see §4.8).

The typical feature of these results is the appearance of a logarithmic term which looks like

$$\ln \frac{kT}{D \exp(\pi\epsilon_d/\Delta)}$$

in the limit $U \rightarrow \infty$, where D is the width of the conduction band. This logarithmic expression characterizes the Kondo effect and will be discussed in detail in §4.

3.5. General results in the Anderson model at zero temperature

This section is devoted to a series of such arguments and results as seem to be valid generally, and some of them are even exact. These results are of great importance in understanding the behaviour of magnetic impurities at zero temperature, even if some of them have attracted relatively moderate attention until now.

(i) *Analyticity in coupling strength.* By changing the coupling constant U , a sharp transition occurs in the HF approximation between the non-magnetic and magnetic regimes. In the Schrieffer and Mattis (1965) theory it is pointed out that the transition from the non-magnetic to the magnetic state is completely smooth, at least in the low-density case investigated. Later Suhl (1967) and several other authors argued in the following way. If one considers a phase transition in a system with dimension lower than three, a sharp transition does not occur because of the strong fluctuations. Studying the dependence on the coupling strength U , one may adopt this idea, concluding that the change in the behaviour of a single impurity must be smooth and analytical even in the region where in lower approximations (as in HF) a sharp transition takes place.

(ii) *Dominance of the non-spin-flip scattering channel in the vicinity of the Fermi level.* As has been previously discussed in §3.2, the dynamical part of the impurity problem is localized on the impurity level. Schrieffer and Mattis (1965) have pointed out that this problem is identical with a problem where there is an interacting electron gas with lorentzian density of states given by equation (3.3) and Coulomb interaction between electrons with opposite spins, but momentum conservation is not required.

This can be checked by looking at the rules of diagram technique. Not much later, Langreth (1966) exploited this idea in many respects, pointing out that the most useful consequence of this equivalence is the fact that in the vicinity of the

Fermi level a many-body system behaves like a free-electron gas. This reflects the fact that any kind of decay of a single excitation into a state containing several (eg n) excitations tends to zero as E^{n-1} as the energy E approaches the Fermi level, because the phase space is strongly reduced as the number of excitations increases in the final state.

In order to put this conclusion in a mathematical form we should consider the one-electron Green function which has the general form

$$G_{d,\sigma}(\omega) = \frac{1}{\omega - \epsilon_d - \Sigma_d(\omega) + i\Delta} \quad (3.34)$$

where the effect of the ‘many-body correlations’ due to the Coulomb interaction is represented by the self-energy $\Sigma_d(\omega)$.

Neglecting Σ_d this formula reduces to equation (3.2). According to the general theorem discussed above, $\text{Im } \Sigma_d(\omega)$ representing the decay processes vanishes at the Fermi level, ie

$$\text{Im } \Sigma_d(\omega = 0) = 0 \quad (3.35)$$

which can be proved in arbitrary order of perturbation theory (Luttinger 1960).

(iii) *The scattering amplitude at the Fermi level can be expressed in terms of phase shifts at $T = 0$.* The results derived in (ii) and given by equations (3.34) and (3.35) can be inserted into expression (3.5) for the scattering amplitude, and then one obtains

$$\begin{aligned} t_{kk',\sigma}(\omega = 0 + i\delta) &= V_{kd} \frac{1}{\omega - \epsilon_d - \text{Re } \Sigma_{d,\sigma}(\omega) + i\Delta} V_{dk'} \\ &= \frac{1}{\pi \rho_0} \frac{\Delta}{\omega - (\epsilon_d + \text{Re } \Sigma_{d,\sigma}(\omega = 0)) + i\Delta}. \end{aligned} \quad (3.36)$$

It is easily seen that the conduction electron scattering amplitude can be given in terms of a single phase shift at the Fermi level if one compares our recent result (3.36) with that in the HF approximation which was obtained by inserting equation (3.2) into the form of $t_{kk'}$ given by equation (3.5); then the two forms are identical if $E_{d,\sigma}$ is replaced by $\epsilon_d + \text{Re } \Sigma_{d,\sigma}(\omega = 0)$. Thus the scattering amplitude can be expressed in terms of a single phase shift as in the HF approximation (see equation (3.17)):

$$\delta_\sigma(\omega = 0) = \cot^{-1} \left(\frac{\epsilon_d + \text{Re } \Sigma_{d,\sigma}(\omega = 0)}{\Delta} \right). \quad (3.37)$$

This means that the elastic non-spin-flip scattering channel being the only one which is open at the Fermi level at $T = 0$, the scattering can be characterized by a phase shift.

(iv) *Friedel sum rule at $T = 0$.* After deriving the results listed in (ii) and (iii), Langreth (1966) has given a general rigorous derivation of the Friedel sum rule. The general form of the sum rule, assuming that the scattering can be described in terms of phase shifts, expresses the total number N of extra electrons associated with the impurity in terms of phase shifts as

$$N = (1/\pi) \sum_{lm\sigma} \delta_{lm\sigma}(\omega = 0) \quad (3.38)$$

where $\delta_{lm\sigma}$ is the phase shift in the angular momentum channel l with azimuthal quantum number m and spin σ . In a different way Anderson and McMillan (1967) have found another exact derivation for the sum rule; furthermore, Langer and Ambegaokar (1961) have concluded that the electron-electron interaction in the conduction band cannot affect the sum rule.

In the following we will assume that only the channel with $l = 2$ contributes to the sum rule, and the other phase shifts can be neglected.

(v) *At $T = 0$ the phase shifts are independent of m and σ in the dominant scattering channel $l = 2$.* Supposing that no external field is applied and making use of (i), saying that the Coulomb interaction can be continuously switched on, one can conclude that the ground state must be rotationally invariant (singlet), because for $U = 0$ the non-magnetic state is rotationally invariant. In the case of a singlet state the phase shifts in each angular momentum channel are equal; thus they depend only on l , but are independent of m and σ . Mattis (1967) and Schrieffer and Mattis (1965) have made several attempts to prove that the ground state is indeed singlet, ie rotationally invariant, and they succeeded in making it at least very plausible. Furthermore, Anderson (1967b) argued that a ground state for the impurity must be built up from a linear combination of different states in order to assure the rotational invariance. Finally, the experimental facts to be discussed later show that the magnetic moment associated with the impurity disappears at zero temperature; thus the ground state is indeed singlet.

(vi) *If the scattering channel with $l = 2$ dominates then $\delta_{l=2} = \pi N/10$ at $T = 0$.* Assuming that at zero temperature the impurity charge is screened completely and in the case of impurities of d type only the channel with $l = 2$ contributes essentially to the Friedel sum rule given by equation (3.38), one obtains for the phase shifts

$$\delta_l = \begin{cases} \pi N/10, & l = 2 \\ 0, & l \neq 2 \end{cases} \quad (3.39)$$

which can be referred to as a consequence of ‘charge neutrality’.

The ‘charge neutrality’ implies a series of predictions for those measurable quantities which at $T = 0$ can be expressed by the value of the scattering amplitude taken at the Fermi level.

By inserting the phase shift given by equation (3.39) into formulae (3.16) and (3.8) of the scattering amplitude, one obtains

$$t_{kk}(\omega = 0 + i\delta) = t_{l=2}(\omega = 0 + i\delta) = \frac{5}{\pi\rho_0} \left[\exp\left(i\frac{\pi N}{10}\right) \sin\left(\frac{\pi N}{10}\right) \right]. \quad (3.40)$$

According to equation (3.22) the zero-temperature resistivity can be obtained as a function of N as

$$R(T = 0) \sim \frac{5}{\pi\rho_0} \sin^2\left(\frac{\pi N}{10}\right). \quad (3.41)$$

Deviations from this formula can be expected if the contributions of the other scattering channels are not negligible. This result does not depend on whether the system behaves as magnetic or non-magnetic in the HF approximation, as has been pointed out by Grüner and Zawadowski (1972). For non-magnetic impurities in the HF sense this formula has been accepted for a long time (see eg Schrieffer 1967);

however, for magnetic impurities there is some confusion in the literature. Thus Schrieffer (1967) has studied the magnetic case with a crystal field splitting of the d levels larger than their width Δ , and has drawn the conclusion that the phase shifts can be different for different orbitals in the same angular momentum channel, in contrast to (v). The width of the d level, however, is so large that the crystalline splitting can be neglected; therefore Schrieffer's argument is not relevant to 3d impurities, but it can be applied to 4f impurities.

3.6. Hartree-Fock picture versus singlet ground state at $T = 0$.

In this section we argue along two different lines using the HF approximation and the assumption of a singlet ground state. The results of the two approaches are essentially different in the magnetic limit.

At high temperatures the many-body correlation effects are not strong enough to result in an essential modification of the HF results. In the HF theory if the total density of states for the localized electrons is split, exhibiting two fairly well-separated peaks, then the conduction electron scattering is described with two different phase shifts δ_σ and $\delta_{-\sigma}$.

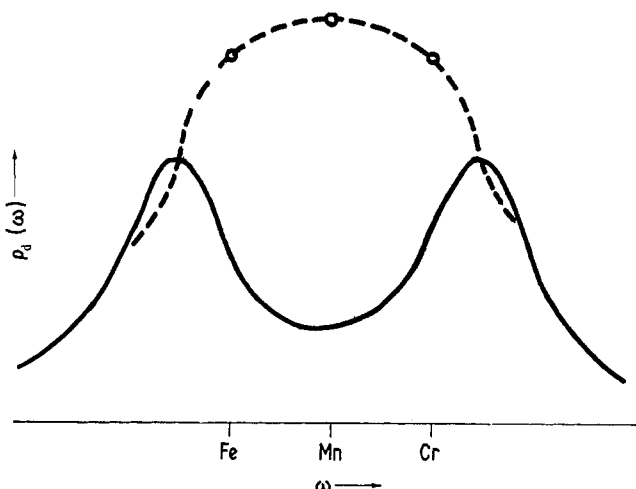


Figure 6. The HF density of states as a function of energy for a magnetic case. The density of states at the Fermi level as predicted by charge neutrality (circles) is shown for Fe, Mn and Cr impurities.

Thus in the absence of an external magnetic field the magnetic moment of the impurity orbital can be directed parallel or antiparallel to the spin of the incoming electron, and the two different phase shifts correspond to these possibilities. Therefore in conduction electron scattering there is not a uniquely defined phase shift, but rather there is a choice between δ_σ and $\delta_{-\sigma}$ with the same probability. On the other hand, at zero temperature there is a well-defined single phase shift $\delta = \pi N/10$ which is formed as a consequence of many-body correlation effects; thus $\delta = \frac{1}{2}(\delta_\sigma + \delta_{-\sigma})$.

The shape of the total density of states is represented in figure 6 in a schematic way. The Fermi levels are given for Cr, Mn and Fe impurities, and for all three

cases it can be found between the two peaks. Furthermore, using the result of the charge neutrality limit by making use of equations (3.40), (3.6) and finally (3.1), one obtains for the density of states at the Fermi level

$$\rho_d(0) = \frac{1}{\pi\Delta} \sin^2 \left(\frac{\pi N}{10} \right). \quad (3.42)$$

$\rho_d(0)$ is plotted in figure 6 as circles for different impurities with $N = 4, 5$ and 6 for Cr, Mn and Fe respectively. These are far from the density of states predicted on the basis of the HF theory, and the question to be answered is how the total density of states obtained from the HF approximation should be modified at low temperature to reach the predicted 'charge neutrality' values at E_F for $T = 0$.

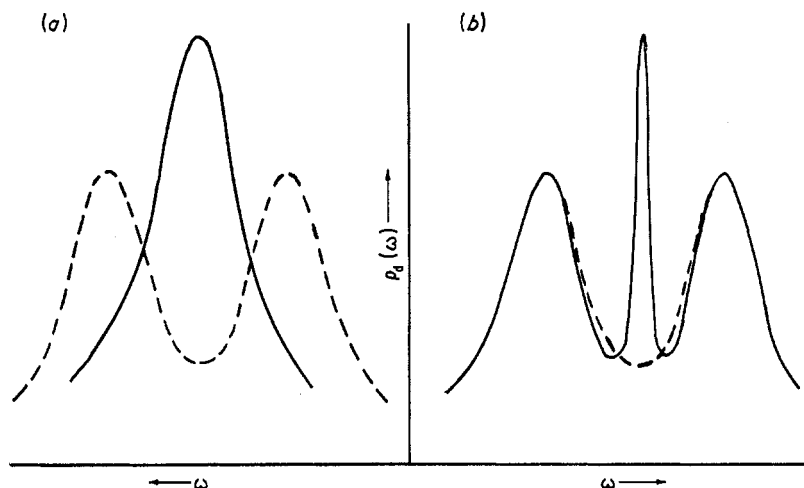


Figure 7. The two possible modifications of the HF density of states for $T = 0$ which satisfy the charge neutrality condition.

In principle there are two possible ways of resolving this problem (see Grüner and Zawadowski 1972).

(i) At low temperatures the density of states changes in such a way that at $T = 0$ the total density of states is going to exhibit a single maximum corresponding to the non-magnetic HF solution shown in figure 7(a). This would mean a large re-ordering of the density of states with an energy scale comparable with U and Δ (ie on a scale of the order of 1 eV, which is associated with 10^4 K), and therefore no drastic effect can be expected in the temperature range available in experiments.

(ii) At low temperatures an additional peak appears due to correlation effects superimposed on the HF density of states. The width of this resonance is relatively narrow on the HF scale and is formed at the Fermi level, as shown in figure 7(b). The maximum of this narrow peak is determined by the 'charge neutrality' condition. Recalling the relation between density of states and scattering amplitude given by equation (3.6), one can speak of a narrow resonance formed at the Fermi level. As will be discussed later, this narrow resonance is very probably connected with the Kondo effect discussed in § 4, and in that case the resonance is referred to as Abrikosov-Suhl resonance.

4. Kondo effect and s-d model

The most striking discovery in the subject was made by Kondo in 1964, who realized that, by calculating the conduction electron scattering amplitude of a conduction electron scattered by an impurity spin in the s-d model, the result diverges at the Fermi level as $\ln(\omega/D)$ in third order of perturbation theory, where ω is the energy of the conduction electron and D is the width of the conduction band. According to this calculation the impurity resistivity due to a magnetic impurity must increase with decreasing temperature, as it has been observed to do for many years (see eg van den Berg 1964). This result has suggested that some kind of resonance is formed at the Fermi level which cannot be described by applying a simple perturbation method at zero temperature.

The formation of this resonance might resolve the question raised at the end of the previous section about the behaviour of the density of states for magnetic impurities at $T = 0$.

4.1. s-d model

This simple model, usually referred to as the s-d exchange model, is based on the supposition that if a magnetic moment is formed at the impurity then the moment can be described as a quantum mechanical spin with quantized total angular momentum $[S(S+1)]^{1/2}$, where $S = \frac{1}{2}, 1, \frac{3}{2}, \dots$. In the present case this spin is embedded in a simple metal, and an effective exchange interaction couples the conduction electron and impurity spins. Similar models have previously been applied to different problems. The basic idea of the model goes back to Zener (1951), who assumed that in ferromagnets the s electrons from the conduction band and the d levels are localized at the atomic sites; the s and d electrons interact by exchange interaction. A similar model has been proposed by Fröhlich and Nabarro (1940) for the exchange interaction between nuclear moments and the conduction electron spins in a metal. Later Rudermann and Kittel (1954) applied this model to describe the interaction of two nuclear spins through the conduction band. Similar calculations have also been performed by Kasuya (1956) and Yosida (1957) in the s-d model.

The derivation of the model was given by Kasuya (1956). The s-d hamiltonian can be written as

$$H = H_0 + H_1 \quad (4.1)$$

where

$$H_0 = \sum_{k,\alpha} \epsilon_k a_{k\alpha}^+ a_{k\alpha}, \quad \alpha = \pm \frac{1}{2} \quad (4.2)$$

and

$$H_1 = - \sum_{k,k',\alpha,\alpha'} (J_{kk'}/N) \mathbf{S}(a_{k'\alpha'}^+ \boldsymbol{\sigma}_{\alpha'\alpha} a_{k\alpha}). \quad (4.3)$$

ϵ_k is the energy of the conduction electron with momentum k and spin α . The electrons are described in terms of creation and annihilation operators $a_{k\alpha}^+$ and $a_{k\alpha}$. The second term H_1 contains the effective exchange integral $J_{kk'}/N$; \mathbf{S} is the impurity spin operator and $\boldsymbol{\sigma}$ is the Pauli operator for conduction electron spins. The notation $J_{kk'}/N$ was introduced by Kasuya (1956), who considered the exchange integral between a Wannier function of the conduction band and the localized d orbital. N is the number of elementary cells in unit volume, and it enters into the calculation as a normalization factor for the Bloch wavefunction expressed as

Wannier functions. Although the atomic integrals result in a positive coupling, J may be negative due to some effective interaction to be discussed in §4.8 (Schrieffer-Wolff transformation).

The spin product in the hamiltonian H_1 can be written in a more detailed form as

$$H_1 = -(J/N) \sum_{k,k'} [S^z(a_{k'\uparrow}^+ a_{k\uparrow} - a_{k'\downarrow} a_{k\downarrow}) + S^+ a_{k'\downarrow}^+ a_{k\uparrow} + S^- a_{k'\uparrow}^+ a_{k\downarrow}] \quad (4.4)$$

where the first term is the diagonal part of the interaction, and the second and third terms correspond to spin-flip scattering. The operators S^+ and S^- raise and lower respectively the z component of the impurity spin.

Generally the exchange integral $J_{kk'}$ depends on the momenta k and k' and on the angle between them. The usual assumption is that $J_{kk'}$ does not depend essentially on k and k' and can be taken as constant. This restriction is not serious, because if $J_{kk'}$ acts only in some part of the conduction band then the momentum dependence can be formally eliminated by modifying the density of states of the conduction band, ie taking a non-vanishing of states only in that range where the interaction is effective. The angular dependence is usually disregarded as well, because it does not affect the final results in most cases.

Supposing that the d level has the symmetry $l = 2$, one can find the angular dependence

$$J_{kk'} = J_{l=2} P_{l=2}(\cos \gamma_{kk'}) \quad (4.5)$$

where P_l is the Legendre polynomial and $\gamma_{kk'}$ is the angle between k and k' .

One can assume that in addition to the s-d term the impurity represents also a static potential, and this interaction is then given by the hamiltonian

$$H_V = \sum_{k,k',\alpha} \frac{V_{kk'}}{N} a_{k'\alpha}^+ a_{k\alpha} \quad (4.6)$$

where $V_{kk'}$ is the matrix element of the potential.

4.2. Kondo effect in third order of perturbation theory

The first physical quantity calculated beyond the first Born approximation by using the s-d model was the electrical resistivity. In this section we briefly represent the calculation of the electrical resistivity in the first and second Born approximations. It is assumed that the contribution of the impurities to the electrical resistivity is additive, ie impurity-impurity interaction is negligible. In this case the inverse lifetime of the conduction electrons is proportional to the concentration of the impurities.

The calculation in the first Born approximation was carried out by Kasuya (1956) and Yosida (1957).

The probability of spin-conserving scattering can be obtained by using the 'golden rule', and the first part of the hamiltonian given by equation (4.4) yields

$$W(\uparrow M_z \rightarrow \uparrow M_z) = 2\pi(J/N)^2 M_z^2 \rho_0 \quad (4.7)$$

where ρ_0 is the density of states in the conduction band near the Fermi level, and M_z is the z component of the impurity spin. By averaging over the spin direction, a factor $S(S+1)/3$ is obtained instead of M_z^2 .

The contribution from the spin-flip terms can be obtained in a similar way:

$$W(\uparrow M_z \rightarrow \downarrow M_z + 1) = 2\pi(J/N)^2 [S(S+1) - M_z(M_z+1)] \rho_0 \quad (4.8)$$

and

$$W(\downarrow M_z \rightarrow \uparrow M_z - 1) = 2\pi(J/N)^2 [S(S+1) - M_z(M_z-1)] \rho_0. \quad (4.9)$$

The lifetime of a spin-up electron (for example) is obtained by adding equations (4.8) and (4.9) together and by averaging over the z component of the impurity spin M_z . Thus the transition probability

$$W = 2\pi c(J/N)^2 S(S+1) \rho_0 \quad (4.10)$$

where c is the concentration of the impurities.

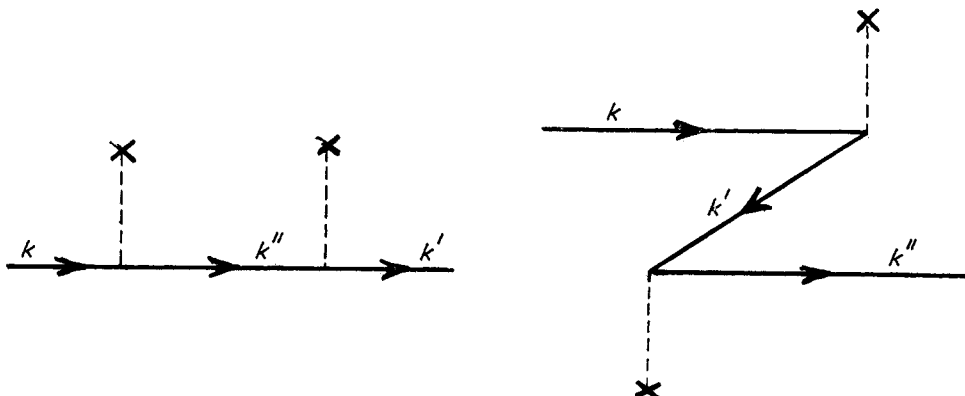


Figure 8. Two time-ordered diagrams corresponding to the conduction electron scattering amplitude in second order of perturbation theory. The full lines represent electrons or holes; the broken lines with a cross at the end represent the exchange interaction.

Kondo (1964) performed this calculation in the next order of perturbation theory. The conduction electron scattering amplitude can be calculated in second order by writing the formula

$$H_1 \frac{1}{\epsilon_k - H_0} H_1 \quad (4.11)$$

where ϵ_k is the energy of the electron in the initial state. The scattering amplitude obtained in this way describes two successive scattering processes. As far as the intermediate state is concerned there are two possibilities:

(i) First the electron with momentum k is scattered from the initial state into the intermediate state with momentum k'' , and then this electron with k'' is scattered into the final state with k' .

(ii) In the first scattering process an electron-hole pair is created by the spin of the impurity, and in the second process the created hole annihilates the electron with momentum k leaving the created electron in the final state.

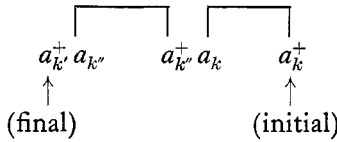
These processes are represented by diagrams in figures 8(a) and (b) respectively. The scattering amplitude for an electron with momentum k is expressed by the following two formulae corresponding to the two diagrams in figure 8:

$$\left(-\frac{J}{N}\right)^2 [S(S+1) - \sigma S] \sum_{k''} \frac{1 - n_{k''}}{\epsilon_k - \epsilon_{k''}} \quad (4.12)$$

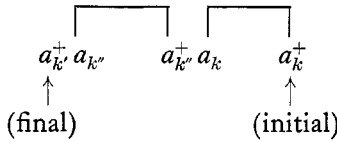
and

$$-\left(-\frac{J}{N}\right)^2 [S(S+1) + \sigma S] \sum_{k'} \frac{n_{k''}}{\epsilon_k - (\epsilon_k - \epsilon_{k''} + \epsilon_{k'})} \quad (4.13)$$

where the following pairing of the electron operators are considered:

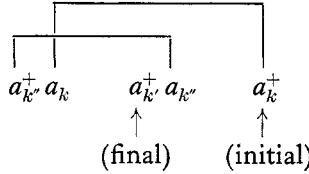


(final)

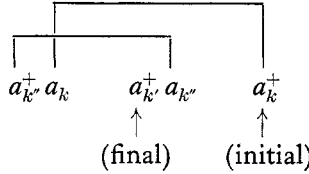


(initial)

and



(final)



(initial)

The second expression has a minus sign due to the fermion character of the operators. The occupation number $n_{k''}$ takes care of the Pauli exclusion in the intermediate state.

By adding these two expressions two different integrals are obtained:

$$\sum_{k''} \frac{1}{\epsilon - \epsilon_{k''}} \approx \int d\epsilon_{k''} \frac{1}{\epsilon - \epsilon_{k''}} \rho_0(\epsilon_{k''}) \quad (4.14)$$

and

$$g(\epsilon) = \sum_{k''} \frac{n_{k''}}{\epsilon - \epsilon_{k''}} \approx \int d\epsilon_{k''} \frac{n_{k''}}{\epsilon - \epsilon_{k''}} \rho_0(\epsilon_{k''}) \quad (4.15)$$

where $\rho_0(\epsilon_{k''})$ is the density of conduction electrons, and $\epsilon = \epsilon_k = \epsilon_{k'}$ due to energy conservation.

The first integral is small, and in the case of a symmetric half-filled conduction band it goes to zero as $\epsilon \rightarrow 0$. The second integral diverges, however, at $T = 0$ as $\epsilon \rightarrow 0$. In order to perform this integral we take a simple form of $\rho_0(\epsilon)$:

$$\rho_0(\epsilon) = \begin{cases} \rho_0, & \text{if } -D < \epsilon < D \\ 0, & \text{otherwise.} \end{cases} \quad (4.16)$$

The integral (4.15) can then be calculated for $T = 0$ and

$$g(\epsilon) = -\rho_0 \ln \left(\frac{|\epsilon|}{(D^2 - \epsilon^2)^{1/2}} \right) \approx -\rho_0 \ln \left(\frac{|\epsilon|}{D} \right) \quad (4.17)$$

for $|\epsilon| \ll D$. Its temperature dependence can be approximated in a similar way for $\epsilon = 0$, and one obtains

$$-\rho_0 \ln \left(\frac{kT}{D} \right) + \text{const.} \quad (4.18)$$

In this way the inverse relaxation time τ^{-1} can be calculated using equations (4.12), (4.13) and (4.18), and

$$\frac{1}{\tau} \approx 2\pi\rho_0 c \left(\frac{J}{N} \right)^2 S(S+1) \left[1 + \frac{4J}{N} \rho_0 \ln \left(\frac{kT}{D} \right) \right]. \quad (4.19)$$

This formula shows remarkable features: (i) for an antiferromagnetic coupling the inverse relaxation time, and therefore the resistivity, decreases with increasing

temperature; (ii) at low temperatures the logarithmic expression dominates, and it diverges at $T = 0$. The occurrence of this divergence indicates that at low temperatures one should calculate further terms of the perturbation series because the first correction is not small.

It is important to compare this calculation of Kondo with a similar calculation for simple potential scattering. In the latter case spin factors do not occur and in the sum of expressions corresponding to (4.12) and (4.13) the occupation number disappears; thus the logarithmic anomaly is specific to magnetic impurities. This is because the potential scattering is a typical one-body problem, in contrast to the scattering on a magnetic impurity which shows many-body character.

4.3. Kondo effect in leading logarithmic orders

As we have seen in the previous section the first correction to the scattering amplitude is of the order of $(J/N)\rho_0 \ln(|\epsilon|/D)$ or $(J/N)\rho_0 \ln(kT/D)$ for $D \gg |\epsilon| \gg kT$ and $D \gg kT \gg |\epsilon|$ respectively. These logarithmic terms can be so large that $(J/N)\rho_0 \ln()$ is not a small correction even for $|(J/N)\rho_0| \ll 1$. The terms in the perturbation expansion can be classified according to the following schema:

$$\begin{aligned} & \left(\frac{J}{N}\rho_0\right)^p \ln^0(), \\ & \left(\frac{J}{N}\rho_0\right)^{p+1} \ln(), \quad \left(\frac{J}{N}\rho_0\right)^{p+1} \ln^0(), \\ & \left(\frac{J}{N}\rho_0\right)^{p+2} \ln^2(), \quad \left(\frac{J}{N}\rho_0\right)^{p+2} \ln(), \quad \left(\frac{J}{N}\rho_0\right)^{p+2} \ln^0(), \\ & \vdots \\ & \left(\frac{J}{N}\rho_0\right)^n \ln^{n-p}(), \quad \left(\frac{J}{N}\rho_0\right)^n \ln^{n-p-1}(), \quad \dots, \quad \left(\frac{J}{N}\rho_0\right)^n \ln^0(). \end{aligned} \quad (4.20)$$

Let us consider some quantity in perturbation theory, and denote the lowest non-vanishing order by p , eg $p = 1$ for the scattering amplitude and $p = 2$ for the resistivity. Thus in n th order the highest power of the logarithm is $n - p$. According to Landau's school, the approximation in which we keep only those terms which are in the first column is called the 'logarithmic approximation'. The terms in the second column will be referred to as 'next to leading logarithmic terms'.

We notice by looking at the integral $g(\epsilon)$ given by equation (4.17) that (i) the shape of the density of states $\rho(\epsilon)$ does not affect the leading logarithmic terms, only the next to leading logarithmic terms, and (ii) adding a small imaginary part in the denominator of equations (4.14) and (4.15) results in imaginary terms belonging to the next to leading logarithmic order.

In this section we briefly review the results obtained in the logarithmic approximation. One can derive these results in a straightforward perturbation expansion up to a given order, and many of these results can be found in Kondo's (1969) review article.

In order to carry out these approximations in a more systematic way one should apply diagrammatic representation. Without further manipulation, however, the interaction of conduction electrons with an impurity spin cannot be represented by diagrams in the way appropriate to potential scattering. This is due to the fact that

the spin is a dynamical variable rather than a static potential. The different states of the spin, however, can be represented by some fictitious particles, eg fermions, and so one arrives at the different drone fermion techniques. The most widely applied method is the so-called Abrikosov pseudofermion representation (Abrikosov 1965). This method has an equivalent form where the spin is represented by a particle with heavy mass (Brenig and Götze 1968). There are a large number of other representations (eg Spencer and Doniach 1968) which will not be discussed here.

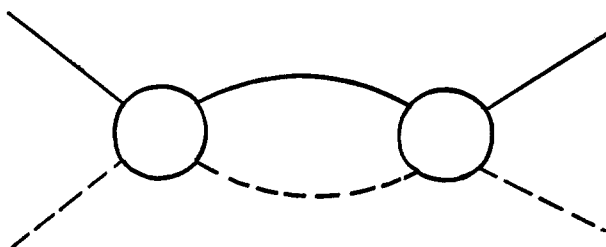


Figure 9. General form of the conduction electron-impurity spin vertex function with one electron or hole excitation in the intermediate state. The full line represents electrons; the broken line represents pseudofermions; and the circle is the vertex.

Let us recall the idea of the Abrikosov representation. $2S+1$ pseudofermions are introduced corresponding to the $2S+1$ states of the impurity spin with z component $M_z = S, S-1, \dots, -S$. The pseudofermions are considered as quantum particles described by creation and annihilation operators $a_{M_z}^\dagger$ and a_{M_z} . An arbitrary spin operator is mapped to the pseudofermion space according to the relations

$$S \rightarrow \sum_{M_z, M_z'} a_{M_z}^\dagger \langle M_z' | S | M_z \rangle a_{M_z} \quad (4.21)$$

where the angle brackets represent the spin matrix elements. The only difficulty remaining is that the real spin states are represented by pseudofermion states with single occupation; thus those elements of Hilbert space where more than one pseudofermion state is occupied have no meaning. These states can be eliminated by assuming that the pseudofermions have a large energy $\lambda \gg kT$; furthermore, one can notice that the vacuum state with zero occupation gives no contribution in an actual calculation. In that way all of the results must be normalized to the probability of single occupation $(2S+1) \exp(-\lambda/kT)$ with $\lambda \rightarrow \infty$.[†] Usually in diagrams the full lines represent electrons and the broken lines pseudofermions. It is interesting to note that due to single occupation the interaction vertices are time-ordered along the pseudofermion line. Therefore this representation can be simply formulated using time-ordered diagrams as well (Brenig and Götze 1968).

Abrikosov (1965) has pointed out that only those diagrams contribute to the leading logarithmic approximation which by cutting simultaneously one electron and one pseudofermion line fall into two distinct parts, and after such successive cuts the elementary vertices are recovered. Therefore in the logarithmic approximation the electron-pseudofermion scattering amplitude must have the structure shown in figure 9, where the diagram falls into two pieces by cutting one electron

[†] This normalization has recently been proved by Sólyom, Tüttö and Zawadowski to be generally correct; thus the correction term in the previous work by Zawadowski and Fazekas (1969) is incorrect.

and one pseudofermion line. This means that only those processes are considered where there is only one excited particle (electron or hole) in the intermediate state. The diagrams of this type are shown in the two lowest orders in figure 10. As can be shown, all the other diagrams contribute to lower powers of the logarithmic term. This class of diagrams is called ‘parquet’ diagrams according to the Russian school, and they are calculated with logarithmic accuracy. This method has been worked out by Landau’s school in great detail, and the best description of the method is given by Nozières and his co-workers (Roulet *et al* 1969, Nozières *et al* 1969).

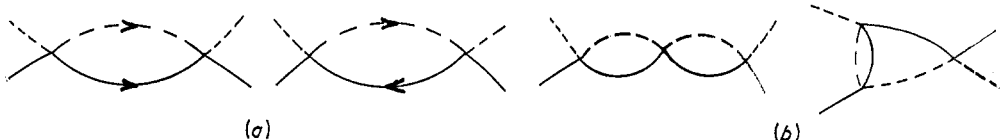


Figure 10. (a) The first-order corrections to the vertex. (b) The second-order corrections to the vertex (the directions of the lines are not indicated).

The general form of the conduction electron scattering amplitude with one electron or hole in the initial and final states can be written as

$$T_{M_z \alpha', M_z \alpha}(\epsilon) = t(\epsilon) \delta_{M_z M_z'} \delta_{\alpha \alpha'} + \tau(\epsilon) \langle M_z' | S | M_z \rangle \sigma_{\alpha' \alpha} \quad (4.22)$$

where the energies of the particles in the initial and final states are on the energy shell, and the spin variables are α , M_z in the initial state and α' , M_z' in the final state.

The real part of the scattering amplitude for $\epsilon = 0$ was obtained by Abrikosov (1965) as

$$\tau(\epsilon = 0) = \frac{J/N}{1 - 2(J/N) \rho_0 \ln(kT/D)}. \quad (4.23)$$

This term contributes to the leading logarithmic approximations, and thus to $p = 1$. The imaginary part of the spin-conserving part of the scattering amplitude is

$$\text{Im } t(\epsilon = 0) = \frac{S(S+1)(J/N)^2 \rho_0}{[1 - 2(J/N) \rho_0 \ln(kT/D)]^2}. \quad (4.24)$$

The resistivity $R(T)$ is proportional to $\text{Im } t(\epsilon = 0)$: see the optical theorem given by equation (3.22); thus its temperature dependence is

$$R(T) \sim \frac{S(S+1)(J/N)^2}{[1 - 2(J/N) \rho_0 \ln(kT/D)]^2}. \quad (4.25)$$

In a similar way the susceptibility has been calculated by several authors (see references in Kondo’s review of 1969) up to a given order. The susceptibility localized on the impurity site is given in this approximation as

$$\lim_{H \rightarrow 0} \mu \frac{\langle S^z \rangle}{H} = \frac{\mu^2 S(S+1)}{3kT} \left(1 + \frac{[2(J/N) \rho_0]^2 \ln(kT/D)}{1 - 2(J/N) \rho_0 \ln(kT/D)} \right) \quad (4.26)$$

where the magnetic field H is in the z direction, and μ is the magnetic moment of the impurity spin. This formula can be derived by using Abrikosov’s method (eg Zawadowski and Fazekas 1969†, Ting 1971). Yosida and Okiji (1965) pointed out

† Before the logarithmic term a factor of two was missing in that calculation because of the incorrect normalization mentioned in the previous footnote. A large number of papers contain the same mistake (eg Yosida and Okiji 1965).

that the conduction electrons are polarized as well, in addition to the Pauli term; however, this contribution appears only in the next to leading logarithmic approximation. Other quantities can be calculated in a similar way (see Kondo 1969).

The calculations in the logarithmic approximation exhibit drastically different behaviour for ferromagnetic and antiferromagnetic coupling in a crucial manner. Thus in the ferromagnetic case the logarithmic expression (4.23) for the scattering amplitude decreases on lowering the temperature. However, in the case of anti-ferromagnetic coupling this expression diverges as T reaches the temperature T_K , where

$$T_K = D \exp\left(\frac{1}{2(J/N)\rho_0}\right). \quad (4.27)$$

This characteristic temperature is usually called the Kondo temperature, and $T_K \ll D$ for weak antiferromagnetic coupling, $-1 \ll (J/N)\rho_0 < 0$. This divergency shows that for τ the leading logarithmic approximation breaks down as T approaches T_K . The expression (4.27) derived for the characteristic temperature shows a non-analytical behaviour in the coupling J , with a strong resemblance to the superconducting transition temperature in the BCS theory. In the theory of superconductivity a similar divergence indicates a phase transition; in the case of a single impurity, however, no phase transition can occur, as has been discussed in §3.5. It is interesting to note that in the theory for zero temperature, $T = 0$, a similar divergence occurs at energy $\epsilon = kT_K$. Similar behaviour is shown by the susceptibility χ given by equation (4.25). This result can be written in the form of a Curie law by introducing an effective moment for the impurity

$$\chi(T) = c \frac{S(S+1)\mu_{\text{eff}}^2(T)}{3kT} + \text{Pauli polarization} + 2 \frac{J}{N\rho_0} c \frac{S(S+1)\mu_{\text{eff}}^2(T)}{3kT} \quad (4.28)$$

where

$$\mu_{\text{eff}}(T) = \mu \left(1 + \frac{1}{2} \frac{[2(J/N)\rho_0]^2 \ln(kT/D)}{1 - 2(J/N)\rho_0 \ln(kT/D)} \right)$$

and c is the concentration of the impurities. The last term in expression (4.28) corresponds to the Zener polarization of the conduction electrons, which is induced by the polarization of the impurity spins through the exchange interaction. The physical reality of this term is, however, questionable, as will be discussed in §4.8. According to the first term the effective magnetic moment decreases on lowering the temperature, due to the screening by the conduction electrons. In other words, at low temperatures a strong correlation between the impurity spin and conduction electrons with opposite spin direction is built up. This spin compensation in the conduction electron gas is usually called the 'spin compensation cloud'. By noticing that only those electrons are strongly scattered by the impurity whose energy is not much further from the Fermi level than the characteristic Kondo energy kT_K , one can realize that the spatial extension of this compensation cloud may be characterized by the length

$$\xi_K = \frac{v_F}{kT_K}$$

which is the coherence length in the Kondo problem; v_F is the Fermi velocity (note the similarity to the coherence length in superconductivity). This compensation cloud and coherence length will be discussed in §§4.8 and 4.9 in more detail.

Summarizing these results one can say that a spurious divergency occurs in most of the quantities if they are calculated in the leading logarithmic approximation. Abrikosov (1965) and Suhl (1965, 1966) have noticed that the appearance of the singularity indicates the formation of a resonance in the conduction electron-impurity scattering amplitude given by equation (4.23), which is centred at the Fermi level. This resonance is called Abrikosov-Suhl resonance. The leading logarithmic approximation breaks down as the temperature approaches the Kondo temperature, and therefore this method is incapable of describing this resonance properly.

There are two ways to improve upon the leading logarithmic approximation:

(i) To calculate the same diagrams as before with one electron or hole in the intermediate state, but with better accuracy. This means including the imaginary part of the scattering amplitude and keeping terms in the real part beyond the leading logarithmic approximation.

(ii) To include a wider class of diagrams.

Method (i) will be the subject of the next section, while the problem of including more diagrams is left to § 6, which deals with more recent developments in the theory.

4.4. Different methods in the one-particle intermediate state approximation

Soon after the realization of the formation of a resonance at the Fermi energy, three different methods were developed to go beyond the leading logarithmic approximation, but keeping only one electron or one hole in the intermediate state. In this section we briefly review these methods: (i) equation of motion for Green functions; (ii) dispersion relations; (iii) summation of diagrams.

We will not give many details because these methods have already been reviewed by others (see Kondo 1969, Fischer 1970). Here we present the starting point of the methods, and the results obtained will be discussed in the next section.

(i) *Equation of motion for Green functions.* Nagaoka (1965) has tried to attack the problem in terms of double-time thermodynamic Green functions. Following the general method worked out by Bogoliubov's school he studied the equation of motion for the most simple Green functions. These equations connect the simple Green function to more complicated ones, and a hierarchy of equations can be derived in this way. The basic idea of the method is to cut this hierarchy after some finite step and to approximate the higher-order Green functions in terms of the lower-order ones. Nagaoka started with the one-particle Green function

$$G(t - t') = -i\theta(t - t') \langle (a_{k\alpha}(t), a_{k\alpha}^+(t'))_+ \rangle \quad (4.29)$$

where

$$\theta(t - t') = \begin{cases} 1, & t > t' \\ 0, & t < t' \end{cases} \quad (4.30)$$

and $a_{k\alpha}^+(t)$ is the electron creation operator in the Heisenberg representation; furthermore, $\langle \dots \rangle$ stands for the statistical average.

In the next step he considered the Green functions of type

$$\Gamma(t - t') = -i\theta(t - t') \langle (a_{k'\downarrow}(t) S^-(t), a_{k'\uparrow}^+(t'))_+ \rangle. \quad (4.31)$$

The Green functions appearing in the equations of motion of Γ were factorized in the following manner:

$$\begin{aligned} & \langle (a_{k'}\uparrow(t) a_{l'}^+(t) a_{l'}\downarrow(t) S^-(t), a_{k'}^+(t'))_+ \rangle \\ &= \langle (a_{l'}\downarrow(t) S^-(t), a_{k'}\uparrow(t'))_+ \rangle \langle a_{k'}\uparrow a_{l'}^+ \rangle - \langle (a_{k'}\uparrow(t), a_{k'}^+(t'))_+ \rangle \langle a_{l'}^+ a_{l'}\downarrow S^- \rangle. \end{aligned}$$

By applying this decoupling scheme Nagaoka derived a closed set of equations. These equations can be solved exactly by including the imaginary part of the Green functions. Because these equations are singular, their analytical structure had to be treated with special care. The general method of solving singular integral equations of this type is given in Muskhelishvili's (1953) book. Following partly the method outlined in this book, the analytic structure of the solution was studied by Hamann (1967), Falk and Fowler (1967), Fowler (1967) and Bloomfield and Hamann (1967), and finally Zittartz and Müller-Hartmann (1968) gave a general exact solution.

(ii) *Dispersion relations.* Suhl (1965, 1966) realized that this problem has a strong resemblance to meson-nucleon scattering, which has been extensively studied in high-energy physics. Suhl applied the method of Chew and Low, who have derived a closed set of equations for the scattering amplitude.

Assuming that one considers only those initial and final states in which there is only one electron or hole, the scattering amplitude can be written in the form of equation (4.22), where $t(z)$ and $\tau(z)$ are the amplitudes in the spin-non-flip and the spin-flip channels. The Chew-Low equation derived by Suhl for the scattering on the impurity spin at finite temperature can be written as

$$t(z) = \frac{V}{N} + \int \frac{|t(x+i\epsilon)|^2 + S(S+1)|\tau(x+i\epsilon)|^2}{z-x} \rho(x) dx \quad (4.32)$$

$$\tau(z) = \frac{J}{N} + \int \frac{\tau(x+i\epsilon)t(x-i\epsilon) + \tau(x-i\epsilon)t(x+i\epsilon) - |\tau(x+i\epsilon)|^2(1-2n_F(x))}{z-x} \rho(x) dx \quad (4.33)$$

where J/N and V/N are the exchange and potential scattering amplitudes of the hamiltonians given by equations (4.3) and (4.6), x is the energy variable on the real axis, and $\rho(x)$ is the density of states for conduction electrons. It is important to note that the Fermi distribution function occurs in the second equation (4.33) only for the spin-flip scattering. If only potential scattering is considered, $\tau \equiv 0$ and $n_F(x)$ does not play any role, in agreement with our previous discussion in §4.2.

These equations were solved generally by Suhl and Wong (1967). Similar results were also derived by Maleev (1966, 1967).

The approximation applied in the derivation of these equations is that only the one-particle intermediate states are considered. In other words, the scattering processes into and out of the intermediate states are given by the one-particle scattering amplitudes $t(z)$ and $\tau(z)$, and the density of states for the intermediate state is replaced by $\rho(x)$.

(iii) *Summation of diagrams.* Brenig and Götze (1968) considered the parquet diagrams and derived rigorous equations for the scattering amplitude. They solved these equations by similar methods to those discussed in (i) and (ii).

It turns out that the three methods discussed above are exactly equivalent. Actually it has been shown by Duke and Silverstein (1967) that the summation of parquet diagrams is equivalent to Suhl's equations. Schotte (1968) and Zittartz (1968a,b) have shown that Suhl's and Nagaoka's equations are also equivalent. Thus all the three methods correspond to the one-particle intermediate state approximation which is obvious for the method described in (ii) and (iii). Although the solutions of these equations are known, it is not trivial in many cases to express the physical quantities by $t(z)$ and $\tau(z)$. The general features of the solution and their consequences will be discussed in the following section.

4.5. Results in the one-particle intermediate state approximation and the unitarity limit

The methods discussed in the previous section were aimed at improving upon the leading logarithmic approximation, especially to include imaginary parts of different quantities. In order to check the accuracy concerning imaginary parts, let us discuss the unitarity condition. According to the 'optical theorem' the imaginary part of the forward scattering amplitude is proportional to the total cross section, and this relation is equivalent to the requirement that the scattering operator is a unitary operator. In the case of Kondo scattering the optical theorem has the form

$$\begin{aligned} \text{Im } t(x - i\epsilon) &= \pi\rho_0[|t(\omega)|^2 + S(S+1)|\tau(\omega)|^2] \\ &+ (\text{one electron or hole} + \text{electron-hole pairs in the final state}). \end{aligned} \quad (4.34)$$

All the possible scattering processes contribute to the right-hand side of this equation, the spin-conserving and spin-dependent scattering channel with one excitation in the final state, and in addition the other processes in which a number of electron-hole pairs as well are created. It is of importance to note that all these contributions are non-negative.

One can see easily that the maximum value of $\text{Im } t(\omega)$ is reached in the case† when $\text{Re } t(\omega)$ and all the other contributions are zero. This limit is called the unitarity limit, where

$$\text{Im } t(\omega - i\epsilon) = 1/\pi\rho_0 \quad (4.35)$$

and

$$\begin{aligned} \text{Re } t(\omega) = \tau(\omega) &= (\text{contribution of one electron or hole} \\ &+ \text{electron-hole pairs}) = 0. \end{aligned} \quad (4.36)$$

Furthermore, the unitarity condition provides an upper limit also for τ ,

$$\tau \leq \frac{1}{2\pi\rho_0} \frac{1}{[S(S+1)]^{1/2}}.$$

This upper bound is strongly violated in the leading logarithmic approximation where τ diverges (see equation (4.23)).

The great advantage of the methods discussed in the previous section is that the solutions provided by them are in agreement with the unitarity condition. Namely, by taking the imaginary part of Suhl's first equation (4.32) one obtains equation (4.34), but without the contribution of the electron-hole pair creation processes, in agreement with our previous statement that these are not included in

† Equation (4.34) can be rewritten as $|\text{Im } t(\omega)| = \pi\rho_0 |\text{Im } t(\omega)|^2 + (\text{positive terms})$, and the solution of this equation has an upper bound given by equation (4.35), in which case all of the other non-negative terms are zero.

Suhl's equations. Actually, the unitarity condition is built into the Chew-Low equations at the very beginning.

Furthermore, as it is easy to show, in this approximation the scattering amplitudes must go to the unitarity limit for energy $\omega = 0$ in the case $T = 0$. Let us suppose that $\tau(0 + i\epsilon) \neq 0$, then $\tau(z = 0)$ diverges because of the term proportional to $1 - 2n_F(x)$ in Suhl's second equation (4.33). That divergent contribution is proportional to

$$\int \frac{|\tau(x + i\epsilon)|^2}{x} \operatorname{sgn}(x) \rho(x) dx \quad (4.37)$$

where $\operatorname{sgn}(x)/x$ is an even function of x ; thus $\tau(0 + i\epsilon) = 0$. Furthermore, because of the electron-hole symmetry

$$|t(x + i\epsilon)|^2 = |t(-x + i\epsilon)|^2, \quad |\tau(x + i\epsilon)|^2 = |\tau(-x + i\epsilon)|^2$$

and $\rho(x) = \rho(-x)$; therefore the right-hand side of equation (4.32) is purely imaginary if $V = 0$. Thus from equation (4.32) one obtains $\operatorname{Im} t(0 - i\epsilon) = 1/\pi\rho_0$, which is the unitarity limit given by formula (4.35). The case $V \neq 0$ will be discussed in the following section.

We have seen again that the crucial term of Suhl's equation is that one which is proportional to the factor $1 - 2n_F(x)$ occurring in the spin-flip scattering term.

The solution has a simple form for $\omega = 0$ at finite temperature $T = 0$ (Hamann 1967):

$$t(\omega + i\epsilon) = \frac{1}{2\pi i\rho_0} \left(1 - \frac{\ln(T/T_K)}{\{[\ln(T/T_K)]^2 + S(S+1)\pi^2\}^{1/2}} \right) \quad (4.38)$$

and

$$\tau(\omega) = \frac{1}{2\rho_0} \frac{1}{\{[\ln(T/T_K)]^2 + S(S+1)\pi^2\}^{1/2}} \quad (4.39)$$

where in the weak coupling limit

$$kT_K = D \exp \left(2 \frac{J}{N} \rho_0 \right). \quad (4.40)$$

The energy dependence at $T = 0$ is very similar to the temperature dependence at $\omega = 0$; t is monotonically decreasing starting from the unitarity value at $\omega = 0$. On the other hand, $\tau = 0$ at the Fermi energy, exhibits a peak at energy $|\omega| = kT_K$, and then decreases with increasing temperature. Considering $\operatorname{Im} t(\omega)$ at $T = 0$, a resonance is found at the Fermi level which is symmetric in energy and has a width of kT_K . This resonance is gradually smeared out with increasing temperature.

The solution shows the following features:

- (i) The behaviour of the solution is logarithmic at low and high temperature (see equations (4.37) and (4.38)) and at small and high energies as well.
- (ii) $\operatorname{Im} t$ tends to the unitarity limit as $\omega/T_K, T/T_K \rightarrow 0$. In this case the scattering is spin-conserving at the Fermi level, in agreement with the general statement (ii) in § 3.4.
- (iii) In the region $T/T_K \gg 1$ or $|\omega|/T_K \gg 1$ the solution is in agreement with those obtained in the leading logarithmic approximation (see equations (4.24) and (4.23)).

The impurity resistivity is determined by the temperature dependence of $|\text{Im } t(\omega)|_{\omega=0}$ as

$$R(T) = \frac{2\pi c}{\rho_0 e^2 k_F} \left(1 - \frac{\ln(T/T_K)}{\{[\ln(T/T_K)]^2 + S(S+1)\pi^2\}^{1/2}} \right) \quad (4.41)$$

where c is the concentration of the impurities (number in unit volume), k_F is the Fermi momentum, and e is the electron charge.

The zero-temperature resistivity is determined only by the unitarity limit (the expression in the large bracket in equation (4.41) is equal to 2) and does not depend on the value of spin S .

Similarly to the impurity resistivity, other physical quantities—such as the susceptibility, the heat capacity and the change of entropy ΔS —have been calculated on the basis of this approximation. Zittartz (1968b) determined the susceptibility assuming that the g factors for the conduction electrons and the impurity spin are equal. The following expression was obtained for $\ln(T_K/T) \gg 1$:

$$\chi(T) = \frac{1}{3kT} (g\mu_B)^2 \left[S(S+1) - (S+\frac{1}{2}) + \frac{S(S+1)}{\ln(T_K/T)} \right] + \text{Pauli term} + O\left[\ln^{-2}\left(\frac{T_K}{T}\right)\right]. \quad (4.42)$$

This expression goes to a Curie law at very low temperature. Thus the effective moment $\mu_{\text{eff}}(T)$ determined from the susceptibility using equation (4.27) does not disappear as $T \rightarrow 0$. In other words, this result does not agree with the expectation that the ground state is singlet and its magnetic moment is zero (see § 3.4).

The heat capacity was also calculated; it exhibits a peak at $T = \frac{1}{3}T_K$, and the energy change related to the formation of the ground state is of order kT_K (Bloomfield and Hamann 1967). According to this result the heat capacity $c(T) \rightarrow 0$ with some power of T as $T \rightarrow 0$. The entropy change related to the formation of the ground state was calculated as well by Zittartz and Müller-Hartmann (1968), and it was found that

$$\Delta S = -k_B[(2S+2)\ln(2S+2) + 2S\ln(2S) - 2(2S+1)\ln(2S+1)]. \quad (4.43)$$

This result depends on the value of the spin S ; it does not show, however, that the transition would take place between a singlet ground state and a free spin with degree of freedom zero and $2S+1$ respectively.

Summarizing the results obtained in the one-particle intermediate state approximation one can conclude that at high temperature it reproduces the perturbational result at least in the leading logarithmic approximation. At lower temperature it provides an imaginary part to the scattering amplitude in such a way that the unitarity condition is satisfied, and at zero temperature the scattering amplitude tends to the unitarity limit. However, the other results for low temperatures are very questionable. The problem remains to make clear how much the low-temperature behaviour can be affected by including the contributions of the many-particle intermediate states. This question can be answered either by comparing the theoretical expressions with the experimental results, or on theoretical grounds by using renormalization and scaling arguments. This will be discussed in § 6.

4.6. Kondo effect including potential scattering

The discussion presented in the previous section about the unitarity limit is based on the assumption that the interaction is pure exchange scattering and $V = 0$

in the hamiltonian (4.6). Actually, the main features of the formation of resonance are not influenced by the potential scattering, but our conclusion that $\text{Re } t(\omega)|_{\omega=0} = 0$ for $T = 0$ is not generally valid; see the real part of equation (4.32). The problem with potential scattering has been worked out in the framework of Nagaoka's equation (Fischer 1967, Schotte 1968, Kondo 1968, Nagaoka 1969).

The Kondo scattering is very sensitive to the density of states at the impurity site. The potential V changes this density of states, and this results in two different effects.

The result can be expressed in terms of the conduction electron phase shift δ_V due to the potential scattering. The potential V reduces the density of conduction electrons at the Fermi level by a factor $\cos^2 \delta_V$; thus $(J/N) \rho_0$ must be replaced by $(J/N) \rho_0 \cos^2 \delta_V$, which can be done in a formal way by introducing an effective exchange interaction

$$\bar{J} = J \cos^2 \delta_V. \quad (4.44)$$

Furthermore, in Nagaoka's scheme the resistivity is essentially changed compared to equation (4.41), and (Nagaoka 1969)

$$R(T) = \frac{2\pi c}{\rho_0 e^2 k_F} \left[2 \sin^2 \delta_V + \cos 2 \delta_V \left(1 - \frac{\ln(T/T_K)}{\{[\ln(T/T_K)]^2 + S(S+1)\pi^2\}^{1/2}} \right) \right] \quad (4.45)$$

which is in agreement with equation (4.41) if $\delta_V = 0$. The value of the resistivity at $T = 0$ is reduced by a factor $\cos^2 \delta_V$ with respect to the unitarity limit. This result has been derived in the framework of the one-particle intermediate state approximation. However, we emphasized at the end of the previous section that at low temperature this approximation breaks down; therefore the validity of this expression even for $T = 0$ is not well justified.

As was first pointed out by Fischer (1967), the sign of the logarithmic terms in the expression for the resistivity depends on δ_V ; thus it may be opposite to that of the original Kondo results (where $\delta_V = 0$) if $\delta_V \geq \pi/2$. Furthermore, the potential scattering may have an important effect on the thermopower. Namely, if the electron-hole symmetry holds, the Kondo resonance is symmetric to the Fermi level, $t(\omega + i\epsilon) = t(-\omega + i\epsilon)$, and thus the thermopower is zero because it is proportional to the antisymmetric part of the scattering amplitude. The presence of the potential scattering, however, breaks this symmetry, and the thermopower is finite.

4.7. Variational calculations for the ground state

We have already discussed the formation of the Abrikosov-Suhl resonance in the electron-impurity scattering at low temperatures. At zero temperature several authors have considered this resonance as a bound state built up from the impurity spin and from the conduction electron polarization. This bound state is formed in such a way that the total spin of this state is zero; thus the conduction electrons screen the impurity spin. Although several attempts have been made to construct variational wavefunctions to describe this bound state, these calculations do not lead to a better theoretical treatment than those we have described before. The main drawback of these approaches is that in most cases it is hard, or even impossible, to estimate the accuracy achieved. However, these attempts lead to a better understanding of the main difficulties and are therefore very instructive.

Methods of the first type are the variational calculations of the Japanese group, which are reviewed by Yosida (1971) in considerable detail. In the first step one constructs a wavefunction in which a single electron is attached to the impurity spin while the other electrons are unperturbed. This wavefunction can be written in the simple form (see Yosida 1966a,b, Okiji 1966, Heeger and Jensen 1967)

$$\psi_0 = \sum_{k>k_F} \Gamma_k (a_{k\downarrow}^+ \alpha - a_{k\uparrow}^+ \beta) \psi_V \quad (4.46)$$

where α and β are the spin states with $\sigma_z = 1$ and $\sigma_z = -1$, and ψ_V is the wavefunction of the free-electron gas with Fermi momentum k_F . The binding energy E_B is obtained by variational calculation of the coefficient Γ_k , and the binding energy is given by

$$E_B = \begin{cases} D \exp\left(-\frac{2}{J\rho_0}\right), & \text{if } J > 0 \\ D \exp\left(\frac{2}{3} \frac{1}{J\rho_0}\right), & \text{if } J < 0. \end{cases}$$

This result contradicts the expression for the Kondo temperature given by equation (4.40) because it gives bound states for ferromagnetic coupling ($J > 0$) as well; furthermore, the binding energy is smaller than the Kondo temperature T_K given by equation (4.26), because the factor $\frac{1}{2}$ in the exponent of the Kondo temperature is replaced by $\frac{2}{3}$. This result can also be derived using diagrams, and then this simple wavefunction with one excited electron corresponds to summation of ladder diagrams where the ladder is formed by parallel electron and impurity spin lines (see eg the first diagrams in figures 10(a) and (b)). In this case the electron and impurity spin form a bound state with binding energy given above (see eg Sólyom 1966), and the exponents obtained are characteristic of the approximations where only diagrams simpler than the parquet diagrams are summed up (see discussion in § 4.3). Yosida (1966a,b) recognized this problem and included an additional electron-hole pair into the wavefunction, which then has the new form

$$\begin{aligned} \psi = \psi_0 + & \sum_{k_1 k_2 k_3} \Gamma_{k_1 k_2 k_3}^{(1)} (a_{k_1\downarrow}^+ a_{k_2\downarrow}^+ a_{k_3\downarrow} \alpha - a_{k_1\uparrow}^+ a_{k_2\uparrow}^+ a_{k_3\uparrow} \beta) \psi_V \\ & + \sum_{k_1 k_2 k_3} \Gamma_{k_1 k_2 k_3}^{(2)} (a_{k_1\uparrow}^+ a_{k_2\downarrow}^+ a_{k_3\uparrow} \alpha - a_{k_1\downarrow}^+ a_{k_2\uparrow}^+ a_{k_3\downarrow} \beta) \psi_V. \end{aligned} \quad (4.47)$$

The presence of the electron-hole pair improved the coefficient in the exponent of the binding energy, and 0.62 was obtained instead of $\frac{2}{3}$; this correction is in the direction of the value of $\frac{1}{2}$. This sort of calculation was extended by Yoshimori (1968), who considered an infinite number of electron-hole pairs, and by this method the expected exponent $\frac{1}{2}$ was obtained. In this calculation a set of coupled integral equations, which was shown by Nakajima (1968) to be equivalent to Abrikosov's vertex equation with logarithmic accuracy, has been solved.[†] Thus the parquet or leading logarithmic approximation leads to a ground state where already an infinite number of electron-hole pairs are excited. It was not possible to make further progress along this line without improving the calculation technique in an essential way. This has been done by Sakurai and Yoshimori (1973), who have built the renormalization group technique into this schema (see § 6).

[†] This type of calculation was extended to the case of an external magnetic field as well (see Yosida's 1971 review).

A different construction of the ground state wavefunction was given by Kondo (1966) and Appelbaum and Kondo (1968). Without going into a discussion in detail, we only remark that this attempt was a very good example of how difficult it is to estimate the accuracy of the method (see Hamann and Appelbaum 1969). By now it is generally accepted that it is very hard to get reliable information on the properties of the Kondo state by constructing sophisticated ground state wavefunctions except those obtained by the systematic method developed by the Japanese group (see the review by Yosida and Yoshimori 1973).

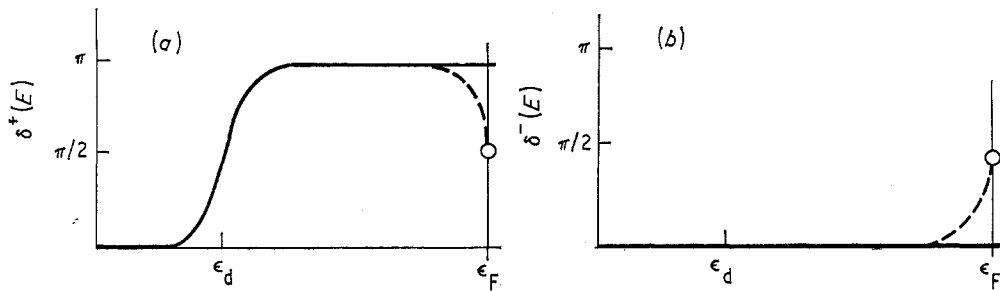


Figure 11. Energy dependence of the phase shifts for (a) spin-up and (b) spin-down electrons in Anderson's construction of the ground state. The full curve is the HF solution; the broken curve represents the modification due to the Kondo effect.

Other types of ground state wavefunction were suggested starting from the Anderson model, and two of them are very instructive. Anderson (1967a) focused his attention on the construction of a singlet wavefunction expressed in terms of conduction electron phase shifts which depend strongly on energy. The basic idea has a strong resemblance to the discussion of § 3.6. The starting point is an HF-like picture where the phase shifts δ_+ and δ_- increase from zero to π in the energy range of the d level, or remain constant depending on whether the d level with that spin direction is occupied or not. This is in accordance with the Friedel sum rule in the HF approximation (see full curve in figure 11). For the ground state, however, the phase shifts provide a correct description of the system at the Fermi level; furthermore, as the ground state is singlet the phase shifts must be the same for the two spin directions (see discussion in §§ 3.5 and 3.6). Anderson's main idea was to modify the phase shifts occurring in the construction of the ground state wavefunction in such a way that they are altered only in the vicinity of the Fermi energy and are equal at the Fermi energy (see broken curve in figure 11). In our general discussion (§ 3.6) we argued that the HF picture is essentially correct at large energies or at high temperatures; thus the phase shifts are 0 or π in the energy region between the d levels, and this is in accordance with the broad structure of the d level density of states (see figures 6 and 7). In the discussion of § 3.6 the problem of two phase shifts 0 and π and the uniform phase shift $\pi/2$ at the Fermi energy was resolved by assuming the formation of a resonance at the Fermi level. In order to describe this situation, Anderson modified the phase shifts in the constructed wavefunction just in the region of the Abrikosov-Suhl resonance.

Finally, recent work by Okada and Yosida (1973) has to be mentioned. They started from five-fold degenerate impurity levels in the Anderson model and derived an effective hamiltonian by applying a transformation of the Schrieffer-Wolff type; however, the effective hamiltonian is more complicated than in the simple s-d model. Further, a ground state wavefunction was constructed by a

generalization of the procedure reviewed at the beginning of this section. The most striking conclusion obtained is that at zero temperature the electrical resistivity is proportional to $\sin^2(N\pi/10)$, in agreement with the general analysis of the present authors (Grüner and Zawadowski 1972) and with the resistivity formula (3.41); thus this work provides confirmation of the discussion of §§ 3.5 and 3.6. This result shows again that when studying low-temperature properties one should turn to the Anderson model rather than apply a simple s-d model which leads, according to our present knowledge, to a residual resistivity independent of the spin of the impurity (see equation (4.41)).

4.8. Derivation of the s-d model from the Anderson model: Schrieffer-Wolff transformation

Throughout the present section the existence of a magnetic moment at the impurity site has been taken for granted, as the moment is built in to the s-d hamiltonian (4.2). Previously, however, on the basis of the Anderson model, the necessary condition for formation of the magnetic moment has been discussed in the HF approximation, where in order to have a moment the intra-atomic Coulomb interaction must be large enough, ie $U \gg \pi\Delta$. The goal of this section is to find a more rigorous relationship between these two models.

Let us treat the most simple case where the atomic orbital is non-degenerate. If in the Anderson hamiltonian given by equation (2.3) $\epsilon_d < 0$, $2\epsilon_d + U > 0$, then the impurity level is singly occupied in the limit $V_{kd} \rightarrow 0$. The effect of the s-d mixing V_{kd} which results in the conduction electron scattering on the impurity can be considered as a perturbation. This scattering can be treated in the second order of perturbation theory as

$$H_V \frac{1}{E_i - E_m} H_V \quad (4.48)$$

where H_V is the mixing term of the hamiltonian (2.3), the transition rate is given by V_{kd} , and E_i and E_m are the energies of the initial and intermediate states respectively. Let us assume that there is one excited conduction electron with energy ϵ_k in the initial state, and the impurity level is singly occupied, and so $E_i = \epsilon_k + \epsilon_d$. Scattering can occur through two different intermediate states:

- (i) First the conduction electron jumps on the d level to make it doubly occupied with energy $E_m = 2\epsilon_d + U$.
- (ii) The d level first becomes empty by exciting a conduction electron with momentum k' , and in the second step the excited conduction electron occupies it; thus $E_m = \epsilon_k + \epsilon_{k'}$. These processes are shown in figure 12. In the final state the impurity level is singly occupied, and one conduction electron is in the excited state with momentum k' . The transition may be either spin-flip or spin-conserving scattering, which can be formally described by the hamiltonian given by equations (4.3) and (4.6). The coupling strengths $J_{kk'}$ and $V_{kk'}$ can be chosen to fit the transition amplitudes obtained in the Anderson model; then

$$\begin{aligned} \frac{J_{kk'}}{N} &= V_{kd} V_{dk'} \left(\frac{1}{\epsilon_k - \epsilon_d - U} + \frac{1}{\epsilon_d - \epsilon_{k'}} \right) \\ \frac{V_{kk'}}{N} &= \frac{1}{2} V_{kd} V_{dk'} \left(\frac{1}{\epsilon_k - \epsilon_d - U} - \frac{1}{\epsilon_d - \epsilon_{k'}} \right) \end{aligned} \quad (4.49)$$

where the two denominators correspond to the two different intermediate states. As only those matrix elements are of importance in the Kondo effect in which the excited conduction electron energies are near the Fermi level, $\epsilon_k, \epsilon_{k'} \approx 0$. In this way the expressions for $J_{kk'}$ and $V_{kk'}$ are simplified to

$$\frac{J}{N} = -|V_{kd}|^2 \frac{U}{|\epsilon_d|(U - |\epsilon_d|)} < 0 \quad (4.50)$$

$$\frac{V}{N} = \frac{1}{2} |V_{kd}|^2 \frac{U - 2|\epsilon_d|}{|\epsilon_d|(U - |\epsilon_d|)} > 0. \quad (4.51)$$

Thus the effective exchange interaction due to these processes is always negative. These expressions were first derived by Clogston and Anderson (1961), de Gennes

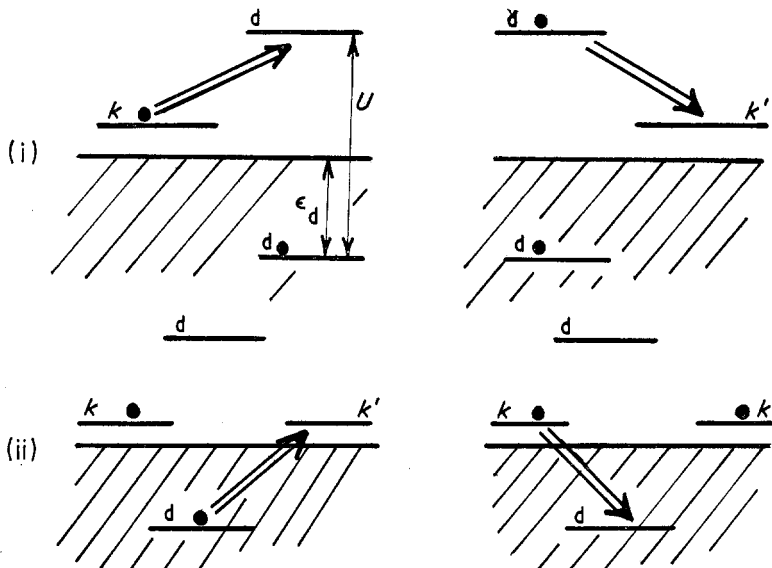


Figure 12. The two possible processes (i) and (ii) for scattering of a conduction electron on a singly occupied impurity level. The shaded region is the Fermi sea, the d levels are labelled by 'd', and the transitions are shown by double arrows. The circles are the electrons taking part in the scattering.

(1962) and Kondo (1962). A canonical transformation was applied by Schrieffer and Wolff (1966) in order to arrive at the above result, whose generator S is given by

$$S = \left(\sum_{k,\sigma} \frac{V_{kd}}{\epsilon_k - \epsilon_d - U} n_{d-\sigma} a_{k\sigma}^+ a_{d\sigma} + \sum_{k,\sigma} \frac{V_{kd}}{\epsilon_k - \epsilon_d} (1 - n_{d-\sigma}) a_{k\sigma}^+ a_{d\sigma} \right) - cc \quad (4.52)$$

and the new form of the hamiltonian is $(\exp S)H\exp(-S)$. These results were generalized by Schrieffer (1967) and Mühlischlegel (1968) for the degenerate Anderson model, and for this situation the result given in equation (4.50) was modified by a factor $1/2S$, where S is the spin of the impurity. This general relationship between the s-d model and the Anderson model is usually described in the literature as the Schrieffer-Wolff transformation.

Several physical quantities (eg resistivity, susceptibility) have been calculated in the framework of the Anderson model by carrying out a perturbation expansion

in V_{kd} (eg Scalapino 1966, Dworin 1967, Hamann 1966). In these calculations, as has already been mentioned in § 3.4, it is assumed that $U, |\epsilon_d| \gg \Delta$ and the logarithmic approximation is applied. The most careful comparison of the results in the Anderson model with those obtained using the s-d model was performed by Keiter and Kimball (1971), who found that in general the leading logarithmic contributions can be calculated correctly on the basis of the s-d model with exchange coupling given by equation (4.50), though the further terms are rather dubious. Furthermore, the assumption $U \gg \Delta$ plays an important role, because it means that the split d levels are far from the Fermi level and their tails can be neglected in that region. This assumption is certainly well justified for Mn impurities in Cu, Ag or Au as host, and less so for Al as host, where Δ is larger; but it is, however, not the case for other impurities, Fe and Cr for example, in Cu and Au, because the d levels are partially occupied and the density is quite large at the Fermi level. In other words, either $|\epsilon_d| \gg \Delta$ or $|\epsilon_d + U| \gg \Delta$ does not hold. Furthermore, it is obvious that the Schrieffer-Wolff transformation is valid for rather large U/Δ values, and breaks down progressively with decreasing U/Δ .

So far the discussion has been limited to a comparison of the scattering amplitudes obtained in the two models. Looking at the form of the Schrieffer-Wolff transformation (equation (4.52)), however, the question of how this transformation mixes the s and d states can be raised. In a recent paper Stewart and Grüner (1973) calculated the magnetic moment M of the impurity in the limit $|\epsilon_d|, |\epsilon_d + U| \gg \Delta$ by using the HF approximation, when the overlap of the d levels is small. The result is

$$\begin{aligned} M &= \mu_B(\langle n_{d+} \rangle - \langle n_{d-} \rangle) \\ &= \mu_B \left[\left(1 - \frac{1}{\pi} \frac{\Delta}{|\epsilon_d|} \right) - \left(\frac{1}{\pi} \frac{\Delta}{U + \epsilon_d} \right) \right] \\ &= \mu_B \left(1 - \frac{|J|}{N} \rho_0 \right) \end{aligned} \quad (4.53)$$

where the first expression comes from the asymptotic expansion of equation (3.11) and the second form is obtained by using the Schrieffer-Wolff transformation (4.48) and equation (3.1) for Δ . Moreover, in the susceptibility the factor $M^2 \sim (1 - |J| N^{-1} \rho_0)^2 \sim (1 - 2|J| N^{-1} \rho_0)$ occurs. As already mentioned, the susceptibility is completely localized to the d level in the HF approximation (see Anderson's compensation theorem in § 3.2). In contrast to this result in the s-d model the first correction to the susceptibility is the Zener term, which has exactly the same amplitude (see equation (4.27)) but is located at the conduction band. This discrepancy was studied by Zawadowski and Grüner (1974), who found that it is an artefact of the Schrieffer-Wolff transformation which—although it conserves the total momentum—mixes the d level and conduction band polarizations. With respect to localization the main features of this transformation can be summarized in the following way. In the HF approximation the total momentum is localized to the d level and is less than that which would correspond to $S = \frac{1}{2}$; therefore it cannot be described by a spin operator. By means of the Schrieffer-Wolff transformation a new set of d and conduction electron states are introduced by the new annihilation operators

$$\bar{a}_{k\sigma} = (\exp S) a_{k\sigma} \exp(-S) \quad \text{and} \quad \bar{a}_{d\sigma} = (\exp S) a_{d\sigma} \exp(-S),$$

and the new states are not completely localized to the d level and to the conduction

band; thus they are slightly mixed into one other. In the new representation the momentum on the d level is increased by the factor $(1 - 2|J|N^{-1}\rho_0)^{-1}$ to achieve a localized spin with $S = \frac{1}{2}$. As the total spin is conserved, a spin deficit occurs in the conduction band, which is the well-known Zener term. The conclusion, therefore, is that the occurrence of the Zener term in the dilute alloy problem is artificial and is entirely due to the assumption that a spin with half-integer value is formed on the impurity site. Although this consideration is limited to the HF approximation, it implies that the distinction between the spin and conduction band is somewhat artificial in the s-d model.

4.9. Conduction electron density of states and charge oscillation around the impurities

Friedel (1954) first pointed out that impurities in metals perturb the conduction electron states. This perturbation is called the Friedel oscillation, and at large distances r the charge perturbation $\Delta\rho(r)$ has the asymptotic form

$$\Delta\rho(r) = -\frac{(2l+1)\sin\delta_l(0)}{4\pi^2r^3} \cos(2k_F r - l\pi + \delta_l(0)) \quad (4.54)$$

where r is measured from the impurity site, and l is the angular momentum quantum number (in general there is a summation over l). The conduction electron density of states can be calculated from the one-particle Green function G , which is expressed by the unperturbed Green function $G^{(0)}$ and by the spin-conserving part of the scattering amplitude t as $G = G^{(0)} + G^{(0)}tG^{(0)}$. We have seen previously that at $T = 0$ and at the Fermi energy this scattering amplitude can be given in terms of phase shifts $\delta_l(0)$ (see § 3.5), and this phase shift enters in the expression (4.54).

Recently a series of calculations have been performed to investigate the pre-asymptotic behaviour of this perturbation. The most detailed study of the density of states $\rho(r, \omega)$ at energy ω measured from ϵ_F is given by Mezei and Zawadowski (1971a). Three characteristic distances are important for this behaviour: (i) the atomic distance ($\sim k_F^{-1}$) and two coherence lengths; (ii) $\xi_\omega = V_F/\omega$; and (iii) $\xi_{\Delta'} = V_F/\Delta'$, where Δ' is a characteristic energy related to the momentum dependence of the scattering amplitude, and V_F is the Fermi velocity ($\Delta' \sim V_F \delta k$, where δk is the momentum region in which the scattering amplitude is large). The energy Δ' must be of the order of the broadened atomic energy levels; thus $\xi_{\Delta'}$ should be around 5–10 Å. This quantity may be important in the case of tunnel junctions with an impurity layer (Mezei and Zawadowski 1971b), but not in the present context.

In experiments the charge oscillation rather than the density of states is important. The two quantities are related by

$$\rho(r) = \int_{-\epsilon_F}^0 \rho(r, \omega) d\omega. \quad (4.55)$$

In $\rho(r)$ the energy dependence of the spin-conserving scattering amplitude $t(\omega)$ has a crucial role. In order to study this effect, Mezei and Grüner (1972) considered a free-electron gas with one impurity which is a simple resonant scatterer; in this case the scattering amplitude has the form

$$t_l(\omega) = \frac{1}{\pi\rho_0} \frac{\Delta}{\omega - \omega_0 + i\Delta} \quad (4.56)$$

in the angular momentum channel $l = 2$, where Δ is the width and ω_0 the position of the resonance. The charge perturbation is written in the form

$$\Delta\rho(r, \omega) = -\frac{(2l+1)\sin\delta_l(0)}{4\pi^2} \frac{a(r)}{r^3} \cos(2k_F r - l\pi + \delta_l(0) + 2\phi(k_F r) - \eta(r)) \quad (4.57)$$

where the derivation from the asymptotic form (4.54) is expressed in terms of $a(r)$ and $2\phi(k_F r) - \eta(r)$,† which describe the radial dependence of the amplitude and phase respectively. The function $a(r)$ is plotted in figure 13 for different values of ω_0 . One can see that for $r < \xi_\Delta = V_F/\Delta$ there is a strong reduction in the amplitude, while in the asymptotic region $r \rightarrow \infty$, $a(r) \rightarrow 1$ and reproduces expression (4.54). In the case of our interest Δ is of the order of 1 eV; therefore $\xi_\Delta \sim 10 \text{ \AA}$ and should be measurable by experiment.

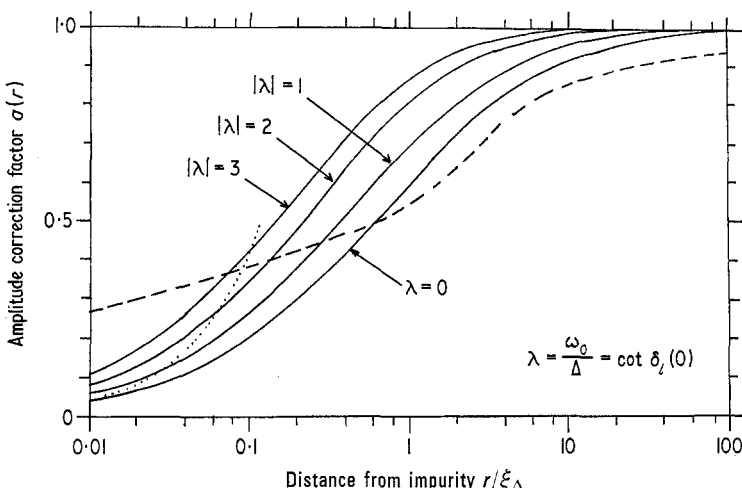


Figure 13. The amplitude of the charge perturbation $a(r)$ as a function of r/ξ_Δ ; the parameter $\lambda = \omega_0/\Delta = \cot\delta_l(0)$ characterizes the position of the resonance (after Mezei and Grüner 1972).

In the Kondo effect, the narrow resonance appearing in the scattering amplitude should show up in the charge perturbation in an essential way, as the width kT_K of this resonance can be small; therefore the corresponding coherence length ξ_{kT_K} is rather large. Although the detailed radial dependence depends on the form of the Suhl–Abrikosov resonance, the main effect is the reduction of the oscillation amplitude at distances $r < \xi_{kT_K}$. Indeed, calculation of $\rho(r)$ on the basis of the s-d model (Bloomfield *et al.* 1970, Klein 1969) shows this reduction near to the impurities; $\rho(r)$ obtained in this way is shown in figure 14. Far from the impurities $\Delta\rho(r)$ goes as r^{-3} , but saturates near the impurity; this saturation is the consequence of the reduced amplitude. The overall behaviour is the same as that calculated by Mezei and Grüner (1972), if Δ is replaced by kT_K .

These results can be formulated in a more general way. Let us consider some arbitrary scattering amplitude shown in figure 15, which has a structure with a characteristic width $\delta\omega$ in the region near the Fermi energy. Looking for the effect of this structure in the charge oscillation one can find that at distances $r \gg \xi_{\delta\omega}$ this

† For the meaning of these see the original publication by Mezei and Grüner (1972).

structure contributes to the charge oscillation amplitude since it is determined by $t(0)$ only. At distances $r \ll \xi_{\delta\omega}$, however, this structure does not contribute to the charge perturbation. In other words, at distances r one observes the effect of a scattering amplitude $t(\omega)$ smeared out on an energy scale $\delta\omega$ where $r \sim \xi_{\delta\omega}$. In this way the pre-asymptotic behaviour of the charge perturbation is a powerful tool for studying the shape and width of the resonances.

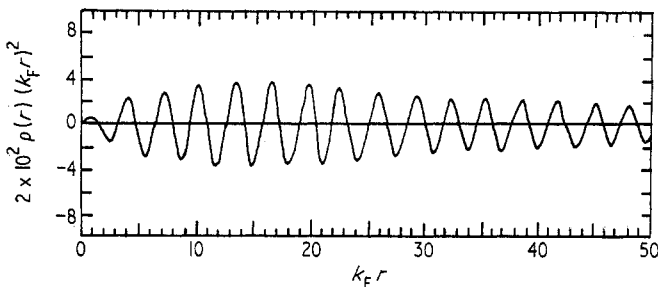


Figure 14. Radial dependence of the charge perturbation derived from the s-d model (after Bloomfield *et al* 1970).

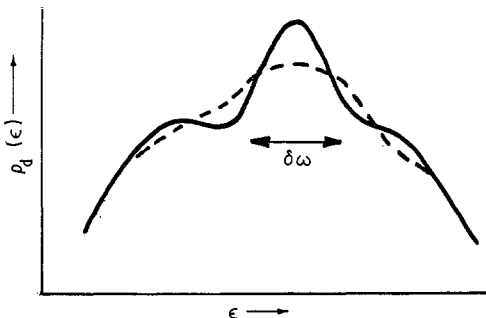


Figure 15. A schematic plot of the scattering amplitude (full curve) which shows a structure with a width $\delta\omega$ at the Fermi level. At distances $r \ll \xi_{\delta\omega}$ the charge perturbation amplitude $a(r)$ is related to a scattering amplitude $t(\omega)$ smeared out on a scale $\delta\omega$ (broken curve).

Another advantage of the charge perturbation is that the temperature dependence of the oscillation amplitude in the asymptotic region is determined only by the temperature dependence of $t(0)$, in contrast to the transport properties where the energy and temperature dependence are mixed together (Grüner and Hargitai 1971).

4.10. Spin perturbation in the s-d model and the spin compensation cloud

In § 4.8 the various contributions to the magnetic moment were discussed. In the s-d model, the term $-J\rho_0$ in equation (4.53) is the consequence of the polarization of the electron gas by the impurity spin. This polarization, however, is not uniform, but decreases going away from the impurity and has an oscillatory form similar to the charge perturbation. In the HF approximation of the Anderson model this spin perturbation is simply the difference between the charge perturbations for the spin-up and spin-down conduction electrons. For a well-split virtual

bound state this perturbation has the form

$$\Delta\sigma(r) = (\alpha'/r^3) \cos(2k_F r + \phi') \quad (4.58)$$

with

$$\begin{aligned} \alpha' \cos \phi' &= (\sin \delta_\uparrow \cos \delta_\uparrow - \sin \delta_\downarrow \cos \delta_\downarrow) \\ \phi' \sin \phi' &= (\sin^2 \delta_\uparrow - \sin^2 \delta_\downarrow). \end{aligned} \quad (4.59)$$

From the s-d model one arrives at a similar radial dependence, and then the spin perturbation has the well known Rudermann-Kittel-Kasuya-Yoshida (RKKY) form

$$\Delta\sigma(r) = \frac{J}{N\rho_0} \frac{r \cos(2k_F r) - \sin(2k_F r)}{r^4} \quad (4.60)$$

which reduces to a $\cos(2k_F r)/r^3$ form at large r values. Comparing the amplitudes in equations (4.58) and (4.60) one immediately arrives at the Schrieffer-Wolff result given by equation (4.50) (Blandin 1967).

It was also shown in §4.8 that a finite s band polarization is probably artificial, and the integral over r of equation (4.60) should be zero instead of $(J/N)\rho_0$. Therefore the radial dependence should be slightly modified; this modification should be the most dominant near the impurities (see eg Geldart 1972).

Naturally, the Kondo effect should modify the above results, as the singlet state itself is the result of a spin correlation. The static magnetic susceptibility has been discussed in §4.3. The main feature of the results presented there is that at very high temperatures $T \gg T_K$ the spin is practically uncoupled from the conduction electron, but by lowering the temperature the screening of the magnetic moment of the impurity by polarization of the conduction band sets in at $T > T_K$. Below the Kondo temperature, on the other hand, the screening becomes stronger; and at $T = 0$, on the basis of general arguments (see §3.5), a singlet ground state, ie a complete screening, occurs. In the region $T > T_K$ perturbation theory with logarithmic accuracy is appropriate; at $T \sim T_K$, however, the approximation with one particle in the intermediate state breaks down and fails to predict a singlet ground state (see equation (4.42)). This singlet ground state can be visualized in such a way that the impurity spin is rigidly coupled to the screening spin polarization cloud, and this coupled system is rotating. This polarization cloud is frequently called the 'compensation cloud'. This screening should be formulated in terms of a correlation function. The spin density of the conduction electron will be denoted by the operator $\sigma(r) = \sum_{\alpha\beta} \psi_\alpha^+(r) \sigma_{\alpha\beta} \psi_\beta(r)$ if the total spin is

$$S + \frac{1}{2} \int \sigma(r) d^3r. \quad (4.61)$$

Assuming that the ground state is singlet, ie that it is an eigenstate of the total spin operator, it follows that

$$\left\langle S \left(S + \frac{1}{2} \int \sigma(r) d^3r \right) \right\rangle_{T=0} = 0. \quad (4.62)$$

Thus

$$\left\langle S \int \sigma(r) d^3r \right\rangle_{T=0} = -2S(S+1) \quad (4.63)$$

as $\langle SS \rangle = S(S+1)$. The energy associated with the formation of the compensation cloud must be of the order of the Kondo energy kT_K . This restriction immediately

rules out the possibility that the radius of the compensation cloud is of the order of the atomic distance or, in other words, localized to the impurity site and to its nearest neighbours, because the energy in question would be then of the order of 1 eV. The other characteristic length which may be anticipated is given by equation (4.28). This quantity is rather large for small Kondo temperatures, and might be expected to cause measurable effects in different experiments, like NMR and neutron scattering. The actual situation, however, is rather complicated. First of all it would be quite obvious to anticipate that in an external magnetic field the compensation cloud is polarized throughout its whole volume; however, it appears that this is not the case. The polarizability at a given distance can be expressed as

$$\lim_{H \rightarrow 0} \frac{\langle \sigma^z(r) \rangle_{T,H}}{H} = \mu_B \left\langle \sigma^z(r) \left(S^z + \frac{1}{2} \int \sigma^z(r') d^3r' \right) \right\rangle \quad (4.64)$$

where the external magnetic field is in the z direction. The second form follows from the expansion of the statistical density matrix with respect to H . The polarizability can be split into two terms: (i) the conduction electron spin density–impurity spin correlation $\langle \sigma^z(r) S^z \rangle$; and (ii) the conduction electron spin density self-correlation $\frac{1}{2} \langle \sigma^z(r) \int \sigma^z(r') d^3r' \rangle$.

As we have already seen, the first correlation cannot be well localized. The situation is similar for the second term, and to see this let us consider the total spin self-correlation. Assuming again that the ground state is singlet, one obtains for $T = 0$ that

$$\left\langle \left(S + \frac{1}{2} \int \sigma(r) d^3r \right)^2 \right\rangle = -S(S+1) + \frac{1}{4} \left\langle \left(\int \sigma(r) d^3r \right)^2 \right\rangle \quad (4.65)$$

where equation (4.63) has been used. As $\langle (\int \sigma(r) d^3r)^2 \rangle = 4S(S+1)$ one may repeat the previous arguments for $\langle \sigma(r) S \rangle$, and thus $\langle \sigma(r) \int \sigma(r) d^3r' \rangle$ must be rather extended. In this way the polarizability of the conduction electrons at distance r is the difference between the two positive terms, both with large spatial extension. Therefore one cannot decide whether the expression (4.64) is localized inside a few atomic distances or not without a more detailed investigation. Similarly to the situation for other physical quantities, however, no reliable results are expected for temperatures $T \ll T_K$. In the logarithmic approximation, the behaviour of these two terms can be studied at least at high temperatures. The most detailed study is due to Müller–Hartmann (1969, and references therein), who used Nagaoka's schema for the Green function decoupling. This investigation shows the following behaviour:

- (i) At low temperatures the correlation becomes strong and independent of the temperature, in agreement with our conclusion that this correlation can be expressed only in terms of S .
- (ii) $\langle S\sigma(r) \rangle$ contains an oscillating part proportional to r^3 in the asymptotic region (RKKY-like behaviour).
- (iii) The terms $\langle \sigma(r) S \rangle$ and $\langle \sigma(r) \frac{1}{2} \int \sigma(r') d^3r' \rangle$ have a long-range non-oscillating contribution of the form of $r^{-3} S(S+1)/[\ln(r/\xi_{T_K})]^2$, but with opposite sign; furthermore, these terms cancel each other in expression (4.64).

Even if this result is reliable only at $T > T_K$, it shows that a complete cancellation in the conduction electron polarization may occur at large distances. This cancellation is very probably quite general and indicates that no long-range behaviour occurs in the non-oscillating polarization caused by the external magnetic field.

As we will see in §5, this idea is supported by experiment. Looking for the long-range behaviour, therefore, the correlations $\langle \sigma(r) S \rangle$ and $\langle \sigma(r) \int \sigma(r') d^3r' \rangle$ must be studied directly, and only neutron scattering is an appropriate tool for this.

Summarizing these results, one may conclude that the compensation cloud has a very large extension; however, only the centre part of the spin-compensated state can be polarized by the external field. Finally, we should mention that the applicability of the s-d model may be questioned (see §4.8) with respect to the above problem too, but on the other other hand no detailed study is known which starts from the Anderson model.

What must be emphasized, however, is that, independently of whether one uses the s-d model or the Anderson model, the spin compensation cannot be localized on the d level only, because it would be associated with a double occupation, resulting in a large intra-atomic Coulomb energy.

4.11. General remarks

In the course of §3 we discussed the structure of the d level density of states $\rho_d(\omega)$. We argued that a broad structure corresponding to the split d level (broad one-particle resonance of the Friedel–Anderson type) must exist; this is indicated in the HF approximation. Furthermore, as a consequence of the singlet ground state and charge neutrality it was suggested in §3 that a narrow resonance must be built up at the Fermi level at $T = 0$, although its dynamical origin was not discussed there. In this section we have turned to the problem of the Kondo effect which shows up in the form of a resonance at the Fermi level. According to the general relation between the conduction electron scattering amplitude and the density of the d level, the Abrikosov–Suhl resonance must be superimposed on the broad d level resonances.

The theory of the Kondo effect was discussed in the s-d model on the basis of the Schrieffer–Wolff transformation, and in that limit of the Anderson model where the d level density of states is negligible at the Fermi surface. Thus the essential assumption of the theories is that the overlap of these two different resonances is small. It is strongly believed that the occurrence of the Abrikosov–Suhl resonance does not depend on this assumption; only the mathematical treatment is simplified in that limit.

The general case seems to be too hard for the existing theoretical methods. If one considers the broadening of the d level first, the treatment of the narrow resonance is extremely difficult, as one starts with the HF approximation in which the rotational symmetry is broken. The main task would be to restore this symmetry by some mathematical trick which has not yet been found. On the other hand, starting with $V_{kd} = 0$ and treating this term as a perturbation one cannot arrive at a broad d level overlapping the Abrikosov–Suhl resonance. It is generally believed that although the mathematical details have not yet been worked out, the physical picture is correct.

There are further difficulties in the description of the Abrikosov–Suhl resonance. If one deals with $T \gg T_K$ or $|\omega| \gg kT_K$ there is a mathematical guideline—the logarithmic approximation. In the one-particle intermediate state approach this method is extended to lower temperature without further mathematical justification. It is a success of this method that all of the physical quantities remain finite, but it fails to predict the singlet ground state and the correct entropy change. At this

point we can state that at low temperature or energy a more general method is required; however, one can be convinced that many of the main features of these results, such as the monotonically increasing resistivity and decreasing effective moment with decreasing temperature, and the bump in the heat capacity around $T = T_K$, are correct. At high temperatures the logarithmic behaviour is certainly well justified; however, at low temperature there are no reliable predictions.

A further problem is that the simple s-d model probably results in the unitarity value for the zero-temperature resistivity for all the spin values $S = \frac{1}{2}, 1, \frac{3}{2}$, and that contradicts charge neutrality. This problem could be solved in a phenomenological way by assuming a small static potential scattering in addition to the exchange interaction; this procedure, however, seems to be artificial. Therefore a complete description can be expected only on the basis of the Anderson model.

Recently Zlatic *et al* (1974) made an attempt to construct a scattering amplitude in a semiphenomenological way by adding a narrow resonance of lorentzian form to the broad resonance structure. Thus they have been able to demonstrate the general feature shown by figure 7(b); the narrow resonance does not, however, show any logarithmic behaviour of Kondo type.

5. Experiments on dilute alloys

5.1. Introduction

Although the phenomenon itself—the resistance minimum and the logarithmic dependence of the resistivity on T —was well known by experimentalists for about 30 years, a more or less complete experimental situation emerged only at the end of the sixties.

The main reason for this is that it is often difficult to separate the single-impurity properties from interaction effects; these interactions usually have a great influence on the measured parameters. The main source of interaction is the RKKY perturbation, which provides a long-range indirect coupling between the impurities, and relatively distant impurities can be coupled together. An additional effect which may be even more important occurs when the impurities are in the Kondo state. From arguments presented in § 4 it follows that the screening of the impurity spin is performed by electrons in the energy range kT_K around the Fermi level. Therefore, for a free-electron band with a bandwidth D , the relative number of conduction electrons which take part in the screening is of the order of kT_K/D , and so for an impurity concentration $c_i > kT_K/D$ there are simply not enough conduction electrons for screening. If $T_K \sim 10$ K, then for $D = 10$ eV this critical concentration is around 10 ppm! Naturally this concentration is larger for larger T_K , but then the phenomena connected with the Kondo effect are weaker, and the separation of the effect due to the impurities from the matrix properties is more difficult.

Local methods like the Mössbauer effect (ME), nuclear magnetic resonance (NMR) and nuclear orientation (NO), which do not suffer from the above limitations, have played an essential role in this field due to the local character of the problem; other methods like electron spin resonance (ESR) and neutron scattering have not been widely applied, and the experiments are not fully understood.

In the following we discuss the experimental situation for alloys which are expected to be appropriately described by the Anderson model, and use the information obtained mainly for 3d impurities in noble metal or aluminium hosts. Our

goal is to answer the questions raised in the previous sections, and the experimental facts will be summarized around the following points.

(i) *Basic parameters of the Anderson model.* Here the HF approximation provides the theoretical background; experiments performed at high temperatures, where many-body correlations are absent, are essential in this respect.

(ii) *Properties in the Kondo state.* The experimental data will be organized to support the assumptions of the previous sections as well as to demonstrate the consequences of these assumptions. In particular, the evidence for the singlet ground state at $T = 0$ and the charge neutrality will be discussed. In connection with the experimental features of the Abrikosov–Suhl resonance and of correlation effects, questions concerning the validity of the various approximations will be raised as well.

(iii) *Relation between the Friedel–Anderson and the Abrikosov–Suhl resonances.* Here we examine the T_K values of various alloys; this provides an experimental test of the Schrieffer–Wolff transformation and of the validity of the s–d model itself.

Finally we attempt to collect those main experimental facts and indications which still await theoretical explanation; attempts to answer these problems are left to § 6, where the latest theoretical developments on the Kondo problem will be discussed.

5.2. Basic parameters of the Anderson model; HF analysis

In order to gain insight into the nature of the Friedel–Anderson resonances discussed in § 2, experiments with an energy range comparable with the basic parameters U and Δ are ideal. Macroscopic thermal, transport and magnetic properties give only indirect information on this resonance formation through Fermi surface effects. Local properties are on the one hand closely related to the macroscopic properties, and therefore reflect low-energy processes; but in some cases energy distributions well away from ϵ_F are also sampled by these techniques.

Optical experiments are the most important in this context, as the excitation energies involved in the optical absorption process are several eV. In spite of serious limitations (a considerable impurity concentration of around 1 at% is needed to arrive at a measurable extra absorption, and the class of alloys is limited mainly by the absorption properties of the host, etc), these experiments proved to be the most valuable. One expects an absorption peak at $E_{d,\sigma}$ with a width somewhat larger than Δ due to the inherent width of the absorption process itself.

Available optical data fully confirm the Friedel–Anderson picture of the resonance formation, in particular the classification of alloys according to the parameter $(U+4J)\rho_d(\epsilon_F)$. Thus only a single absorption was found in CuNi (Drew and Doezena 1972), centred well below the Fermi level. The resonance is near lorentzian, $\Delta = 0.27$ eV and $E_d = 0.75$ eV. With these parameters the total number of electrons in the resonance $N_d = 8.9 \pm 0.1$, in accordance with the charge neutrality, as originally there are 9 electrons in the d shell of the Ni atom. As the resonance is nearly full $\rho_d(\epsilon_F)$ is small, and therefore this impurity is well within the non-magnetic limit $(U+4J)\rho_d(\epsilon_F) \ll 1$. In the middle of the 3d series, where the density of states is expected to be large, well-separated absorption peaks appear; these are particularly well pronounced in AgMn (Myers *et al.* 1968) and AuMn (Steel and Therene 1972). One resonance is well below, the other well above ϵ_F . $E_{d,\sigma} - E_{d,-\sigma} = 4.8$ eV in these cases, and this value should be rather near, although

somewhat smaller than $U+4J$; see equation (3.20). $\Delta \sim 0.5$ eV for both alloys. With these parameters $(U+4J)\rho_d(\epsilon_F) \sim 3$; therefore both systems are well beyond the HF boundary in the magnetic limit. Other relevant data (for references see Rizzuto 1974, Grüner 1974) on Au alloys are absorbed in figure 16, where the arrows show the position of the Fermi level with respect to the broad resonances; the relative positions of the resonances were inferred from the observed absorption peaks. The precise widths of the resonances were not obtained from the experiments; we can, however, assume that Δ is practically constant (about 0.5 eV), and $U+4J$ should be reasonably constant around 5 eV. The virtual bound state seems

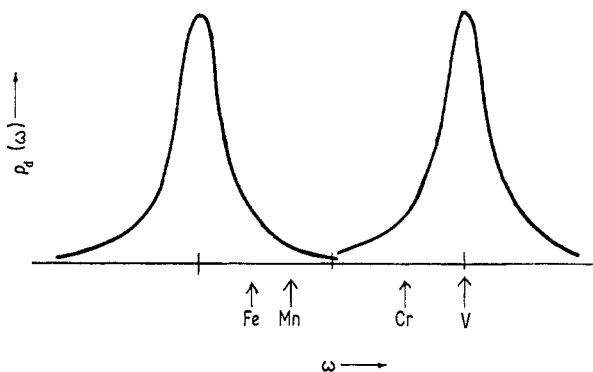


Figure 16. Virtual bound states of 3d impurities in gold, inferred from the optical experiments.

to be double-peaked in these cases, except possibly for **AuV**, where the experimental situation is not completely clear and $(U+4J)\rho_d(\epsilon_F) \sim 1$. **AuNi**, however, is similar to **CuNi**, and only one resonance was observed (Drew and Doezena 1972). A similar situation is expected to hold for Ag and Cu alloys, although clear-cut experiments are not available. For Al alloys optical experiments would be ideal to answer the important question of the parameters which determine the magnetic behaviour. It is expected that Δ is increased compared to noble metal hosts due to the larger density of host states, and a reasonable increase by a factor of two or three would result in a ‘borderline’ situation where $(U+4J)\rho_d(\epsilon_F)$ is near to one in the middle of the series.

The variation of $\rho_d(\epsilon_F)$ when moving along the 3d series shown in figure 16 is reflected in the high-temperature impurity resistivities of these alloys. Figure 17 shows the incremental resistivity $R/\text{at}\%$ for the alloys in question at room temperature; the double-peaked structure, due to the double-peaked virtual bound state, is evident both for Au and Cu hosts. The HF expression for the resistivity, equation (3.22), describes the main features of the above behaviour, and several authors, following Daniel (1962), have performed a quantitative analysis using two phase shifts δ_σ and $\delta_{-\sigma}$ coupled together by the Friedel sum rule, equation (3.18). Such a type of analysis, however, is not entirely correct; the main objection probably is that the HF expression neglects the spin-flip scattering, only the potential scattering being retained. The neglect of the spin-flip process might be most important for Mn impurities, because here one resonance is well below, the other well above ϵ_F ; the potential scattering is fairly small and the impurity represents a well-formed spin. In fact, in these cases the resistivity is described reasonably well by the

expression, derived from the s-d model,

$$R = 2\pi\rho_0 c(J/N)^2 S(S+1) \quad (5.1)$$

with $S = \frac{5}{2}$ and $J = 0.25$ eV. We shall see later that this value of J is in accordance with other estimations.

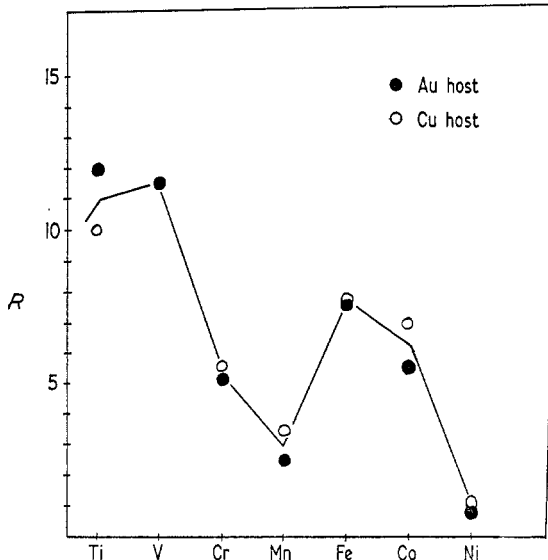


Figure 17. Impurity resistivities at room temperature in Au- and Cu-based alloys.

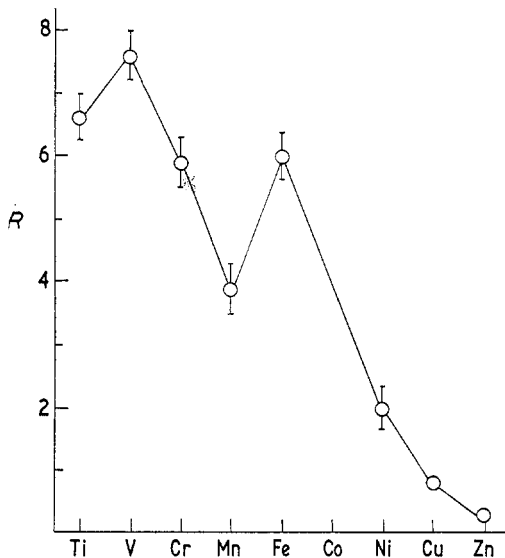


Figure 18. Impurity resistivities at $T = 930$ K in Al-based alloys (after Kedves *et al* 1972).

Although many-body correlations are effective even at room temperature in Al-based alloys, recent high-temperature resistivity measurements, shown in figure 18, suggest again the appearance of a double-peaked virtual bound state, at least for Mn, implying that $(U+4J)\rho_d(\epsilon_F) > 1$ for this case. The separation

between the two peaks is probably not so well pronounced as for noble metal hosts, due to the larger width Δ .

While the resistivity is sensitive to $\rho_d(\epsilon_F)$ only (see equation (3.22)), and the temperature dependence of R is expected to be small due to the broad (and so weakly energy-dependent) d states (at least in the HF approximation), the thermoelectric power (TEP) reflects the energy derivative of the density of states at ϵ_F . In the non-magnetic limit of the HF approximation

$$S = \frac{\pi}{3} \frac{k^2}{e} \frac{T}{\Delta} \sin(2\eta_2(\epsilon_F)).$$

However, correlation effects should have a drastic influence on this parameter. In fact the deviations of the measured TEP from that expected on the basis of the Friedel–Anderson picture with virtual bound state widths as derived before indicate the strength of these many-body correlations. Indeed Δ derived from the TEP agrees with that obtained from the optical experiments only for cases where $(U+4J)\rho_d(\epsilon_F)$ is small compared to 1; a classic example is **CuNi** (Klein and Heeger 1966). Δ_{TEP} evaluated from the low-temperature thermoelectric power, however, decreases drastically as the correlation increases; in **CuCo** for example it is three times smaller, about 0.15 eV, and the situation is similar for **AuV**. This effect is clearly seen in Al-based alloys, where Δ_{TEP} decreases drastically in the sequence Co, Fe, Mn and then increases again going towards the beginning of the series.

The situation is similar for the specific heat, as this parameter is also influenced by low-lying fluctuations. The electronic specific heat coefficient

$$\gamma = \frac{3\pi^2}{2} k \rho_d(\epsilon_F) = \frac{3\pi}{2} k \frac{\sin^2(N\pi/10)}{\Delta} \quad (5.2)$$

in the non-magnetic limit and again allows us to evaluate Δ (see equation (3.42)). The drastic reduction of the virtual bound state width evaluated by this method compared with the optical data in Al-based alloys and in **AuCo** and **AuV** points again to important correlation effects. Although the TEP for magnetic cases like **CuMn** can be accounted for by a phase shift analysis similar to that suggested for the resistivity, it is rather hard to estimate the correctness of such a type of analysis. No valuable specific heat experiments were performed on magnetic alloys, mainly due to the fact that impurity interactions are rather important here.

The magnetic properties give the most clear distinction between ‘magnetic’ and ‘non-magnetic’ impurities, although later it will become clear that this distinction is somewhat arbitrary. Without relating the measured temperature dependence of the susceptibility to theoretically derived formulae, it is usually accepted that the observation of a Curie–Weiss susceptibility

$$\chi(T) = \frac{\mu_{\text{eff}}^2}{3k(T+\theta)} \quad (5.3)$$

with a modest θ value is an indication of a well-defined impurity moment, and a Pauli susceptibility shows the absence of the moment. The relation of the above classification to the density of states is clear (at least in the framework of the Friedel–Anderson picture): a double-peaked virtual bound state is connected with a Curie–Weiss, a spin-degenerate virtual bound state with a Pauli susceptibility, as discussed in § 3.2. This connection is borne out from the experiments: Mn, Cr and Fe impurities show a well-defined Curie–Weiss behaviour in noble metal hosts, and

μ_{eff} decreases going from Mn to Cr and Fe in accordance with equation (3.19); θ increases in this sequence from well below 1 K for Mn to about 30 K for CuFe. In CuCr θ is about 1 K. The HF approximation works well for these cases; the non-integral moments are explained by a reduced splitting of the virtual bound state (in phase shift representation $\delta_\sigma < \pi/2$ and $\delta_{-\sigma} > 0$). This approximation, however, cannot account for the finite θ values; here we only mention that it seems to have a strong connection with $\rho_d(\epsilon_F)$ and a larger density of d states results in a drastic increase of the Curie temperature. Alloys where the optical, transport and thermal properties indicate a spin-degenerate virtual bound state have a temperature-independent susceptibility which is often enhanced. This enhancement is small for CuNi and CuTi, but increases with increasing $(U+4J)\rho_d(\epsilon_F)$; this seems to be the situation for Al-based alloys at low temperatures. AuCo and AuV—which are borderline cases according to our previous classification based on the properties of the resonances—cannot be fitted into this scheme; they show a Pauli susceptibility at low temperatures with considerable enhancement; at high temperatures, however, $\chi(T)$ has the form of equation (5.3) with θ of the order of room temperature. These alloys indicate therefore some kind of magnetic–non-magnetic transition if we relate the magnetic properties to the above operational definition based on $\chi(T)$.

It must be mentioned that the first Born approximation of the s-d model is appropriate for describing the properties of strongly magnetic impurities, at least at temperatures $T > T_K$, and then the reduction of the moment from the Hund rule value $g[S(S+1)]^{1/2}$ is explained by the antiferromagnetic polarization of the conduction electron states; this polarization is proportional to $(J/N)\rho_0(\epsilon_F)$. The total effective moment (see equation (4.53))

$$M = g[S(S+1)]^{1/2}[1 - (J/N)\rho_0(\epsilon_F)]. \quad (5.4)$$

Therefore a negative s-d coupling accounts for the observed reduction (see § 4.8).

The most dramatic effect which cannot be understood on the basis of an HF analysis is the giant negative magnetoresistance observed in a number of strongly magnetic alloys; however, the s-d model provides a natural explanation of this observation. In the expression for the resistivity (equations (5.1) and (4.10)), two-thirds of the scattering amplitude comes from spin-flip, one-third from non-spin-flip processes. The spin-flip scattering is frozen out by the application of a magnetic field, leading to a strong decrease of the resistivity with increasing magnetic field. In small external magnetic fields

$$\frac{\rho(H)}{\rho(H=0)} = 1 - \frac{4g^2\mu_B^2H^2}{27(kT)^2} \quad (5.5)$$

(Beal-Monod and Weiner 1968) which explains the experimental findings and gives an estimation of J/N .

The local properties and experiments which are essential in dilute alloys have a further advantage in that these methods are often free from impurity interaction effects. Until now mainly static properties like local charge and spin distributions have been investigated by ME, NMR and NO techniques; dynamical effects measured by ESR and NMR relaxation experiments and which influence the NO experiments are still not well understood.

One may in a somewhat arbitrary way distinguish between properties measured at the impurity site and at the site of host atoms. In the former case the local susceptibility induces a hyperfine field at the impurity site, resulting in a shift of the

NMR line (Knight shift) and a splitting of the Mössbauer line, and has a pronounced effect on the nuclear orientation. This hyperfine field has two contributions, coming from the spin and orbital components of the local susceptibility. The measured field together with the relaxation time can be used to separate the above two components. The relevant experimental data have been summarized by Narath (1972a,b).

The charge perturbation amplitude, which can be measured by NMR techniques (Bloembergen and Rowland 1953), follows the same pattern as the residual resistivity. Available data on Cu-based alloys (Lumpkin 1967, Tompa 1971) indicate a double-peaked dependence on the impurity atomic number, similar to figure 17 (Tompa 1971). In Al-based alloys it is single-peaked at low temperatures; at high temperatures it becomes double-peaked like the impurity resistivity (Grüner and Hargitai 1971, Grüner 1972).

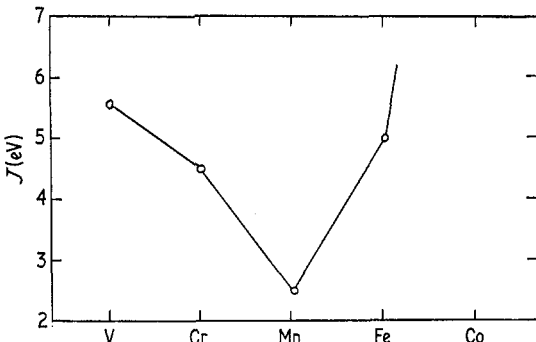


Figure 19. J values evaluated from the line broadening of the host NMR signal.

The measurement of the spin perturbation by NMR methods allows the s-d coupling to be evaluated. This perturbation causes a line broadening proportional to the external magnetic field and to the amplitude of the perturbation. This amplitude is proportional to $(J/N) \rho_0(\epsilon_F) x$, where $x = \langle S^z \rangle / (J/N) \mu_B H$. Using the susceptibility data in the same alloys J/N can be derived by a line shape analysis, and relevant experimental data using both data taken on the host and on the impurity nuclei are shown in figure 19. The overall behaviour, the minimum in the middle of the series, is in agreement with the prediction of the Schrieffer-Wolff transformation and will be discussed later.

5.3. The magnetic-non-magnetic transition: the Kondo effect

The explanation of the resistance minimum, well known by experimentalists for 30 years, gave the first indication of a non-perturbative low-temperature state in certain cases. Although the above effect was thought to be really a low-temperature phenomenon, it was suggested later by Schrieffer (1967) that T_K may vary through several decades from alloy to alloy, from the mK region to well above room temperature.

The main features of the magnetic-non-magnetic transition are readily observable, although the details may be strongly influenced by impurity interactions. As the susceptibility θ is a measure of T_K , a hump in the thermoelectric power and specific heat as well as a strong increase of the resistivity gives a further indication of the Kondo temperature. This behaviour is displayed in several review papers

(van Dam and van den Berg 1970, Rizzuto 1974), and therefore we list only the arguments for an ‘experimental scaling’, ie for the conclusion that the key parameter T_K is the only energy which determines the temperature behaviour of the various physical properties, and these properties are rather similar on a reduced T/T_K scale for various alloys. The most clear-cut evidence has been supplied by Rizzuto *et al* (1973), who measured and collected the temperature dependence of the impurity resistivity of various alloys; this plot is shown in figure 20. While T_K

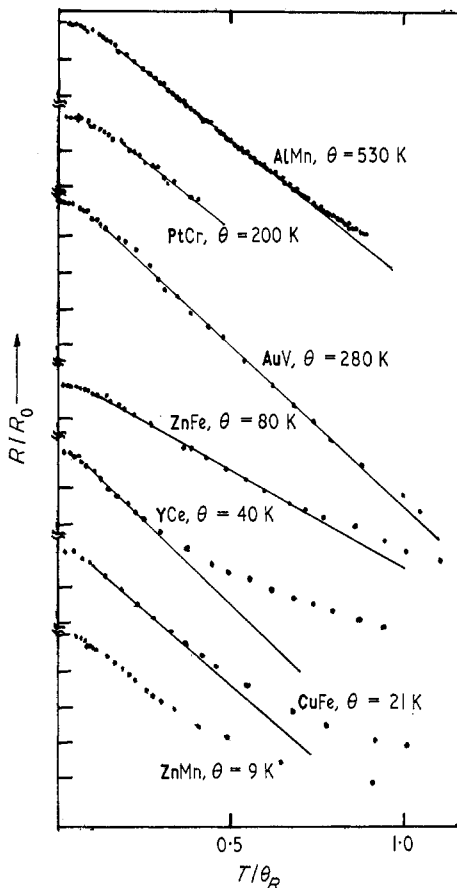


Figure 20. Temperature dependence of R in various alloys on a reduced temperature scale (after Rizzuto *et al* 1973).

varies from 1 K (ZnMn) to 500 K (AlMn), in all cases $R(T) \sim 1 - (T/\theta)^2$ at $T \ll T_K$, then flattens off and becomes logarithmic at $T \gg T_K$, where this temperature range is accessible experimentally. The TEP looks remarkably similar for different alloys, although the sign and magnitude depend on the potential scattering background; this similarity was first noted by Heeger (1969).

A similar conclusion can be reached by inspecting the temperature dependence of the susceptibilities. In the previous section it has been noted that the susceptibility of AuV has a Pauli (temperature-independent) form at low temperatures (with a leading T^2 dependence, van Dam *et al* 1972), which changes gradually to a Curie–Weiss form at higher temperatures. CuFe displays a similar behaviour and below 1 K a susceptibility proportional to T^2 was found, although by an indirect

method (Triplet and Phillips 1971). In **AlMn**, where the temperature dependence of χ_{Al} (pure aluminium) makes the evaluation of the contribution from the Mn impurities somewhat ambiguous, the temperature dependence of the impurity Knight shift (Alloul *et al* 1971) indicates high-temperature Curie-Weiss behaviour too.

These pieces of evidence strongly suggest that the Kondo effect is not restricted to low temperatures, but is a more or less common feature of dilute alloys, although the most pronounced effects are found when T_K is small. This suggestion leads to the speculation that some alloys traditionally thought to be non-magnetic in the HF sense are in fact in a Kondo state, and a smooth transition between the two types of states exists when $(U+4J)\rho_0(\epsilon_F)$ is varied. This continuity hypothesis has not been entirely proved experimentally; various types of experiments, such as NMR measurements reviewed by Narath (1972b), point, however, in such a direction. To reach a final conclusion, however, a closer inspection of the properties of the low-temperature $T \ll T_K$ Kondo state is required.

5.4. Physical properties in the Kondo state

This section is devoted to the discussion of the nature of the Kondo state, and that of the magnetic-non-magnetic transition. Although the arguments presented before suggest that the Kondo effect is a rather general phenomenon, here we mainly use experimental information obtained on alloys where clear-cut magnetic behaviour is observed at high temperatures. Thus the nature of the $T \ll T_K$ state is rather different from the high-temperature behaviour in these cases, and the effect of Kondo correlations is readily observable.

5.4.1. Evidence for a singlet ground state. The susceptibility has been used previously to distinguish between magnetic and non-magnetic impurities; this distinction is based on $\chi(T)$. The Curie-Weiss behaviour can be thought to arise from a temperature-dependent effective moment

$$\chi(T) = \frac{\mu_{\text{eff}}^2(T)}{3kT}. \quad (5.6)$$

The finite susceptibility at $T = 0$ shows that μ_{eff} gradually disappears at $T < \theta$. Using equation (5.6) to interpret the experimental data, the temperature dependence of the effective moment can be evaluated. Figure 21 shows $\mu_{\text{eff}}(T)$ obtained in this way for **AuV** alloys (van Dam *et al* 1972). Although the detailed temperature dependence is slightly different for different V concentrations, for all concentrations $\mu_{\text{eff}} \rightarrow 0$ as $T \rightarrow 0$. This behaviour is reproduced by the temperature dependence of the impurity Knight shift (Narath 1972b), demonstrating that the magnetization disappears at the impurity site and is not due to a negative definite polarization outside the impurity cell. It must be mentioned, however, that the above findings show only that $\langle S^z \rangle = 0$ at $T = 0$, but not S itself; in fact in the Kondo model the latter is constant (see § 4.9).

The specific heat anomaly connected with the transition supplies further evidence for the singlet ground state. The total entropy connected with the transition

$$S = \int_0^\infty \frac{C_V(T)}{T} dT \quad (5.7)$$

can be evaluated from the temperature dependence of the impurity specific heat; for CuCr and CuFe it corresponds to $R \ln(2S+1) = R \ln 4$ (Triplet and Phillips 1971), showing that the high-temperature spin disorder entropy has been removed from the system below T_K , ie the ground state is a singlet.

Although the temperature dependence of the transport properties is not directly related to the singlet nature of the ground state, the strong temperature dependence found in these parameters indicates a strongly temperature- and/or energy-dependent scattering amplitude which builds up at $T < T_K$; the nature of this resonance will be discussed later.

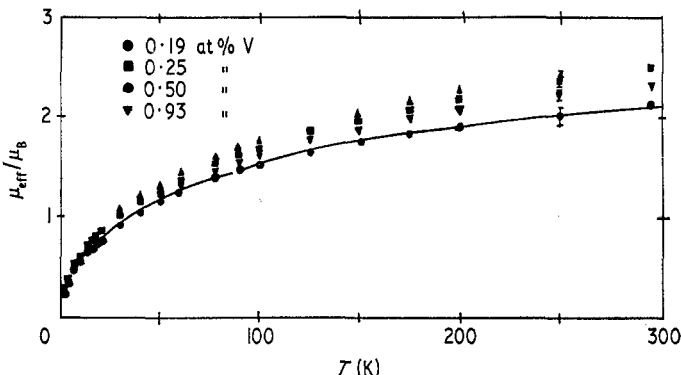


Figure 21. Temperature dependence of the effective moment in AuV alloys (after van Dam *et al* 1972).

5.4.2. Properties of the Kondo resonance. The question raised at the end of § 3.5 must be answered on experimental grounds; this section collects various pieces of evidence which indicate that a narrow resonance is forming at ϵ_F in the Kondo state, and analyses the properties of this resonance. These pieces of evidence are based partly on macroscopic and partly on local properties; the combination of the two types of information is needed to arrive at a firm conclusion. Macroscopic properties—in particular transport properties are essentially of this type—suffer from two limitations:

(i) Being ‘Fermi surface properties’ they are extremely sensitive to small variations of the scattering process near ϵ_F (in the energy region kT), but give no direct information on the density of states far from the Fermi level.

(ii) Both the energy and temperature dependences of the scattering enter in the relevant expressions of the transport properties. For example, the Bethe-Sommerfeld expansion gives for the resistivity

$$R(T) \sim \text{Im } t(\epsilon_F; T) + \frac{\pi^2 k^2 T^2}{6} \left. \frac{\partial^2 \text{Im } t(\omega; T)}{\partial \omega^2} \right|_{\omega=\epsilon_F}. \quad (5.8)$$

Therefore both the T and ω dependences influence $R(T)$; the situation is similar for the TEP and Lorentz number, and also for the thermal and magnetic properties.

The local properties often do not suffer from these limitations; for example, the charge perturbation around the impurities is sensitive to the scattering amplitude far from the Fermi level, and the temperature dependence is driven only by the temperature dependence of the scattering amplitude (see § 4.9). This difference

with respect to the resistivity will be used later to separate the energy and temperature dependences.

The scattering amplitude at $T = 0$, however, is not influenced by the many-body effects which lead to strong energy dependences, and is determined only by the total number of electrons introduced by the impurity; equation (3.41) is independent of the approximations involved and has a general validity. Figure 22 shows the

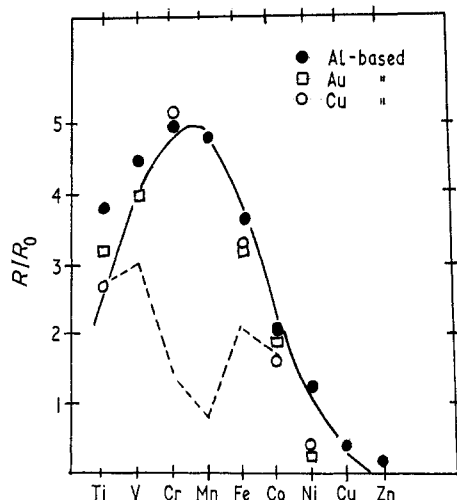


Figure 22. Impurity resistivities normalized to the R_0 values extrapolated to $T = 0$ for Au-, Cu- and Al-based alloys (after Grüner and Zawadowski 1972).

impurity resistivities extrapolated to $T = 0$ for Cu-, Au- and Al-based alloys; for **CuMn**, **CuCr** and **AuMn** the Kondo temperature is so low that no relevant experiments exist below T_K . The full curve is calculated using equation (3.41). The good agreement between the calculated and measured points provides a firm basis for charge neutrality. A further piece of evidence can be given by comparing $\Delta R = R(T \ll T_K) - R(T \gg T_K)$ for **CuFe** and **CuCr**. As the high-temperature spins of the two impurities are nearly identical, ΔR should be the same for the two impurities if it is proportional to S as suggested (Schrieffer 1967), while for charge neutrality to hold it should be given by the difference of the high-temperature ($T \gg T_K$) and low-temperature ($T \ll T_K$) expressions for $R(T)$ (equations (3.22) and (3.41)); this difference is also shown in figure 21. Experimental values of ΔR are $20 \mu\Omega \text{ cm}/\text{at\%}$ for Cr and $8 \mu\Omega/\text{at\%}$ for Fe impurities, clearly favouring the picture we have presented in § 3.6 on the basis of charge neutrality. Charge perturbation amplitudes for Al-based alloys extrapolated to $T = 0$ are also in agreement with the charge neutrality condition, and the oscillation amplitudes can well be described by equation (4.54) with one phase shift which is independent of the spin direction.

We stress again that although equation (3.41) is the same as that obtained on the basis of the HF approximation in the non-magnetic limit, it has a more general validity and does not require a simple Lorentzian density of states.

The energy dependence of the density of states enters into the expression for the temperature dependences of the transport properties, although it is mixed with the temperature dependence of $\rho_d(\epsilon_F)$. Therefore the question about the density of states raised in § 3.5 cannot be resolved by inspecting the transport properties alone.

However, comparing these temperature dependences with that of a related local property, the charge perturbation around the impurities, the energy and temperature dependences can be separated. The reason is that while the low-temperature resistivity is given by equation (5.8) and two terms contribute to the temperature dependence, the charge oscillation amplitude reflects only $t(\epsilon_F; T)$; therefore by this comparison $\partial^2 t(\omega)/\partial\omega^2$ can be evaluated in certain cases (Grüner and Hargitai 1971). Such analysis leads to a strongly energy-dependent scattering amplitude near ϵ_F for AlMn; this can be characterized by a width of about 0.1 eV, which is near to kT_K for this alloy. It supports therefore possibility (ii) in § 3.5, that a sharp resonance is built up at ϵ_F . This is the Abrikosov-Suhl resonance discussed in § 4.

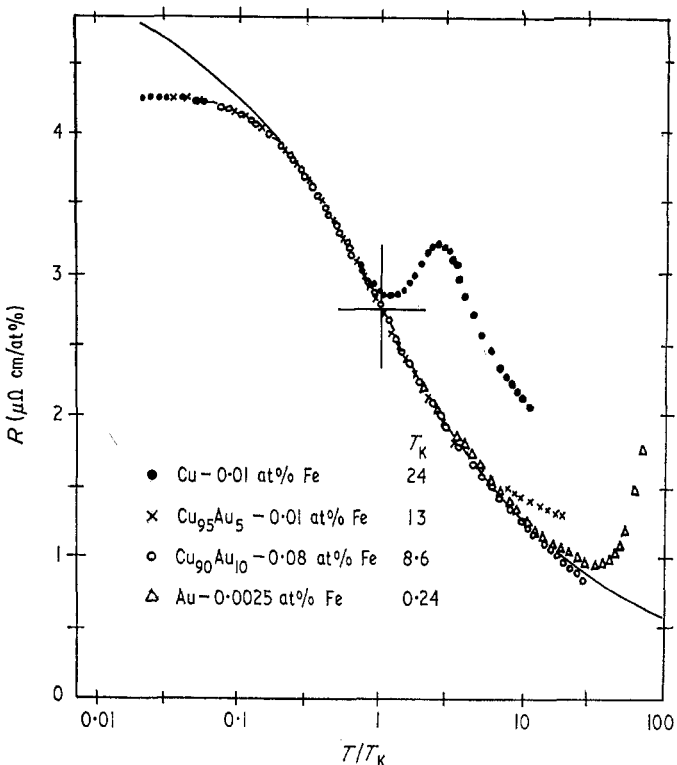


Figure 23. Temperature dependence of the impurity resistivity in $\text{Cu}_x\text{Au}_{1-x}\text{Fe}$ alloys (after Loram *et al* 1970). The full curve is the Hamann curve, equation (4.38).

As the resonance has a width of approximately kT_K , both the low- and high-energy parts of this resonance can be studied if the temperature range of the experiments extends from well below to well above the Kondo temperature.

Theoretical formulae obtained on the basis of the s-d model cover the whole temperature interval in question and can be compared with the experimental findings. Such a comparison is presented in figure 23, where $R(T)$ measured in $\text{Cu}_x\text{Au}_{1-x}\text{Fe}$ alloys is compared with the Hamann curve, equation (4.38). The full curve is calculated by adjusting S to achieve good agreement with experiment; this gives $S = 0.77$ (which is much smaller than the spin $\frac{3}{2}$ observed in the susceptibility). The agreement is poor especially at low temperatures, where $R(T) \sim 1 - (T/\theta)^2$

experimentally, while $\partial R(T)/\partial T$ diverges in Hamann's expression. This disagreement, which holds for the other transport and for the thermal and magnetic properties, is, however, not fundamental as far as the model is concerned, but is probably due to the approximations involved. The above analysis shows that they break down below T_K . The situation is even worse for the ground state models, where drastic deviations from experiment were found (Star *et al* 1972); the good agreement claimed by Heeger (1969) is caused by impurity interaction effects.

In this situation one must abandon the hope of perfect agreement between theory and experiment, and it is more useful to inspect the temperature regions where the physical properties are determined by the same temperature dependences, even though the origin of these dependences is not fully understood. Two temperature regions are essential in this respect: the $T \gg T_K$ and $T \ll T_K$ behaviours of the various alloys. The s-d model as a firm theoretical background where the formulae are expected to work can be used only to account for the $T \gg T_K$ properties; for $T \ll T_K$ we use the assumption of a simple single-particle-like resonance to arrive at a common physical picture.

The high-energy behaviours are controlled by logarithmic dependences, the most famous of them being the logarithmic increase of the resistivity with decreasing temperature. Clear-cut logarithmic behaviours are expected, however, only at $T \gg T_K$; the successive leading logarithmic terms are important even at temperatures one or two orders of magnitude larger than T_K . This feature of the logarithmic approximation provides merely a warning to experimentalists that only alloys with very low T_K are suitable for a straight comparison with perturbational expressions, and strictly speaking only alloys of noble metals with Mn impurities (where T_K is much less than 1 K) are suitable in this respect. Indeed, logarithmic temperature dependences over broad temperature intervals were found only in these cases, and equation (4.19) fits the experimental results with reasonable coupling constants. No such analysis is appropriate for other cases where T_K is larger than 1 K. The Curie-Weiss behaviour of the susceptibility is in fact also in agreement with perturbational expressions based on the s-d model. Equation (4.27) can be approximated by a Curie-Weiss form over a broad temperature interval, with $\mu_{\text{eff}} = g[S(S+1)]^{1/2}/1.22$ and $\theta = 4.5T_K$, T_K being given by equation (4.26). Therefore the high-temperature susceptibilities of 'magnetic' impurities discussed in § 5.2 are in agreement with a logarithmic behaviour of this parameter. No useful specific heat data related to this question are available.

The overall behaviour of the $T \ll T_K$ properties is completely different from the high-temperature logarithmic dependences, and by now it is generally accepted that the low-energy processes are controlled by simple power laws for the temperature. This was first demonstrated by Caplin and Rizzuto (1968) on AlMn. Furthermore, the temperature dependences of the various physical parameters are similar to that for an interacting Fermi gas, ie

$$R(T) = R(0)[1 - (T/\theta_R)^2] \quad (\text{resistivity})$$

$$C_V(T) = (T/\theta)[1 - (T/\theta_C)^2] \quad (\text{specific heat})$$

$$\chi(T) = \chi_0[1 - (T/\theta_\chi)^2] \quad (\text{susceptibility})$$

where the θ values may be somewhat different because $\rho_d(\omega)$ is temperature-dependent too. The TEP is a linear function of the temperature, the magnitude being determined by the potential scattering background. This behaviour of the

transport, thermal and magnetic properties is well-confirmed experimentally, in particular in **CuFe** ($\theta \sim 20$ K), **AuV** ($\theta \sim 300$ K) and **AlMn** ($\theta \sim 10^3$ K). The characteristic temperatures are of the same order of magnitude as the temperature where the magnetic–non-magnetic transition occurs, at least for the first two cases, thus giving evidence that the transition temperature and the width of the many-body resonance are strongly correlated.

This change of regime from logarithmic to simple power laws is the basic unresolved question in this field, and this contrasting behaviour at $T \gg T_K$ and $T \ll T_K$ has generated the family of more sophisticated theoretical techniques to attack the s-d model; these techniques will be discussed in § 6.

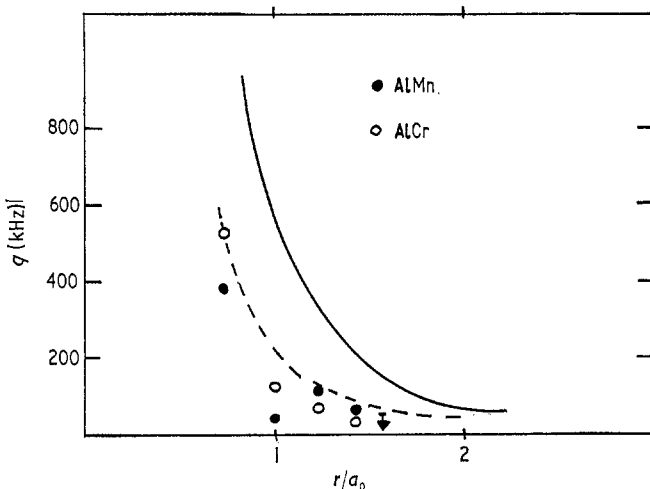


Figure 24. Radial dependence of the charge perturbation around Mn and Cr impurities in aluminium. The full curve is calculated with $\Gamma = 0.5$ eV as explained in the text (after Berthier and Minier 1973).

5.4.3. Correlation effects in the Kondo state. As the Kondo-type screening of the impurity spin is a long-range correlation effect, with a characteristic distance $\xi_K = V_F/kT_K$, the nature of the Kondo state should be manifested in anomalous charge and spin perturbations around the impurity within this distance, as discussed in §§ 4.8 and 4.10. For an impurity with $T_K \sim 10$ K this distance is of about 10^3 Å; therefore this correlation effect should be well observable by studying the properties of the host by local methods. NMR is well suited for such a type of investigation, and indeed both the charge and spin perturbations have been investigated with this technique.

The radial dependence of the charge perturbation has been fully investigated in Al–3d transition metal alloys; this perturbation is reflected through the quadrupole effects on the NMR signal. As discussed in § 4.9, a strong depression of the charge perturbation is expected within the characteristic distance $\xi_{\delta\omega}$ when compared with the asymptotic Friedel expression. Figure 24 shows the radial dependence of the charge perturbation around Cr and Mn impurities in aluminium; the strong depression of $\Delta\rho(r)$ is evident in both cases. A comparison (Berthier and Minier 1973) with the theory discussed in § 4.9 gives a characteristic distance $\xi \sim 10$ Å, and thus an average width $\Gamma \sim 0.5$ eV of the scattering amplitude. The

significance of this result becomes clear when compared with other estimations of the width of the resonances.

(i) It is definitely smaller than the single-particle width Δ which is at least 1 eV for Al-based alloys.

(ii) Γ is much larger than the effective width Δ' determined from the comparison of the temperature dependences of the charge perturbation and resistivity (see § 5.4.2).

The dilemma can be resolved only by assuming that the resonance has a sharp top at ϵ_F . This is reflected by the small Γ ; Δ' , however, has long tails, and therefore the average energy dependence sampled by the pre-asymptotic behaviour is weaker. This behaviour is in full agreement with the representation of figure 22(b), and supplies the basic evidence that the resonance in the Kondo state consists of both the broad single-particle (Friedel-Anderson) and narrow many-body (Abrikosov-Suhl) resonances.

The behaviour of the spatial distribution of the magnetization has been thoroughly investigated in CuFe by various techniques, and various interpretations appeared from time to time to account for the observed anomalies. The experimental information has been supplied by three techniques: macroscopic susceptibility, ME on the iron impurities, and host NMR measurements. Impurity interaction effects have a dominant role in this system, and the contribution of the single impurities to the measured behaviour has been separated only recently. The experimental findings can be summarized as follows:

(i) The macroscopic susceptibility is given by a Curie-Weiss law down to 1 K, where it flattens off and can be represented by a $1 - (T/\theta)^2$ dependence (Toulouse 1969, Tholence and Tournier 1969, Triplett and Phillips 1971).

(ii) The impurity hyperfine field measured by ME has essentially the same temperature dependence, although at low temperatures ($T < T_K$) a slight negative polarization appears (Steiner *et al* 1973).

(iii) The spin perturbation around the impurities has an oscillatory RKKY form, the amplitude of which is temperature-dependent and is enhanced over the non-perturbative RKKY perturbation observed well above T_K (Golibersuch 1970).

(iv) No negative definite spin polarization was found in the Kondo state, as indicated by the absence of a large Knight shift of the Cu nuclei (Golibersuch and Heeger 1969).

These observations show that the negative definite polarization cloud hypothesis advocated by Heeger (1969) has to be abandoned, and no such kind of long-range effect appears in the polarization. The slight difference between the temperature dependence of χ (proportional to μ_{eff}) and the hyperfine field at the Fe nucleus (proportional to $\mu_{\text{eff}}^{\text{imp}}$) can be explained by an extra contribution to the second term on the right-hand side of equation (5.4), which builds up in the Kondo state; from (iii) it follows that it has the same spatial distribution as the perturbative term. Therefore the experimental data can be absorbed phenomenologically into a temperature-dependent s-d coupling, although this suggestion needs confirmation from the theoretical side. The spatial distribution of the polarization, however, may be rather different from the correlation function $\langle \mathbf{S}\sigma(r) \rangle$, which is expected to have a spatial distribution drastically different from the polarization. Unfortunately, recent efforts to measure the correlation function itself by diffuse neutron scattering were not entirely successful (Kroo and Szentirmay 1972, Bauer and Seitz 1972).

In conclusion it appears that the Kondo correlation effect influences the behaviour of the charge perturbation around the impurities, but does not affect the polarization itself. This duality—although being partially resolved by the classical approaches to the Kondo effect discussed in § 4—still awaits a theoretical clarification.

5.5. Relation between the single-particle and many-body resonances

Both the single-particle (Friedel–Anderson) and many-body resonances of the Abrikosov–Suhl type are well confirmed experimentally; however, no relation has been demonstrated to exist between these two types of resonance. Intuitively it is clear that a large single-particle density of states near ϵ_F means that the many-body resonance, which should reach the charge neutrality limit at $T = 0$, can be built up more easily; thus its width (proportional to T_K) is larger. Looking at figure 16, T_K should have a minimum in the middle of the series. The dependence of T_K on the impurity atomic number is shown in figure 25 (see eg Heeger 1969, Grüner

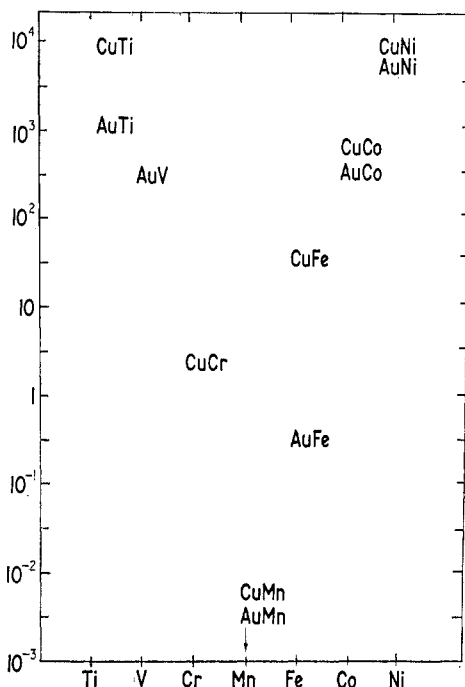


Figure 25. Kondo temperatures of 3d impurities in Cu and Au hosts. For references see Rizzuto (1974) and Grüner (1974).

1974) for Au- and Cu-based alloys. The change in T_K of four orders of magnitude suggests a rather drastic dependence of the Kondo temperature on $(U+4J)\rho_d(\epsilon_F)$. The connection between figures 25 and 16 can be further seen in figure 19, and then T_K has a rather strong dependence on J/N .

Even the non-degenerate Anderson model can explain this behaviour, at least in a certain range of the parameters of the model. Namely the Schrieffer–Wolff transformation (equation (4.49)) connects J/N to the Anderson parameters U and Δ and describes the behaviour of T_K when going through the 3d series, and then the expression of the Kondo temperature accounts for the widespread T_K values.

Although the Schrieffer-Wolff transformation works only for strongly magnetic cases, the inclusion of non-resonant phase shifts (potential scattering) into the s-d model could in principle be used to extend the relation between the Anderson and s-d models.

It should be mentioned that orbital degeneracy certainly plays an important role here; in fact the extension of the Schrieffer-Wolff transformation to orbitally degenerate impurities shows that $J/N \sim 1/S$ and that the application of Hund's rule explains the V-shaped behaviour of the plot of J/N against the impurity atomic number (Daybell and Steyert 1968). This explanation, however, requires the Schrieffer-Wolff transformation to hold for cases other than Mn, and we have seen previously that this hypothesis is confirmed neither experimentally nor theoretically.

In the light of the restricted validity of the Schrieffer-Wolff transformation, the question of the validity of the s-d model itself has to be raised again. The model certainly works for strongly magnetic cases like **CuMn**, but we believe that the main features of the physics behind the s-d model survive also for intermediate situations like **AlMn** and go over progressively to an HF non-magnetic state with decreasing $(U+4J)\rho_d(\epsilon_F)$. The smooth transition from a spin-compensated ground state to a non-magnetic state in the HF sense can be visualized in the following way: the resonance in the Kondo state consists of two well-separated Friedel-Anderson resonances and a narrow Abrikosov-Suhl resonance. With decreasing $(U+4J)\rho_d(\epsilon_F)$ the Friedel-Anderson resonances move closer to each other, while the width of the Abrikosov-Suhl resonance increases rapidly. The distinction between the two types of resonance is progressively smeared out, and finally for $(U+4J)\rho_d(\epsilon_F) \ll 1$ the resonance looks like a single lorentzian. This transition is smooth, since it is similar to the magnetic-non-magnetic transition as a function of temperature. This transition may in fact be described by an s-d coupling constant which increases from the Schrieffer-Wolff value to a unitarity limit as $(U+4J)\rho_d(\epsilon_F)$ goes to zero. On experimental grounds it seems that this value is given by $(J/N)\rho_0(\epsilon_F) = 1$ (see eg Narath 1972b); this suggestion, however, has not yet been confirmed theoretically.

6. Recent theoretical developments: infrared divergencies and scaling laws

As we have discussed in the previous sections, the theoretical problems to be solved are the low-temperature behaviour in the s-d model and a unified theory describing simultaneously the narrow and broad resonances within the Anderson model. In the last few years considerable progress has been achieved in the first field from a realization of the importance of infrared divergencies and scaling laws. This will be discussed in the main part of the present section. The second problem has proved to be more difficult, and the functional integral approach of the Anderson model has been hampered by mathematical difficulties; some remarks on this approach will be given in § 6.6.

6.1. Many particles in the intermediate states

Abrikosov's theory, where only the leading logarithmic terms are considered, breaks down as the Kondo temperature T_K is approached from high temperatures. As was pointed out at the end of § 4.3, there are two drawbacks in the leading logarithmic approximation: omission of all the imaginary parts and the restriction to a certain class of diagrams (the parquet diagrams).

The one-particle intermediate state approximation reviewed in §4.4 suffers, however, only from the second simplification. As was shown in §4, this theory of the Abrikosov–Suhl resonance is still satisfactory except in regions $T \gg T_K$ or $|\omega| \gg T_K$, and is in contradiction with experimental findings (see §5). The main part of this section is devoted to those theories which were constructed to go beyond the one-particle intermediate state approximation.

The milestone of this line is Anderson's (1967b) work, where the Kondo problem is related to infrared divergencies which are already a well-known phenomena in quantum field theory. Namely, a finite energy loss of a particle may be associated with the creation of a very large or even infinite number of excitations if the energy spectrum of these excitations starts at zero energy. In the Kondo problem the relevant excitations are electron–hole pairs with small energy. The production of a large number of these excitations leads to the importance of the many-particle intermediate states.

We discuss first the problem of infrared divergencies and then its application to the Kondo effect. The investigation of the latter problem was started using different approaches.

(i) Anderson *et al* outlined a scaling theory for thermodynamical quantities in a series of papers (Yuval and Anderson 1970, Anderson *et al* 1970a,b, Anderson and Yuval 1971), and the Kondo problem was related to one-dimensional models. This approach will be discussed in §6.3.

(ii) Using the diagram representation Fazekas and Zawadowski (1969) demonstrated that one has to go beyond the parquet approximation. Furthermore, Maleev (1969) included electron–hole pairs in his dispersion theory. This line, to be discussed in §6.4, has been developed by making use of dynamical renormalization groups (Zawadowski and Fowler 1970, Abrikosov and Migdal 1970).

(iii) Wilson's recent contribution to the phase transition theory (see Wilson and Kogut 1974), which is based on renormalization groups, was followed by a numerical treatment of the Kondo effect with great success. We discuss this approach in §6.5.

6.2. Infrared divergencies

In order to demonstrate the origin of the infrared divergencies occurring in different physical problems, Anderson (1967b) considered the very simple case of a non-interacting electron gas in a well-localized impurity potential V (see hamiltonian (4.6)), and thereafter he compared the ground states corresponding to the cases $V \neq 0$ and $V = 0$. The instructive conclusion was that these two ground states have only a small overlap which goes to zero as $\Omega^{-\epsilon}$ ($\epsilon > 0$) if the volume of the electron gas tends to infinity. Thus in the case $\Omega = \infty$ the ground states are orthogonal to each other. This orthogonality is due to the fact that the ground state with potential can be expressed in terms of the unperturbed free-electron states, and the electron–hole pair excitations occur with large relative amplitudes, because these pairs can be excited with arbitrary small energies. One may conclude that if a localized potential is suddenly changed then in the rearrangement of the electron gas an infinite number of electron–hole pairs are involved. The infrared divergencies have been presented by Hopfield (1969) in a simple manner. Mahan (1967) has proposed a simple physical problem where this phenomenon results in measurable quantities, namely x-ray absorption. In a metal the x-ray absorption problem means that a deep-lying electron of an atom is excited by x-rays into the continuum

above the Fermi level. The potential representing the atom is changed, and due to this process a new arrangement in the electron gas is set up to screen this potential. The time dependence of the rearrangement is reflected in the x-ray absorption spectrum near the threshold and shows a particular asymptotic behaviour; namely; the remainder of the old arrangement dies out according to some power function $1/t^\alpha$ instead of the exponential $\exp(-\alpha' t)$ expected in general.

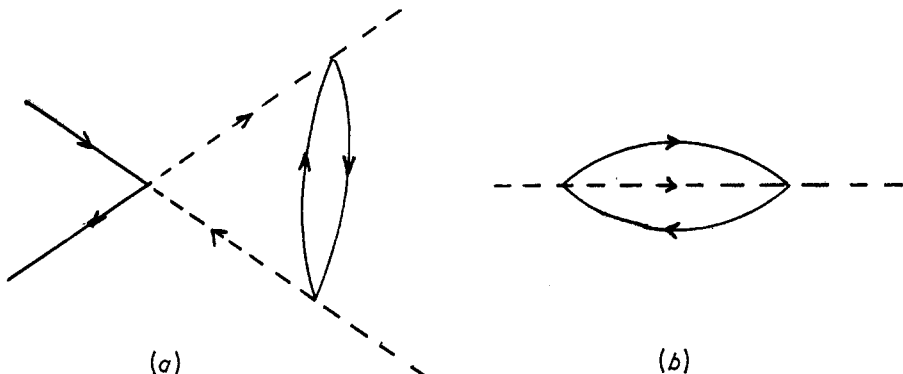


Figure 26. (a) Self-energy and (b) vertex corrections which are not included in the parquet approximation to third order of perturbation theory.

The theoretical formulation of this problem has a strong resemblance to Abrikosov's pseudofermion representation of the impurity spin in the Kondo problem (see § 4.3); the deep-lying electron corresponds to the pseudofermion but without $(2S + 1)$ -fold spin degeneracy, and the interaction between the deep-lying electron and the conduction electron is spin-independent. Nozières and others (Roulet *et al* 1969, Nozières *et al* 1969) developed a theory based on diagram technique where not only the leading logarithmic but also the next leading terms are considered. Starting from perturbation theory the vertex corrections due to parquet diagrams cancel each other, as has already been demonstrated in § 4.2 for the scattering amplitude in second order. Moreover, additional vertex and self-energy corrections occur in third order of perturbation theory; these diagrams are shown in figure 26. These diagrams give the skeletons for Nozières's self-consistent theory. It is important to mention that in the x-ray problem the vertex and self-energy corrections cancel each other, again due to an exact identity of the Ward type. Thus the strength of the scattering is not enhanced as it is for resonant scattering. In order to demonstrate the typical analytical functional forms achieved in the x-ray absorption problem, we refer to the deep-electron Green function given by Nozières *et al* (1969):

$$G(\omega) = -\frac{1}{\omega} \left(\frac{\omega}{D} \right)^{g^2} \quad (6.1)$$

where ω is the energy measured from the absorption edge, the coupling g is proportional to the potential change, and D is the width of the conduction band. The correction to the free propagator $G^{(0)}(\omega) = (-1/\omega)(g = 0)$ shows up as a result of the summation of typical logarithmic terms, namely

$$\left(\frac{\omega}{D} \right)^{g^2} = \exp \left[g^2 \ln \left(\frac{\omega}{D} \right) \right] = \sum_{n=0}^{\infty} \frac{1}{n!} g^{2n} \ln^n \left(\frac{\omega}{D} \right). \quad (6.2)$$

This formula demonstrates how the summation of logarithmic terms results in simple power behaviour.

A more detailed study of the question given by Nozières and de Dominicis (1969) shows that the x-ray absorption is actually a one-body problem where the non-interacting electrons move in a time-dependent potential associated with the excitation of the deep electron, and this becomes obvious in time-dependent representation but is not trivial in energy representation. In this problem no resonance occurs. The time-dependent problem was solved exactly by Nozières and de Dominicis, and the results obtained are similar to those derived by perturbation theory if the coupling is replaced by δ/π , where the phase shift δ corresponds to the scattering on the potential change. The response function of the x-ray absorption which was derived is exact in the asymptotic region with respect to the time variable, and the correction term due to the potential change can be written as

$$(iDt)^{2\delta/\pi - \delta^2/\pi^2}. \quad (6.3)$$

This again exhibits typical power behaviour. This correction, however, is asymptotic, because at small times $t \sim 1/D$ the shape of the conduction band has an important role, and this cut-off problem was treated in an oversimplified way. Finally, we mention that for strong coupling the diagram technique breaks down, because further classes of diagrams enter into the problem, and already the 'envelope' diagram shown in figure 27 is not included. Thus the extension of the theory in a diagrammatic way seems to be too complicated.

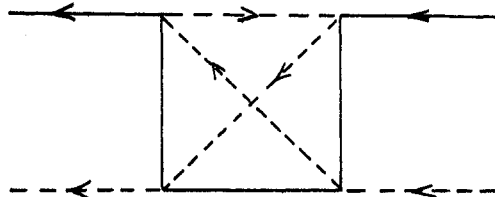


Figure 27. The 'envelope' diagram which is beyond the scope of the x-ray absorption theory worked out by Nozières *et al* (1969).

6.3. Thermodynamical scaling

Anderson and Yuval (Yuval and Anderson 1970, Anderson *et al* 1970a) called attention to the importance of the infrared divergencies in the Kondo effect, arguing in the following way. First of all an anisotropic Kondo model was introduced where the two terms in the hamiltonian (4.4) have different amplitudes; thus

$$H_1 = H_z + H_{\pm} \quad (6.4)$$

where

$$H_z = -J_z \sum_{kk'} S^z(a_{k'\uparrow}^+ a_{k\uparrow} - a_{k'\downarrow}^- a_{k\downarrow}) \quad (6.5)$$

$$H_{\pm} = -J_{\pm} \sum_{kk'} (S^+ a_{k'\downarrow}^+ a_{k\uparrow} + S^- a_{k'\uparrow}^+ a_{k\downarrow}) \quad (6.6)$$

with coupling constants J_z and J_{\pm} for the spin-conserving and spin-flip terms respectively. (In Anderson's work the coupling constants introduced are different by a factor of -2 .) If the z component of the spin is fixed then H_z has an effect on the electron gas like a spin-dependent static impurity potential. The spin-flip due to H_{\pm} is associated with a sudden change of the potential. Therefore one spin-flip

corresponds to the problem discussed by Nozières and de Dominicis (1969) in connection with the x-ray absorption. Their exact asymptotic solution can be applied directly. In the Kondo problem, however, there is a sequence of spin-flip processes, and the necessary generalization was given by Yuval and Anderson (1970) in a very elegant mathematical form working with determinants built up from time-dependent Green functions. They succeeded in giving the partition function in a closed form by evaluating those determinants. The result can be written as

$$\text{Tr} [\exp(-\beta H)]$$

$$= \sum_{n=0}^{\infty} J_{\pm}^{2n} \int_0^{\beta} d\beta_{2n} \int_0^{\beta_{2n}-\tau} d\beta_{2n-1} \times \dots \times \int_0^{\beta_2-\tau} d\beta_1 \exp \left[\sum_{i>j} (-1)^{i-j} (2-\epsilon) \ln \left(\frac{\beta_i - \beta_j}{\tau} \right) \right] \quad (6.7)$$

with

$$\epsilon = 8 \frac{\delta_{\uparrow\downarrow} - \delta_{\uparrow\uparrow}}{\pi} - 2 \left(\frac{\delta_{\uparrow\downarrow} - \delta_{\uparrow\uparrow}}{\pi} \right)^2 \quad (6.8)$$

where $\delta_{\uparrow\uparrow}$ and $\delta_{\uparrow\downarrow}$ are the conduction electron phase shifts in the cases where the conduction electron spin is parallel and antiparallel to the impurity spin, and $\delta_{\uparrow\downarrow}$ and $\delta_{\uparrow\uparrow}$ depend only on J_z . The partition function is given as a product of integrals. As we have already mentioned at the end of the previous section, the solution given by Nozières and de Dominicis breaks down at short times $\tau \sim D^{-1}$ because of the approximate cut-off procedure applied. In order to avoid this difficulty time intervals proceeding the spin-flips are eliminated by modifying the upper limits of the integrals. The approximate nature of this procedure does not lead to any serious problem insofar as the total length of these spurious intervals is negligible compared with the total path of the integrals; thus the spin-flips are not too frequent. Studying the form of the partition function given by equation (6.7) Anderson and Yuval realized that this partition function corresponds to a classical problem at the same time.

In this classical problem a line of length β is divided into rods alternatively charged with positive and negative signs. The interaction between the charges shows logarithmic dependence on the distance as $(-1)^{i-j} \ln(|\beta_i - \beta_j|/\tau)$, and the strength of the interaction is given by $2 - \epsilon$. The 'chemical potential' for the boundary points is proportional to the spin-flip amplitude J_{\pm} standing in front of the integrals. Although the classical problem looks very simple, this partition function cannot be treated exactly. It is interesting to note that by transforming the integrals into sums, a one-dimensional Ising problem is achieved (Anderson and Yuval 1971) with long-range interaction of type $1/r^2$ associated with next-neighbour interaction as well, which has interest on its own right.

In order to study this partition function Anderson and Yuval turned to the scaling with respect to the conduction electron band width, ie the inverse of the short time cut-off τ^{-1} . The idea is to change τ by $d\tau$ and afterwards to modify the coupling strengths J_{\pm} and ϵ in such a way that the partition function remains invariant. This program was worked out and it can be presented in a very simple way (see Anderson *et al* 1970b). However, here we restrict ourselves to the discussion of the scaling properties, which are given by the scaling equations

$$d\epsilon = [(2 - \epsilon)^2 / (2 - \epsilon_0)] (2J_{\pm}\tau)^2 d\tau / \tau \quad (6.9)$$

$$d \ln (J_{\pm}^2 \tau^2) = \epsilon d\tau / \tau \quad (6.10)$$

where in the weak coupling limit $\epsilon = 4J_z\tau$, and $\epsilon_0^2 = \epsilon^2 - (4J_{\pm}\tau)^2$ is an invariant quantity under the scaling. The scaling curves are shown in figure 28 with arrows indicating the direction of increasing τ . The isotropic case scales along the straight lines, and for ferromagnetic coupling the scaling goes towards the weak coupling limit. In the antiferromagnetic case, however, it goes towards the strong coupling regime.

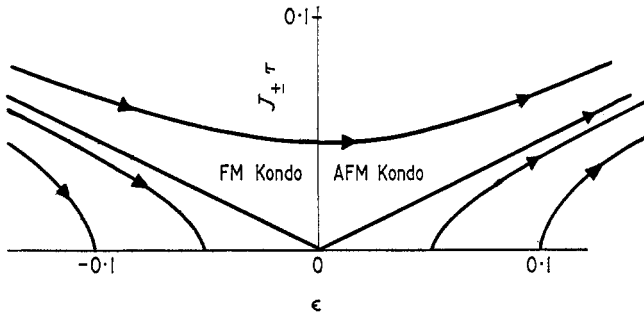


Figure 28. Anderson-Yuval scaling curves for the anisotropic Kondo problem. The straight line corresponds to the isotropic case and the arrows indicate the scaling directions.

The scaling curves below the straight lines connect an Ising-type model ($J_{\pm} = 0$) with the anisotropic Kondo problem. The Anderson-Yuval scaling is exact in the weak coupling limit, but with increasing coupling strength the spin-flip processes become dense in expression (6.7), and a more accurate treatment of the cut-off may be required as was emphasized by Anderson *et al* (1970a). This problem will be discussed in § 6.7 in connection with the value of the Kondo temperature.

The most important consequence of this scaling theory is that the coupling strength becomes infinite along the antiferromagnetic scaling lines. The argument is based on the fact that the problem is related to one-dimensional problems in which there should not be any singular behaviour at finite coupling. Thus there is no singular point on the scaling plane in which the curves may end, and they may therefore go to infinity (see eg Anderson 1972, Fowler 1972). This relies on the plausible assumption that the connection between the Kondo problem and one-dimensional systems holds even in the strong coupling limit.

Finally, we should mention that studying the special case of $\epsilon = 1$ Toulouse (1969) realized that this limit is exactly solvable. This 'Toulouse limit' can be represented by a vertical line on the antiferromagnetic side of the scaling plane somewhere in the medium strong coupling regime of J_z . It is believed that the scaling into the 'Toulouse limit' may be a key to solve the Kondo problem. Numerical predictions, however, have not yet been obtained in that way. The situation becomes more complicated by the fact that it is not clear how accurate expression (6.7) itself is in the strong coupling limit (cut-off procedure).

Emery and Luther (1971) worked out a theory which is in many senses similar to those discussed above. However, there are smaller discrepancies as well. They transformed the problem into another one where the spin is interacting with a boson field, and the treatment is based on the long-time approximation introduced by Nozières and de Dominicis (1969).

6.4. Diagram techniques and the dynamical renormalization group

In order to include the effect of more than one particle in the intermediate states, different techniques have been developed, among others the Nozières'

generalized ‘self-consistent parquet’ approximation and the different versions of the dynamical renormalization group method, but only the most efficient of these will be discussed.

At an early stage of the application of the diagram technique going beyond the simple parquet approximation it became obvious that the self-energy and vertex corrections of the type given in figure 27 yield essential corrections. For example, Fazekas and Zawadowski (1969) and Zawadowski and Fazekas (1969, 1970) concluded that as a consequence the strength of the Abrikosov divergency discussed in §§ 4.4 and 4.5 (see eg expression (4.23)) must be reduced. For $T \gg T_K$ this reduction was given by a temperature-dependent coupling constant to be inserted into Abrikosov’s vertex function given by equation (4.27) as $J\mu_{\text{eff}}(T)/\mu_B$, where $\mu_{\text{eff}}(T)$ is the screened magnetic moment given by expression (4.27). It is important to note that the self-energy and vertex corrections given in figure 26 do not cancel each other in the Kondo problem as they do in x-ray absorption. Actually, a Ward identity can be proved again, but because of different spin factors, $S(S+1)$ and $1 - S(S+1)$, the cancellation is not complete (Zawadowski and Fazekas 1970). This is due to the fact that in the Kondo problem a resonance is formed, while it is not in the x-ray absorption situation.

A complete theory closely following the diagram technique (Nozières *et al* 1969) applied to the x-ray absorption problem was worked out by Nozières and Abrahams (unpublished), where the next leading logarithmic approximation based on the skeleton diagrams shown in figure 27 was performed in a self-consistent way. This method is frequently called the ‘self-consistent parquet approximation’. In this theory the product of the correction factor $d(\omega) = G(\omega)/G^{(0)}(\omega)$ to the pseudofermion Green function $G(\omega)$, the vertex function $\Gamma(\omega)$ and the exchange coupling J plays the role of an effective coupling strength

$$J_{\text{eff}}(\omega) = J\Gamma(\omega) d(\omega) \rho_0 \quad (6.11)$$

where ρ_0 is the density of states of the conduction electrons, and in the vertex function $\Gamma(\omega)$ only the pseudofermion variable ω is kept. This quantity is enhanced as the energy and the temperature decrease, and goes to $J_{\text{eff}} = 2$ at $\omega = 0$ and $T = 0$. This already indicates that all of the diagrams must be simultaneously considered, and therefore the diagram technique breaks down at low temperatures. Furthermore, the result for the vertex violates the unitarity limit as the imaginary parts are completely neglected. The most important conclusion is that the logarithmic behaviour disappears at low temperatures as in the x-ray absorption problem (see eg equation (6.1)), and a power dependence is left. The Nozières method has been applied to the Kondo problem by several other authors, among them Murata (1971) and Fukushima (1971). It is worth mentioning that these theories provide a T^2 dependence for the low-temperature resistivity, but this square form is rather dubious because it relies entirely on the self-consistent parquet approximation which breaks down there. To include the imaginary parts as well seems to be a rather hopeless problem, at least in this theory.

To sum up a certain class of diagrams in logarithmic problems the renormalization group method is very adequate (Bogoliubov and Shirkov 1959), and it may lead to scaling. On the other hand, Anderson (1970) has suggested a very simple scaling idea. First, because of its simplicity, this elementary scaling will be presented in a form generalized by Sólyom and Zawadowski (1974) to make it capable of taking into account many-particle intermediate states.

The conduction electron scattering amplitude is considered in Schrödinger perturbation theory, and the amplitude is normalized according to the norm of the initial and final states $|i\rangle$ and $|f\rangle$ with momenta k and k' near the Fermi surface. This normalized scattering amplitude is

$$T(\omega/D; J_{\pm}, J_z) = \frac{\left\langle f \left| \sum_{n=0}^{\infty} H_1 \{ [1/(\omega - H_0)] H_1 \}^n \right| i \right\rangle}{\left(\left\langle f \left| \sum_{n=0}^{\infty} \{ [1/(\omega - H_0)] H_1 \}^n \right| f \right\rangle \left\langle i \left| \sum_{n=0}^0 \{ [1/(\omega - H_0)] H_1 \}^n \right| i \right\rangle \right)^{1/2}}. \quad (6.12)$$

This quantity is closely related to the effective coupling given by equation (6.11). The scaling idea for a fixed energy ω can be formulated as a change of the conduction electron band width and the coupling constants by ΔD and ΔJ_{\pm} , ΔJ_z respectively, in such a way that the normalized scattering amplitude remains invariant; thus

$$\frac{\partial T(\omega/D; J_{\pm}, J_z)}{\partial D} \Delta D + \frac{\partial T(\omega/D; J_{\pm}, J_z)}{\partial J_{\pm}} \Delta J_{\pm} + \frac{\partial T(\omega/D; J_{\pm}, J_z)}{\partial J_z} \Delta J_z = 0. \quad (6.13)$$

These equations (one in the isotropic and two in the anisotropic case) establish the scaling. If the derivatives are known, effective ω/D -dependent coupling constants can be defined as the solutions of this equation, which agree for $J_{\pm} = J_z$ with the one introduced by equation (6.11). These derivatives are calculated in Schrödinger perturbation theory. The first-order scaling is achieved by calculating the numerator of expression (6.12) up to second order, and the effective coupling obtained is equivalent to the spin-flip scattering amplitude in Abrikosov's theory, and furthermore in the weak coupling limit to that derived in the Anderson-Yuval theory. In second-order scaling the numerator is calculated up to third order and the denominator up to second order; thus the diagrams in figure 27 are included as well. The differential equation obtained, for example, for the isotropic case is

$$\frac{\partial}{\partial \ln(D/\omega)} J_{\text{eff}}\left(\frac{\omega}{D}\right) = - \left[J_{\text{eff}}\left(\frac{\omega}{D}\right) - \frac{1}{2} J_{\text{eff}}^2\left(\frac{\omega}{D}\right) \right] \quad (6.14)$$

and the solution of this equation remains finite in the whole energy interval, as is shown by figure 29. Furthermore, its behaviour is smoother than the Abrikosov first-order scaling, in agreement with the expectation discussed at the beginning of the present section.

The scaling idea can be summarized in such a way that the problem with large $\ln(\omega/D)$ and small J is equivalent to another one where $\ln(\omega/D)$ is not so large but J becomes larger. The scaling can be formulated in terms of energy and cut-off as well, and the temperature dependence is similar to the energy dependence. As with the summation of diagrams (eg the self-consistent parquet approximation), the dynamical scaling also breaks down at large effective coupling, and thus at small energy and low temperature since the coefficients of equation (6.13) are calculated by using perturbation theory. It may be mentioned that in the anisotropic case there is a singular point on the antiferromagnetic side of the scaling plane where all the scaling curves concur. The existence of such a singular point is rather dubious (see the discussion at the end of §6.3). Furthermore, by solving equation (6.14) for small energies it can be demonstrated that the logarithmic behaviour is changed

to power T^2 and ω^2 dependence at $\omega = 0$ and $T = 0$, but the square dependence is again doubtful.

Historically, the second-order scaling was first derived on the basis of renormalization groups by Zawadowski and Fowler (1970) and Abrikosov and Migdal (1970). The method was suggested by Gell-Mann and Low (see Bogoliubov and Shirkov 1959), and it has been proved to be very adequate in the case of logarithmic problems where scaling occurs (for a review see Zawadowski 1973). The main idea is as follows.

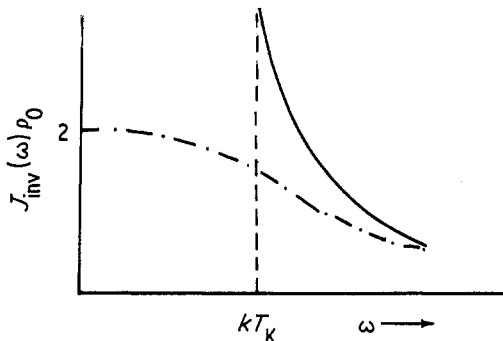


Figure 29. The invariant coupling as a function of the energy in the dynamical scaling law. Chain curve: Abrikosov's result. Full curve: result obtained with infinitesimal generator calculated up to second order.

The quantities in a Green function theory such as the vertex $\Gamma(\omega)$ pseudofermion and electron Green functions, $G(\omega)$ and $G'(\omega)$ respectively, and also the coupling constant J are multiplied by arbitrary constant factors Z_1 , Z_2 and Z_3 in the following way

$$G \rightarrow Z_1 G, \quad G' \rightarrow Z_2 G', \quad \Gamma \rightarrow Z_3^{-1} \Gamma \quad \text{and} \quad J \rightarrow Z_3 Z_1^{-1} Z_2^{-1} J \quad (6.15)$$

and this transformation leaves the mathematical structure of the theory invariant. This transformation forms a continuous symmetry group, and the properties of this group are used. In logarithmic problems the analytical form of the new quantities is not altered by the transformation if the effective coupling defined by equation (6.11) and a new cut-off D' are introduced; thus, for example, for the function $d(\omega)$

$$d\left(\frac{\omega}{D'}, J_{\text{eff}}\left(\frac{\omega}{D}\right)\right) = Z_1 d\left(\frac{\omega}{D}, J\right). \quad (6.16)$$

As shown by Sólyom, this equation with energy-independent Z holds even if the imaginary parts are included. For a continuous group the infinitesimal transformation can be cast into the form of a Lie equation, which is given here for the effective coupling (frequently called invariant coupling) itself:

$$\frac{\partial}{\partial \ln(\omega/D)} \ln J_{\text{eff}}\left(\frac{\omega}{D}; J\right) = \frac{\partial}{\partial \xi} \left[\ln J_{\text{eff}}\left(\xi; J_{\text{eff}}\left(\frac{\omega}{D}, J\right)\right) \right]_{\xi=1}. \quad (6.17)$$

The expression on the right-hand side of this equation is the infinitesimal generator of the group, where the effective coupling constant occurs in the argument. The actual calculation requires us (i) to calculate the generator for those cut-off values where $D \sim \omega$, and (ii) to solve this equation. The main difficulty is that the infinitesimal generator can be determined only in the framework of perturbation theory; thus

$|J_{\text{eff}}(\omega/D, J)| \ll 1$ is assumed. In second-order scaling the diagrams in figures 10 and 27 are considered (see eg Fowler and Zawadowski 1971), and the scaling given by equation (6.14) is recovered.

It is worth mentioning that recently Sakurai and Yoshimori (1973) combined the most advanced variational calculation for the ground state with the dynamical renormalization group discussed before, and the following ground state energy was derived:

$$E_B = -D(J\rho_0/N)^{1/2} \exp(N/2J\rho_0). \quad (6.18)$$

The ground state energy is associated with the Kondo temperature, as it scales the temperature dependence.

The result obtained is in accordance with the expectation discussed at the beginning of this section, because it is much smaller than the Abrikosov expression $kT_K \sim D \exp(N/2J\rho_0)$ derived in the leading logarithmic approximation. For further discussion see § 6.7.

Several consequences of finite J_{eff} at $\omega = T = 0$ have been discussed by Abrikosov and Migdal (1970). The dispersion theories with electron-hole pairs in the intermediate state (see Maleev 1969, 1971, Hübel 1973) seem to be even more complicated, and it is hard to get reliable results. In general the most striking question is whether the effective coupling tends to infinity or remains finite as ω and T tend to zero or, in other words, whether there are singular points on the scaling plane or not, depending on whether the infinitesimal generator has not or has zeros. This question cannot be settled in the present schema, because in the case of strong coupling these methods break down, as has been discussed before. The arguments at the end of § 6.4 and Wilson's theory to be discussed in the next section favour no singularity.

6.5. Wilson's theory

Wilson (1973), realizing that renormalization group methods discussed in the previous section are not capable of solving the question whether the effective coupling remains finite at $T = 0$ and $\omega = 0$ or not, has turned to a new formulation of the problem which allows one to combine the renormalization group method with numerical computer calculations. It is obvious that such a method should not rely on diagram representation. Wilson's aim was to establish a wavefunction calculation for the ground state and its low-lying excitations and to determine the eigenvalues by some numerical iteration procedure.

First of all he modified the Kondo model to fit his purposes. It was done in three steps:

(i) A discreteness is introduced in the wavenumber of the conduction electron as $(k - k_F) \sim \pm \Lambda^{-n}$, where Λ is an arbitrary number of the order of two, and n is the new quantum number. By this step the conduction electron density of states is distorted, and this distortion is compensated by making the coupling n -dependent in such a way that the contribution of the low-lying energy states (in the neighbourhood of the Fermi energy) to the free energy is not altered. The hamiltonian considered is

$$H = \sum_{n=0,\sigma}^{\infty} \Lambda^{-n} (a_{n\sigma}^+ a_{n\sigma} - b_{n\sigma}^+ b_{n\sigma}) - J(A^+ \sigma A) S \quad (6.19)$$

where

$$A_\sigma = \sum_{n=0}^{\infty} \Lambda^{-n/2} (a_{n\sigma} + b_{n\sigma}) \quad (6.20)$$

$a_{n\sigma}$ and $b_{n\sigma}$ are the electron and hole annihilation operators, and S describes $S = \frac{1}{2}$.

(ii) A new set of basis functions is constructed by an iteration procedure in order to achieve a hopping hamiltonian

$$H = \sum_{n=0,\sigma}^{\infty} \Lambda^{-n/2} \epsilon_n (f_{n\sigma}^+ f_{n+1\sigma}^- + f_{n+1\sigma}^+ f_{n\sigma}^-) - J(f_0^+ \sigma f_0^-) \quad (6.21)$$

where $f_{n\sigma}^+$ is the creation operator on site n , and $A_\sigma \sim f_{0\sigma}$. This hamiltonian has the form of a linear chain with sites labelled by n : the first term describes the hopping between different sites, while the second term shows that the impurity spin is coupled with those electrons sitting on site '0'.

(iii) In a good approximation $\epsilon_n = 1$.

The main idea is that the hopping elements far from the spin do not modify the spectrum in an essential way. Keeping only a few neighbours of the spin, to retain only about 200–500 states, one could diagonalize the problem by computer. In the following step one more neighbour is included and about 100–300 states are dropped from those which have already been computed to keep the states of lowest energy values with the same number as in the previous step. Diagonalizing again and again by performing 50–80 iterations, a reliable energy spectrum is obtained. Without going into details of the computation and accuracy, we confine ourselves only to the conclusion. The spectrum obtained was compared with that which corresponds to a similar hamiltonian but without the spin S and site $n = 0$. It turns out that these two spectra coincide with great accuracy for the lowest states.

This result can be interpreted as if the impurity and the electron on site $n = 0$ were glued together with infinite coupling $J_{\text{eff}}(\omega = 0) = \infty$ to form a singlet. The other electrons behave like a free gas because their energy is not strong enough to break this singlet formed on site $n = 0$.

In order to describe the excited states Wilson introduced a phenomenological extra hamiltonian acting on the electron gas but not on the singlet. The parameters of this pseudohamiltonian have been fitted to reproduce the spectrum calculated numerically, and afterwards this spectrum has been extrapolated to excitations with higher energies. In this way the heat capacity $C_{\text{imp}}(T = 0)$ and the magnetic susceptibility have been evaluated as well. The result can be summarized as

$$\chi_{\text{imp}}(T = 0) \simeq \frac{1}{D} \frac{1}{(2J\rho_0)^{1/2}} \exp\left(\frac{1}{2J\rho_0} + 1.58(2J\rho_0)\right) \quad (6.22)$$

and

$$\lim_{T \rightarrow 0} \frac{C_{\text{imp}}(T)}{T\chi_{\text{imp}}(T)} = \frac{2\pi^2}{3} (1 \pm 0.3) k_B \quad (6.23)$$

where k_B is Boltzmann's constant. This J dependence is a result of the numerical fit of data obtained with different coupling strengths J .

Wilson's theory indicates strongly that in the scaling theories J_{eff} should increase beyond any limit, and that is widely accepted as the final answer.

The question of the Kondo temperature is left to § 6.7. Furthermore, it is still not clear what is the meaning of the 'Toulouse limit' in this theory.

6.6. Functional integral method

It was hoped that the functional integral method would fill the gap between the theories based on the s-d and Anderson models. The starting point is a mathematical identity

$$\exp(a^2) = \int_{-\infty}^{\infty} dx \exp(-\pi x^2 - 2\pi^{1/2} ax) \quad (6.24)$$

which holds even if a is an operator. This formula gives the possibility of linearizing a squared term in an exponent, but an additional integral occurs.

This formula may be applied to the calculation of the partition function

$$Z \sim \left\langle T_\tau \exp\left(-\int_0^\beta d\tau H_1(\tau)\right) \right\rangle \quad (6.25)$$

where $\beta = 1/kT$ and τ is the complex time variable; furthermore, the interaction hamiltonian is given in the interaction representation. When the integral is with respect to τ in the partition function in equation (6.24), a will be τ -dependent and thus the integral becomes a functional integral.

The Anderson model is very appropriate for applying this identity as the Coulomb integral term $U n_{d\uparrow} n_{d\downarrow}$ can be written in the form of squared expressions in different ways; for example,

$$U n_{d\uparrow} n_{d\downarrow} = \frac{1}{4} U(n_{d\uparrow} + n_{d\downarrow})^2 - \frac{1}{4} U(n_{d\uparrow} - n_{d\downarrow})^2. \quad (6.26)$$

Applying the identity discussed above for both terms, a double functional integral is obtained. The idea behind this formal step is that the interaction can be replaced by the problem of free particles moving in fluctuating classical fields acting on the combinations $n_{d\uparrow} + n_{d\downarrow}$ and $n_{d\uparrow} - n_{d\downarrow}$. Thus two fields act on the charge and magnetization fluctuations respectively.

There are, however, statistical weights for the different field fluctuations to control the dynamical behaviour. In actual cases it is very hard to perform the functional integrals. The method in the context of the Anderson model was used by Evenson *et al* (1970) and Hamann (1970). The first success has been that the HF solution can be easily recovered by restricting the possible paths to the time-independent one. It turned out, however, that it is very difficult to reproduce even a single logarithmic term by this method (see discussion and further references in Amit and Keiter 1973). On the other hand, in the strongly magnetic regime of the Anderson model, Hamann (1970) succeeded in relating this method to the Anderson-Yuval-Hamann scaling (see § 6.3) by evaluating the functional integral in a particular regime of the paths which correspond to the spin-flip scattering. Furthermore, Hertz (1971) applied this method in the non-magnetic regime of the Anderson model to achieve scaling by eliminating the contribution of the highest-frequency random field from the functional integral; for further discussion see § 3.4. In spite of this success, the results remained far from expectation. We may finally mention that Yoshimori and Sakurai (1970) applied this method to the s-d model and the most divergent terms were reproduced.

6.7. Some comparisons and some problems to be solved

Concerning the Anderson model, the theoretical part of the problem has not been developed in a satisfactory manner. The study of the s-d model, however, has reached a stage where the phenomena are already well understood and the theoretical description has improved in a significant way.

By taking the excitation of electron-hole pairs into consideration it has been demonstrated at least that the high-temperature logarithmic behaviour is changing to a power dependence at low temperatures. The weak coupling problem becomes stronger by decreasing the temperature, and according to the new developments in the theory the effective coupling tends to infinity at $T = \omega = 0$. The characteristic temperature where the stronger effective coupling enters can be called the Kondo temperature. Starting from high temperature the new T_K can be defined as the temperature where according to the dynamical scaling laws (equation (6.14)) the medium strong coupling occurs; for example, where $0.2 < J_{\text{eff}} < 0.5$. This can be easily determined by using equation (6.14) and calculating the corresponding energy value $\omega = kT_K^{\text{new}}$; thus one finds

$$kT_K^{\text{new}} \approx D(2J\rho_0/N)^{1/2} \exp(N/2J\rho_0). \quad (6.27)$$

This expression seems to be in agreement with the expression for the binding energy E_B derived by Sakurai and Yoshimori (1973) given by equation (6.18), and also with the susceptibility fitting Wilson's numerical results (see equation (6.22)), as the binding energy and the inverse susceptibility are expected to be proportional to the characteristic scaling temperature. It disagrees, however, with the expression published first of that type obtained from the thermodynamical scaling laws by Anderson and Armytage (Anderson 1972), where the factor $(2J\rho_0/N)^{1/2}$ is replaced by $(2J\rho_0/N)^{3/2}$. This is probably due to the approximate treatment of the cut-off procedure, which may play a crucial role in the case of stronger coupling. Summarizing this result, we may conclude that in the weak coupling limit the expression given above is correct and it predicts a much smaller Kondo temperature than that occurring in the one-particle intermediate state approach (see equation (4.27)).

For low temperatures the dynamics has not yet been worked out. On the basis of Wilson's new result that at $T = 0$ the impurity is 'glued' to the electron at the site $n = 0$ in the hopping model, it is expected that at $T = 0$ all the physical properties are analytical, and simple power expansions are adequate. Hence the electrical resistivity should be given by a simple Sommerfeld expansion, and show a T^2 dependence (see for further discussion Anderson 1972, Fowler 1972). This behaviour at low temperatures may be ascribed to spin fluctuations, in the sense that thermal fluctuations in the Kondo state result in the appearance of a small magnetic moment, and has parallels with the T^2 dependence in the LSF theory based on the existence of localized paramagnons (see discussion in § 3.3). It must, however, be emphasized that the detailed dynamics producing the resonance with lorentzian behaviour at small energies is rather different in the two theories. Therefore, although there are formal similarities and in both cases there are thermal fluctuations in non-magnetic states, the ground states in the two models are so different that the parameters of the resonances can be connected only in a formal way which has no physical ground.

The main task for the future is to find a theoretical description of and more detailed justification for the lorentzian behaviour at the top of the Abrikosov-Suhl resonance.

7. Conclusions

In this review we have confined ourselves to those aspects of the dilute alloy problem which are important for an understanding of the resonance formation, and

therefore many questions, rather interesting in their own right, have not been discussed as they are not related directly to this problem.

In particular, the behaviour of the impurities in a superconducting metal has not been mentioned, mainly because it appears that the formation of the resonances is the result of more complicated processes than in normal metals, as the host density of states exhibits a characteristic structure (the energy gap) near the Fermi energy, and a high density of states near to the threshold of the gap. As the Kondo temperature can be larger or smaller than the superconducting transition temperature T_c , widely variable phenomena are expected (and found) depending on the ratio of the two characteristic temperatures. The experimental status is reviewed by Rizzuto (1974) and Maple (1973); the theoretical developments by Müller-Hartmann (1973). Another field which has attracted wide interest, but was not discussed here, is that of metal/metal-oxide/metal junctions with paramagnetic impurities in or near the barrier. The physical phenomena are two-fold: the impurity-assisted tunnelling suggested by Appelbaum (1966) and the change of the electron density of states near to or in the impurity layer; the latter can be discussed in a way similar to that for a single impurity (for references see Mezei and Zawadowski 1971b). The sample preparation, however, is rather difficult, and therefore the real cause of the anomalies found in the I - V characteristics is still unclear. Relaxation phenomena in dilute alloys have also not been discussed, in spite of a belief, held for a long time, that these phenomena can give rather valuable information on the dynamical behaviour of the impurities. It appears, however, that the s-d interaction does not have a dominant role here, because the spins of the impurity and the conduction electrons enter into the dynamics as a whole, if the gyromagnetic factors are the same; this effect is known as 'bottleneck'. The experiments, however, give information on the spin-lattice relaxation (see eg Monod and Schultz 1968). The same can be said for the dynamical susceptibility (see Götze and Schlottmann 1973 and references cited therein), which is connected with the neutron scattering experiments, which should show a maximum at energy transfers near kT_K (Gurgenishvili *et al* 1969). The effect of a magnetic field on the Kondo scattering was also not reviewed, and the giant negative magnetoresistance has only been mentioned. It is clear, however, that an external magnetic field makes the spin-flip scattering inelastic, and therefore the effect of external fields should show up in side bands near the energy μH ; the internal magnetic field due to impurity-impurity interactions leads to similar effects.

The other aspect which has been left out is the influence of anisotropy, crystalline field splitting, spin-orbit interaction, and the influence of the orbital degeneracy on the Kondo scattering. It appears that while these effects may lead to a slight modification of the scattering problem, they do not play such a crucial role here as for impurities with an unfilled 4f shell. Furthermore, it appears that the orbital degeneracy is not fundamental and the non-degenerate model works well if one replaces U by $U+4J$, although the theoretical justification for this is not perfectly clear.

Phenomenological models which attempt to account for the Kondo behaviour should also be mentioned; in particular Souletie (1972) and Loram *et al* (1972) have suggested that the temperature dependences of the transport properties can be described by temperature-dependent phase shifts $\delta_\phi(T)$, which correspond to the non-magnetic HF solution at $T = 0$ and to a magnetic HF solution at $T \gg T_K$. It is clear that a phase shift analysis works at zero temperature, and also gives some

information on the scattering at very high temperatures when spin-flip is properly included. A description in terms of phase shifts is, however, questionable at low temperatures, if it is used to account for temperature-dependent effects. Assuming that the scattering amplitude is an analytic function of T around 0 K, one can make a power expansion of equation (4.34). Keeping only the one-particle scattering amplitudes, the temperature dependence has a leading T^2 term, and furthermore if $|\tau|^2$ can be neglected in (4.34) then $|t|$ can be expressed in terms of the phase shift $\delta(T)$, which means that τ does not contain linear terms. This, however, has no firm theoretical background.

Although many theoretical details of the Kondo problem are still unsolved, we believe that the formation and the nature of the narrow and broad resonances are basically understood. Among questions which still await a solution, the experimental evidence for the spatial distribution of the conduction electron-impurity spin correlation function discussed in §4.10 should be mentioned. Theoretically the most important problem remaining is to work out the dynamical scaling laws in order to describe the t of the Abrikosov-Shul resonance and to justify its T^2 or ω^2 dependence; such a calculation would also give the electrical resistivity for example.

Finally one should stress that although the dilute alloy problem can be regarded as perhaps the most beautiful example of how localization and delocalization occur, and how single-particle and many-particle resonances combine together, the main concepts are not unique to this problem and can be applied in other branches of physics. In particular, chemisorption and molecular reactions have been discussed using rather similar models and theoretical methods. As far as progress towards the understanding of the broader aspects of 3d magnetism is concerned, definite steps have been taken in the description of more concentrated disordered alloys (which are often called 'spin glasses', see eg Coles 1973) or ordered intermetallic compounds (Caplin and Dunlop 1973). In both cases Kondo behaviour is combined with interaction effects, thus giving rise to a broader variety of phenomena than in the case of single impurities. Investigation of such systems may also bridge the gap between the two well-studied aspects of metallic magnetism: the Kondo effect and the highly correlated electron gas.

Acknowledgments

It would be impossible to list all those colleagues and friends with whom we enjoyed numerous stimulating conversations during the writing of this review, but we must at least acknowledge the discussions with Professor A A Abrikosov, Professor P W Anderson, Dr A D Caplin, Professor B R Coles, Dr C Hargitai, Professor A J Heeger, Professor P Nozières, Dr N Rivier and Dr J Sólyom. Professor B R Coles and Dr J Sólyom have also critically read the manuscript.

References

- ABRIKOSOV A A 1965 *Physics* **2** 5
- ABRIKOSOV A A and MIGDAL A A 1970 *J. Low Temp. Phys.* **3** 519
- ALLOUL H, BRENIER P, LAUNOIS H and POUGET J P 1971 *J. Phys. Soc. Japan* **30** 101
- AMIT D J and KEITER H 1973 *J. Low Temp. Phys.* **11** 63
- ANDERSON P W 1961 *Phys. Rev.* **124** 41
- 1967a *Phys. Rev.* **164** 352
- 1967b *Phys. Rev. Lett.* **18** 1049
- 1970 *J. Phys. C: Solid St. Phys.* **3** 2346
- 1972 *Comments Solid St. Phys.* **5** 72

- ANDERSON P W and McMILLAN W L 1967 *Theory of Magnetism in Transition Metals, International School of Physics Course XXXVII, Varenna 1966* ed W Marshal (New York, London: Academic Press) p62
- ANDERSON P W and YUVAL G 1971 *J. Phys. C: Solid St. Phys.* **4** 607
- ANDERSON P W, YUVAL G and HAMANN D R 1970a *Phys. Rev. B* **1** 4664
- 1970b *Solid St. Commun.* **8** 1033
- APPELBAUM J A 1966 *Phys. Rev. Lett.* **17** 91
- APPELBAUM J A and KONDO J 1968 *Phys. Rev.* **170** 542
- APPELBAUM J A and PENN D R 1969 *Phys. Rev.* **188** 874
- 1971 *Phys. Rev. B* **3** 942
- BAUER G and SEITZ E 1972 *Solid St. Commun.* **11** 179
- BEAL-MONOD M T, HURault J P and MAKI K 1971 *Proc. 12th Int. Conf. on Low Temperature Physics, Kyoto 1970* (Tokyo: Keigaku) p727
- BEAL-MONOD M T and WEINER R A 1968 *Phys. Rev.* **170** 552
- VAN DEN BERG G J 1964 *Progress in Low Temperature Physics* vol IV, ed C J Gorter (Amsterdam: North-Holland) p194
- BERTHIER C and MINIER M 1973 *J. Phys. F: Metal Phys.* **3** 1169
- BLANDIN A 1967 *J. Appl. Phys.* **39** 1285
- 1973 *Magnetism* vol V, ed H Suhl (New York: Academic Press) p58
- BLOEMBERGEN N and ROWLAND T J 1953 *Acta Metall.* **1** 731
- BLOOMFIELD P E and HAMANN D R 1967 *Phys. Rev.* **164** 856
- BLOOMFIELD P E, HECHT R and SIEVERT P R 1970 *Phys. Rev. B* **2** 3714
- BOGOLOUBOV N N and SHIRKOV D V 1959 *Introduction to the Theory of Quantized Fields* (London: Interscience) p511
- BRENIG W and GÖTZE W 1968 *Z. Phys.* **217** 188
- CAPLIN A D and DUNLOP J B 1973 *J. Phys. F: Metal Phys.* **3** 1621
- CAPLIN A D and RIZZUTO C 1968 *Phys. Rev. Lett.* **21** 746
- CAROLI B, CAROLI C and FREDKIN D R 1969 *Phys. Rev.* **178** 599
- CLOGSTON A M and ANDERSON P W 1961 *Bull. Am. Phys. Soc.* **6** 124
- COLES B R 1973 *Amorphous Magnetism* ed H Hooper (New York: Plenum Press)
- VAN DAM J E and VAN DEN BERG G J 1970 *Phys. Stat. Solidi* **3** 11
- VAN DAM J E, GUBBENS P C M and VAN DEN BERG G J 1972 *Physica* **62** 389
- DAYBELL M D and STEYERT W A 1968 *Rev. Mod. Phys.* **40** 380
- DREW H D and DOEZEMA R E 1972 *Phys. Rev. Lett.* **28** 1581
- DUKE C B and SILVERSTEIN S B 1967 *Phys. Rev.* **161** 456
- DWORIN L 1967 *Phys. Rev.* **164** 818, 841
- DWORIN L and NARATH A 1970 *Phys. Rev. Lett.* **25** 1287
- EMERY V J and LUTHER A 1971 *Phys. Rev. Lett.* **26** 1547
- EVENSON W E, WANG S Q and SCHRIEFFER J R 1970 *J. Appl. Phys.* **41** 1199
- FALK D S and FOWLER M 1967 *Phys. Rev.* **158** 567
- FAZEKAS P and ZAWADOWSKI A 1969 *Phys. Lett. A* **28** 669
- FISCHER K 1967 *Phys. Rev.* **158** 613
- 1970 *Springer Tracts in Modern Physics* vol 54, ed G Höhler (Berlin, Heidelberg, New York: Springer-Verlag) p1
- 1971a *Phys. Stat. Solidi (b)* **46** 11
- 1971b *Phys. Lett. A* **35** 91
- FOWLER M 1967 *Phys. Rev.* **160** 463
- 1972 *Phys. Rev. B* **6** 3422
- FOWLER M and ZAWADOWSKI A 1971 *Solid St. Commun.* **9** 471
- FRIEDEL J 1954 *Phil. Mag. (Suppl.)* **7** 446
- 1956 *Can. J. Phys.* **34** 1190
- 1958 *Nuovo Cim. (Suppl.)* **7** 287
- 1967 *Theory of Magnetism in Transition Metals, International School of Physics Course XXXVII, Varenna 1966* ed W Marshal (New York, London: Academic Press) p283
- FRÖHLICH H and NABARRO F R N 1940 *Proc. R. Soc. A* **175** 382
- FUKUSHIMA K 1971 *Prog. Theor. Phys., Japan* **46** 1307
- GELDART D J W 1972 *Phys. Lett. A* **38** 25
- DE GENNES P G 1962 *J. Phys., Paris* **23** 510
- GOLIBERSUCH D G 1970 Thesis University of Pennsylvania

- GOLIBERSUCH D G and HEEGER A J 1969 *Phys. Rev.* **182** 584
 GÖTZE W and SCHLOTTMANN P 1973 *Solid St. Commun.* **13** 511
 GRÜNER G 1972 *Solid St. Commun.* **10** 1039
 —— 1974 *Adv. Phys.* in the press
 GRÜNER G and HARGITAI C 1971 *Phys. Rev. Lett.* **26** 772
 GRÜNER G and ZAWADOWSKI A 1972 *Solid St. Commun.* **11** 663
 GURGENISHVILI G E, NERSESYAN A A and KHARADZE G A 1969 *Zh. Eksp. Teor. Fiz.* **56** 2028
 (*Sov. Phys.-JETP* **29** 1018)
 HAMANN D R 1966 *Phys. Rev.* **Lett.** **17** 145
 —— 1967 *Phys. Rev.* **158** 570
 —— 1970 *Phys. Rev. B* **2** 1373
 HAMANN D R and APPELBAUM J A 1969 *Phys. Rev.* **180** 334
 HEEGER A J 1969 *Solid State Physics* vol 23, ed F Seitz, D Turnbull and H Ehrenreich (New York: Academic Press) p283
 HEEGER A J and JENSEN M A 1967 *Phys. Rev. Lett.* **18** 488
 HEINE V 1967 *Phys. Rev.* **153** 673
 HERRING C 1966 *Magnetism* vol IV, ed G T Rado and H Suhl (New York: Academic Press) p1
 HERTZ J A 1971 *J. Low Temp. Phys.* **5** 123
 HOPFIELD J J 1969 *Comments Solid St. Phys.* **2** 40
 HÜBEL H 1973 *PhD Thesis* Technischen Universität, München
 ICHE G 1973 *J. Low Temp. Phys.* **11** 215
 ICHE G and ZAWADOWSKI A 1972 *Solid St. Commun.* **10** 1001
 KAISER A B and DONIACH S 1970 *Int. J. Magnetism* **1** 11
 KASUYA T 1956 *Prog. Theor. Phys., Japan* **16** 45
 KEDVES F J, HORDÓS M and GERGELY L 1972 *Solid St. Commun.* **11** 1067
 KEITER H and KIMBALL J C 1971 *Int. J. Magnetism* **1** 233
 KLEIN A P 1969 *Phys. Rev.* **181** 579
 KLEIN A P and HEEGER A J 1966 *Phys. Rev.* **144** 458
 KONDO J 1962 *Prog. Theor. Phys., Japan* **28** 846
 —— 1964 *Prog. Theor. Phys., Japan* **32** 37
 —— 1966 *Prog. Theor. Phys., Japan* **36** 429
 —— 1968 *Phys. Rev.* **169** 437
 —— 1969 *Solid State Physics* vol 23, ed F Seitz, D Turnbull and H Ehrenreich (New York: Academic Press) p183
 KROO N and SZENTIRIMAY Z S 1972 *Phys. Lett.* **40A** 173–4
 LANGER J S and AMBEGAOKAR V 1961 *Phys. Rev.* **121** 1090
 LANGRETH D 1966 *Phys. Rev.* **150** 516
 LEDERER P and MILLS D L 1967 *Solid St. Commun.* **5** 131
 LEVINE M J, RAMAKRISHNAN T V and WEINER R A 1968 *Phys. Rev. Lett.* **20** 1370
 LEVINE M J and SUHL H 1968 *Phys. Rev.* **171** 567
 LORAM J W, WHALL T E and FORD P J 1970 *Phys. Rev. B* **2** 857
 LORAM J W, WHITE R J and GRASSIE A D C 1972 *Phys. Rev. B* **5** 3659–69
 LUMPKIN H 1967 *Phys. Rev.* **164** 324
 LUTTINGER J M 1960 *Phys. Rev.* **119** 1153
 MAHAN G D 1967 *Phys. Rev.* **163** 612
 MALEEV S V 1966 *Zh. Eksp. Teor. Fiz.* **51** 1940 (*Sov. Phys.-JETP* **24** 1300)
 —— 1967 *Zh. Eksp. Teor. Fiz.* **53** 1038 (*Sov. Phys.-JETP* **26** 620)
 —— 1969 *Zh. Eksp. Teor. Fiz.* **56** 619 (*Sov. Phys.-JETP* **29** 340)
 —— 1971 *Zh. Eksp. Teor. Fiz.* **61** 350 (*Sov. Phys.-JETP* **34** 1869)
 MAPLE M B 1973 *Magnetism* vol V, ed H Suhl (New York: Academic Press) p289
 MATTIS D C 1967 *Phys. Rev. Lett.* **19** 1478
 MENYHÁRD N 1972 *Solid St. Commun.* **11** 423
 —— 1973 *Solid St. Commun.* **12** 215
 MEZEI F and GRÜNER G 1972 *Phys. Rev. Lett.* **29** 1465
 MEZEI F and ZAWADOWSKI A 1971a *Phys. Rev. B* **3** 167
 —— 1971b *Phys. Rev. B* **3** 3127
 MILLS D L, BEAL-MONOD M T and LEDERER P 1973 *Magnetism* vol V, ed G T Rado and H Suhl (New York: Academic Press) p89
 MILLS D L and LEDERER P 1966 *J. Phys. Chem. Solids* **27** 1805

- MONOD P and SCHULTZ S 1968 *Phys. Rev.* **173** 645
 MORE R and SUHL H 1968 *Phys. Rev. Lett.* **20** 500
 MÜHLSCHLEGEI B 1968 *Z. Phys.* **208** 94
 MÜLLER-HARTMANN E 1969 *Z. Phys.* **223** 277
 —— 1973 *Magnetism* vol V, ed H Suhl (New York: Academic Press) p353
 MURATA K K 1971 *PhD Thesis* Cornell University, Ithaca
 MUSKHELISHVILI N I 1953 *Singular Integral Equation* (Groningen: Noordhoff)
 MYERS H P, WALDEN L and KARLSSON A 1968 *Phil. Mag.* **18** 725
 NAGAOKA Y 1965 *Phys. Rev.* **138** A1112
 —— 1969 *Prog. Theor. Phys., Japan* **41** 586
 NAKAJIMA S 1968 *Prog. Theor. Phys., Japan* **39** 1402
 NARATH A 1972a *Solid St. Commun.* **10** 521
 —— 1972b *Crit. Rev. Solid St. Sci.* **3** 1
 NOZIÈRES P and DE DOMINICIS C T 1969 *Phys. Rev.* **178** 1097
 NOZIÈRES P, GAVORET F and ROULET B 1969 *Phys. Rev.* **178** 1084
 OKADA I and YOSIDA K 1973 *Prog. Theor. Phys., Japan* **49** 1483
 OKIJI A 1966 *Prog. Theor. Phys., Japan* **36** 1712
 RIVIER N, SUNJIC M and ZUCKERMANN M 1968 *Phys. Rev. Lett.* **23** 700
 RIVIER N and ZITKOVA J 1971 *Adv. Phys.* **20** 143
 RIVIER N and ZUCKERMANN M 1968 *Phys. Rev. Lett.* **20** 1036
 RIZZUTO C 1974 *Rep. Prog. Phys.* **37** 147
 RIZZUTO C, BABIĆ E and STEWART A M 1973 *J. Phys. F: Metal Phys.* **3** 825
 ROULET B, GAVORET F and NOZIÈRES P 1969 *Phys. Rev.* **178** 1072
 RUDERMANN M A and KITTEL C 1954 *Phys. Rev.* **96** 99
 SAKURAI A and YOSHIMORI A 1973 *Prog. Theor. Phys., Japan* **49** 1840
 SCALAPINO D J 1966 *Phys. Rev. Lett.* **16** 937
 SCHOTTE D 1968 *Z. Phys.* **212** 467
 SCHRIEFFER J R 1967 *J. Appl. Phys.* **38** 1143
 SCHRIEFFER J R and MATTIS D 1965 *Phys. Rev.* **140** 1412
 SCHRIEFFER J R and WOLFF P A 1966 *Phys. Rev.* **149** 491
 SÓLYOM J 1966 *Phys. Lett.* **23** 305
 SÓLYOM J and ZAWADOWSKI A 1974 *J. Phys. F: Metal Phys.* **4** 80
 SOULETIE J 1972 *J. Low Temp. Phys.* **10** 143
 SPENCER H J and DONIACH S 1968 *Phys. Rev.* **171** 515
 STAR W M, BASTERS F B, NAP G M, DE VROEDE E and VAN BAARLA C 1972 *Physica* **58** 585
 STEEL M R and THERENE D M 1972 *J. Phys. F: Metal Phys.* **2** 199
 STEINER P, ZDROJEWSKI W V, GUNPRECHT D and HÜFNER S 1973 *Phys. Rev. Lett.* **31** 355
 STEWART A M and GRÜNER G 1973 *J. Phys. F: Metal Phys.* **3** 843
 STONER E C 1938 *Proc. R. Soc. A* **165** 372
 —— 1939 *Proc. R. Soc. A* **169** 339
 SUHL H 1965 *Physics* **2** 39
 —— 1966 *Phys. Rev.* **141** 483
 —— 1967 *Phys. Rev. Lett.* **19** 442
 SUHL H and WONG D 1967 *Physics* **3** 17
 THOLENCE J L and TOURNIER R 1970 *Phys. Rev. Lett.* **25** 867
 TING C S 1971 *J. Phys. Chem. Solids* **32** 395
 TOMPA K 1971 *Proc. Conf. on the Magnetic and Electric Properties of Dilute Alloys*, Tihany
 TOULOUSE G 1969 *C. R. Acad. Sci., Paris* **268** 1200
 TRIPLETT B B and PHILLIPS N E 1971 *Phys. Rev. Lett.* **27** 1001
 WANG S Q, EVENSON W E and SCHRIEFFER J R 1969 *Phys. Rev. Lett.* **23** 92
 WEINER R A 1971 *Phys. Rev.* **4** 3165
 WILSON K G 1973 *Proc. Nobel Symp. XXIV* (Uppsala: Almqvist and Wiksell Informations-
 Industrie AB) p68
 WILSON K G and KOGUT J 1974 *Phys. Rep.* **12C** 76
 WÖGEL W and ZITTARTZ J 1973 *Z. Phys.* **261** 59
 WOLFF P A 1961 *Phys. Rev.* **124** 1030
 YOSHIMORI A 1968 *Phys. Rev.* **168** 493
 YOSHIMORI A and SAKURAI A 1970 *Prog. Theor. Phys., Japan* **46** 162
 YOSIDA K 1957 *Phys. Rev.* **106** 893

- YOSIDA K 1966a *Phys. Rev.* **147** 223
— 1966b *Prog. Theor. Phys., Japan* **36** 875
— 1970 *Proc. 12th Int. Conf. on Low Temperature Physics, Kyoto 1970* ed E Kanda (Tokyo: Keigaku) p665
YOSIDA K and OKIJI A 1965 *Prog. Theor. Phys., Japan* **34** 505
YOSIDA K and YAMADA K 1971 *Prog. Theor. Phys. (Suppl.)* **46** 244
YOSIDA K and YOSHIMORI A 1973 *Magnetism* vol V, ed H Suhl (New York: Academic Press) p253
YUVAL G and ANDERSON P W 1970 *Phys. Rev. B* **1** 1522
ZAWADOWSKI A 1973 *Proc. Nobel Symp. XXIV* (Uppsala: Almqvist and Wiksell Informations-Industrie AB) p76
ZAWADOWSKI A and FAZEKAS P 1969 *Z. Phys.* **226** 235
— 1970 *J. Appl. Phys.* **41** 1155
ZAWADOWSKI A and FOWLER M 1970 *Proc. 12th Int. Conf. on Low Temperature Physics, Kyoto 1970* ed E Kanda (Tokyo: Keigaku) p954
ZAWADOWSKI A and GRÜNER G 1974 *J. Phys. F: Metal Phys.* **4** L202
ZENER C 1951 *Phys. Rev.* **81** 440
ZIMAN J 1972 *Principles of the Theory of Solids* 2nd edn (London: Cambridge UP) p157
ZITTARTZ J 1968a *Z. Phys.* **217** 43
— 1968b *Z. Phys.* **217** 155
ZITTARTZ J and MÜLLER-HARTMANN E 1968 *Z. Phys.* **212** 380
ZŁATIC V, GRÜNER G and RIVIER N 1974 *Solid St. Commun.* **14** in the press